UNIVERSITEIT VAN PRETORIA
UNIVERSITY OF PRETORIA
YUNIBESITHI YA PRETORIA

Chemical evolution of the Paleoproterozoic Rooiberg Group, Kaapvaal Craton, South Africa: new insights into the formation of a silicic large igneous province (SLIP)

By

Olutola O. Jolayemi

29266476

Submitted in partial fulfilment of the requirement for the degree of Doctor of Philosophy in Geology in the Faculty of Agricultural and Natural Science at the University of Pretoria.

Supervisors: Dr. N. Lenhardt

Dr. R.J. Roberts

July, 2015

UNIVERSITEIT VAN PRETORIA
UNIVERSITY OF PRETORIA
YUNIBESITHI YA PRETORIA

ABSTRACT

With an estimated erupted volume of 300,000 km^3 and an areal extent of more than 200,000 km^2, the Paleoproterozoic (2.06 Ga) silicic volcanic rocks of the Rooiberg Group (Kaapvaal Craton) in northern South Africa forms one of the largest and to the same time oldest silicic large igneous provinces (SLIPs) known. This large volume of rocks can be sub-divided into four formations: the Dullstroom, Damwal, Kwaggasnek and Schrikkloof Formations.

The results of this study show that a clear chemostratigraphy (by using major elements such as TiO_2, SiO_2, Na_2O, K_2O, P_2O_2, MgO, and Fe_2O_3) can be established in the area north of Loskop Dam, dividing the rocks of the study area into the Damwal, Kwaggasnek and Schrikkloof formations. The studied rocks are characterized by aphanitic lavas bearing amygdales, spherulitic textures and flow-bands with some sedimentary and pyroclastic interbeds. The dacites could mainly be described as high-Mg felsites (HMF), whereas the rhyolites could be described as low-Mg felsites (LMF).

The negative Eu anomaly, Nb and Ta values of the upper part of the Rooiberg Group range between 5.38-24.2 and 0.45-1.86 ppm, respectively, similar to crustal compositions. Furthermore, Nb/Ta values range from 10.91-14.83 (also similar to typical crustal compositions) while few samples from the Damwal Formation exhibit higher values of 15.13-16.02, similar to mantle-derived compositions. Tectonic discriminant diagrams show that the rocks used in this study evolved from fractional crystallization of a mafic liquid although all samples plot in fields with crustal signatures. Plot of ε_{Nd} and $^{87}Sr/^{86}Sr$ show a mantle-derived origin for the upper part of the Rooiberg Group. However, ε_{Nd} values of the upper part of the Rooiberg Group range between ~-10 to ~-6, typical of crustal composition or continental basalts formed in the crust.

From the results, the Rooiberg Group exhibit both mantle (as observed in the Dullstroom and lower Damwal formations) and crustal signatures as exhibited by the Kwaggasnek and Schrikkloof formations. This is interprested as a result of the interaction of the thick crust and

a shallow mantle source within the Bushveld Province during magmatism. Furthermore, similarities in geochemical signatures between the Rooiberg Group and selected SLIPs around the world suggest a similar origin for SLIPs by fractional crystallization of a mafic melt and melted (or assimilated) crustal material.

UNIVERSITEIT VAN PRETORIA
UNIVERSITY OF PRETORIA
YUNIBESITHI YA PRETORIA

DECLARATION

I, Olutola Olumayowa Jolayemi declare that this thesis, which I hereby submit for the degree of Doctor of Philosophy in Geology in the Faculty of Agricultural and Natural Sciences at the University of Pretoria, is my own work and has not previously been submitted by me for a degree at this or any other tertiary institution.

Signature

Date

UNIVERSITEIT VAN PRETORIA
UNIVERSITY OF PRETORIA
YUNIBESITHI YA PRETORIA

LIST OF PUBLICATIONS AND PRESENTATIONS

Journal articles

Jolayemi, O.O., Lenhardt, N., Roberts, J., Masango, S.M. (in review) Chemical evolution of the Paleoproterozoic Rooiberg Group, Kaapvaal Craton, South Africa: new insights into the formation of silicic large igneous provinces (SLIPs). *Journal of Volcanology and Geothermal Research*.

Lenhardt, N., Masango, S.M., Jolayemi, O.O., Lenhardt, S.Z. (in review) First facies analysis of a Palaeoproterozoic (2.06 Ga) intracratonic, silicic Large Igneous Province – the Rooiberg Group, Kaapvaal Craton, South Africa. *Bulletin of Volcanology*.

Contributions to conferences

Jolayemi, O.O., Lenhardt, N., Roberts, J., Masango, S.M. (2013) Chemical evolution of the Paleoproterozoic Rooiberg Group, Kaapvaal Craton, South Africa: new insights into the formation of silicic large igneous provinces (SLIPs) 24th Colloquium of African Geology, Addis Ababa, Ethiopia, 09.-13.01.13.

Masango, S.M., Lenhardt, N. Jolayemi, O.O. (2013) First lithofacies analysis on and the geodynamic setting of a Palaeoproterozoic silicic large igneous province: the Rooiberg Group, Kaapvaal Craton, South Africa. 24th Colloquium of African Geology, Addis Ababa, Ethiopia, 09.-13.01.13.

Jolayemi, O.O., Roberts, J., Lenhardt, N. (2013) The Paleoproterozoic Rooiberg Group, South Africa: new insights into the formation of the silicic large igneous provinces (SLIPs). Goldschmidt Conference, Italy, 2013. Mineralogical Magazine, 77(5), 1402.

UNIVERSITEIT VAN PRETORIA
UNIVERSITY OF PRETORIA
YUNIBESITHI YA PRETORIA

ACKNOWLEDGEMENT

I would like to acknowledge individuals that have – in their own special way – guided, encouraged, assisted and supported me. Without them this thesis would not have been completed.

I like to express sincere gratitude to Dr. Nils Lenhardt and Dr. R.J. Roberts, Geology Department at the University of Pretoria, for their wonderful supervision, support and advice. I further like to acknowledge the members of department, especially the Stoneman Building for their assistance and guidance during sample preparation and analysis, while sincere gratitude is expressed to Mrs. Sukanya Lenhardt for her ever-ready and kind assistance with using the GIS.

Sincere gratitude is given to the outgone head of department of Geology, University of Pretoria, Prof. P.G. Eriksson for his support and guidance as well as Prof Annette Götz, the new head of department, for her kind assistance and support.

Lastly, I would like to thank my family, especially my parents for their assistance, encouragement and prayerful support during this project.

UNIVERSITEIT VAN PRETORIA
UNIVERSITY OF PRETORIA
YUNIBESITHI YA PRETORIA

CONTENTS

UNIVERSITEIT VAN PRETORIA
UNIVERSITY OF PRETORIA
YUNIBESITHI YA PRETORIA

LIST OF FIGURES

UNIVERSITEIT VAN PRETORIA
UNIVERSITY OF PRETORIA
YUNIBESITHI YA PRETORIA

LIST OF TABLES

CHAPTER 1

INTRODUCTION

1.1 Motivation and Aims

The volcanic rocks of the Paleoproterozoic (~2.06 Ga; Walraven, 1997) Rooiberg Group in the northeastern part of South Africa have an estimated eruptive volume of 300,000 km^3 and a present (after erosion) aerial extent of 50,000-67,000 km^2 (Twist and French, 1983). The rocks thus form one of the largest and oldest silicic large igneous provinces (SLIPs) known (Twist and French, 1983). The Rooiberg Group comprises the accumulation of volcanic rocks prior to the emplacement of the mafic to ultramafic Bushveld Complex (Twist, 1985). These volcanic rocks represent the youngest, most silicic and most voluminous unit of the Transvaal Supergroup that unconformably overlie the 2.32-2.06 Ga Pretoria Group that was deposited on the stable Kaapvaal Craton (Lenhardt and Eriksson, 2012). Although the Rooiberg Group stratigraphy is associated with the Transvaal Supergroup, it is petrogenetically linked to the larger Bushveld magmatic event (Twist and French, 1983; Eriksson et al., 1993; Buchanan et al., 2004).

Silicic large igneous provinces (SLIPs) occur in continental and oceanic intraplate settings similar to the commonly more mafic large igneous provinces (LIPs) (McPhie et al., 2008). SLIPs are described as exclusively continental by Shellnut et al. (2012) and are dominated by voluminous felsic lavas with some pyroclastic and or sedimentary interbeds. Most SLIPs are similar in size to LIPs ($\geq 10^5$ km^3) and formed during the Phanerozoic (Agangi et al., 2012). However, it is important to note that some LIPs also contain felsic rocks, notably the Karoo-Ferrar LIP and the Central Atlantic Magmatic Province (CAMP) (Greenough and Dostal, 1992; Shellnut and Jahn, 2010; Xu et al., 2010). These felsic rocks are believed to have evolved by fractional crystallization of mafic magmas or partial melting of underplated mafic rocks (Shellnut and Jahn, 2010; Shellnut et al., 2012). It should further be noted that the amount of silicic rocks seen in the different LIPs vary; for example the Permian Panjal Traps of northern India are described to have volumetrically minor silicic rocks that are suggested to be products of basaltic rock differentiation (Ganju, 1944; Nakazawa et al., 1975) while the Gawler Range Volcanics is a silicic dominated LIP (McPhie et al., 2008).

Some SLIPs are described as voluminous, extensive lava units that are comparable to flood basalts such as the Gawler Range Volcanics (Agangi et al., 2012; Allen and McPhie, 2002)

whereas others are dominated by ignimbrites such as the Rogerson Graben of the Snake River Plain (Andrews et al., 2008). The study of SLIPs from different locations provides a detailed understanding of their emplacement mechanisms.

This study aims to identify the different formations of the Rooiberg Group in different localities as well as to establish a chemostratigraphy in the northern Loskop Dam area using major and trace element signatures. This study will utilize geochemical characteristics to further ascert the model of formation of the Rooiberg Group as well as compare these signatures to other major silicic large igneous provinces around the world. The SLIPs used for comparison are randomly selected, independent of composition, location and age. Similarities between the selected SLIPs and the Rooiberg Group, independent of these three characteristics (composition, location and age) will further support and improve the probability that SLIPs around the world evolved from similar sources and processes.

Geology of the Rooiberg lavas

The ~2.06 Ga Bushveld Complex (Walraven, 1997; Buick et al., 2001) intruded a stable cratonic setting, the Kaapvaal Craton (Cawthorn and Walraven, 1998), representing the upper part of the Transvaal Sequence (Twist, 1985) that evolved in a slowly evolving intra-cratonic depression termed the Transvaal basin (Tankard et al., 1982). This basin is believed to have shrunk during its final waning phase (Coertze et al., 1977). The term “Bushveld Complex” was described by the South African Commission for Stratigraphy to include ultramafic-mafic layered rocks, sills beneath the intrusion, and the granitic and granophyric roof rocks (South African Commision on Stratigraphy, 1980). The Bushveld Complex was also described to include the volcanic rocks that predate the emplacement of the ultramafic-mafic rocks (Cawthorn and Walraven, 1998). As a result of the inclusion of the various rock types such as mafic rocks of the Rustenburg Layered Suite, volcanics of the Rooiberg Group as well as granitic and granophyric rocks, the term Bushveld Magmatic Province will be employed to describe this igneous province, a term earlier used by Buchanan et al. (1999; 2002) and Mathez et al. (2013). Figure 1 shows the general extent of the Bushveld Magmatic Province with the Rustenburg Layered Suite representing the ultramafic-mafic rocks. The cyclic units of the ultramafic-mafic unit represent different zones (Cawthorn and Spies, 2003; Cawthorn, 2013). These zones include the Lower Zone, Critical Zone, Main Zone and Upper Zone, whereas the volcanics that predate these rocks include the Dullstroom, Damwal, Kwaggasnek

and Schrikkloof formations (Schweitzer et al., 1995; Hatton and Schweitzer, 1995, Buchanan et al., 1999; 2002; 2004).

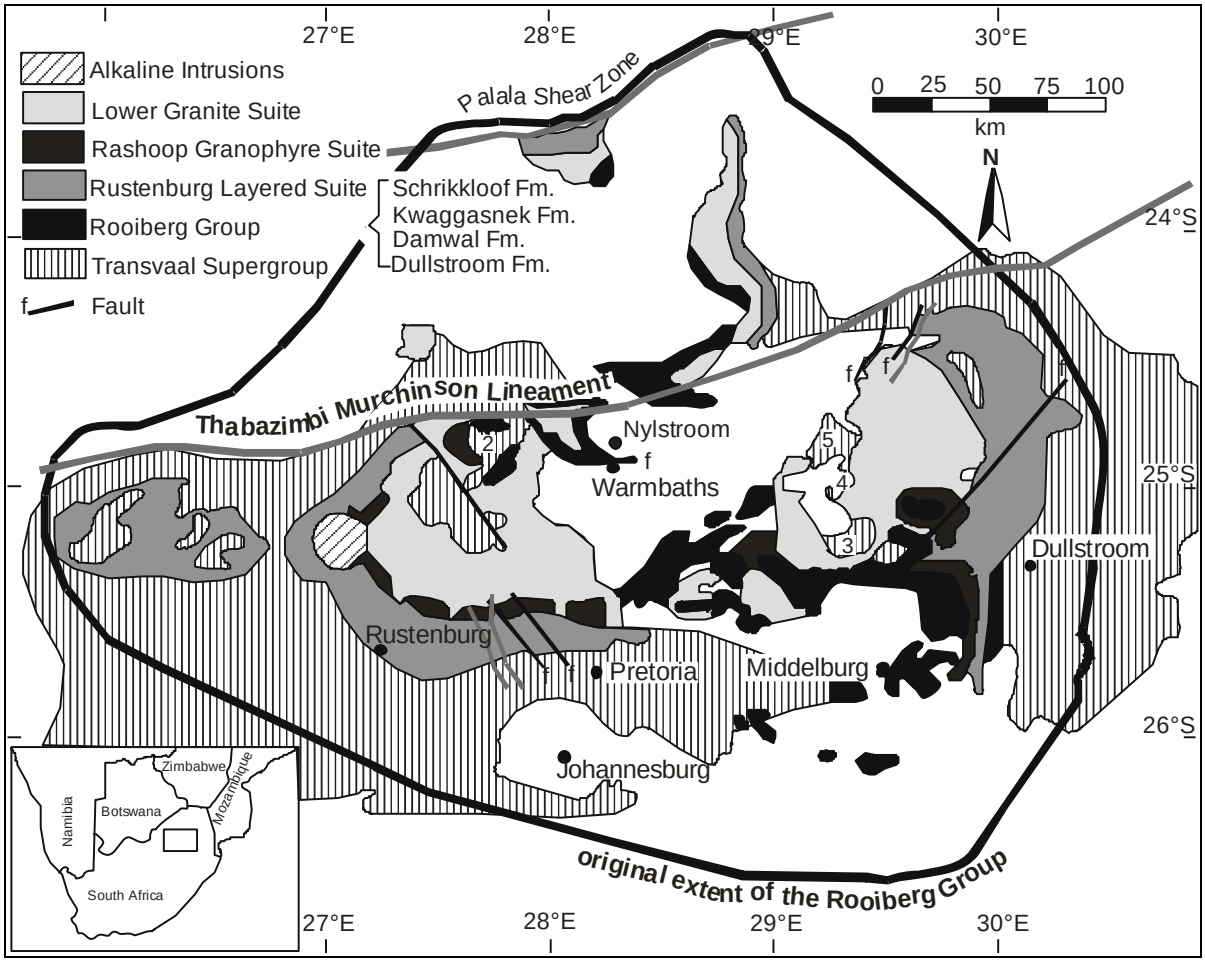

Figure 1: Map showing the extension of the Rooiberg Group together with other parts of the Bushveld Magmatic Province in the north of South Africa (Lenhardt and Eriksson, 2012). The square in the inset in the lower left corner shows the location of the Rooiberg Group in South Africa. 1. Crocodile River Fragment; 2. Rooiberg Fragment; 3. Dennilton Fragment; 4. Marble Hall Fragment; 5; Stavoren (Makeckaan) Fragment.

The Rooiberg rhyolites consist of several thousands of metres of lava flows erupted from fissural volcanism with minor sedimentary units of shale and greywacke (Twist and French, 1983; French and Twist, 1983; Twist, 1985; Harmer and Farrow, 1995; Schweitzer et al., 1995; Hatton and Schweitzer, 1995). The extrusion of the vast Rooiberg Group rocks preceded the emplacement of the Rustenburg Layered Suite in the northern part of the craton. The Rooiberg Group includes the Dullstroom, Damwal, Kwaggasnek and Schrikkloof formations in order of appearance from the bottom to top (Schweitzer, 1987; Eriksson et al., 1993; Buchanan et al., 1999; 2002). This stratigraphy was disrupted by three suites of rocks in the Bushveld Magmatic Province: the mafic to ultramafic rocks of the Rustenburg Layered Suite, the Rashoop Granophyres and the Lebowa Granite Suite (Schweitzer et al., 1995; Buchanan et al., 2004). All four formations, with the lower part of the Dullstroom Formation detached from the upper part of the Rooiberg Group, occur in the SE of the Rooiberg Group (Fig. 1). The Damwal Formation is also restricted to this general area and immediately to the west (Lenhardt and Eriksson, 2012). The upper Kwaggasnek and Schrikkloof formations are much more widespread in the south-central and northwestern parts of the Rooiberg Group where they lie unconformably on Transvaal sedimentary strata in the so-called Rooiberg Fragment (Hatton and Schweitzer, 1995; Lenhardt and Eriksson, 2012). The Rooiberg lava flows in the east are spatially associated with the Rustenburg Layered Suite (Hatton and Schweitzer, 1995).

Twist and French (1983) described the Rooiberg Group as the youngest, most siliceous, as well as most voluminous, volcanic rocks that concluded the formation of the Transvaal basin and at the same time commenced the emplacement of the Bushveld Magmatic Province. Major lithological units within the Rooiberg Group were described by Twist and French (1983) to include the felsite lavas, pyroclastic rocks, sedimentary rocks and xenoliths (quartzite inclusions; Twist and French, 1983). Twist and French (1983) described the felsite lavas as dense, massive aphanitic rocks that are usually red-brown to grey and black. These felsites bear flow-banding, amygdales, vesicles, lithophysae, and spherulites, all features typical of extrusive lava flows (Twist and French, 1983). The agglomerates and tuffs that constitute the pyroclastics are seen in layers, ranging from a few meters to tens of meters in thickness (Twist and French, 1983), and occurring in between the dense lava flows. The agglomerates, as described by Twist and French (1983), are coarse and blocky, consisting of fragments that range from a few millimetres to more than 20 cm across, although fragments of up to 1 m in size are also observed. Ash-flow tuffs which constitute only a minute portion

of the Rooiberg Group, show good welded and shard structures (Twist and French, 1983), and are interpreted as the replacement of original glass with calcite or cryptocrystalline silica (Lenhardt and Eriksson, 2012).

Sedimentary intercalations including sandstones and shales were observed interbedded between the dense lava flows of the Rooiberg Group (Twist and French, 1983). Twist and French (1983) described the numerous feldspathic sandstone layers to range from a few meters to 100 m in thickness. Shales constitute a minor part of the Rooiberg Group. These shales are described as the product of tuffs, tuff-shales or partly chemical precipitates (Twist and French, 1983). Finally, Twist and French (1983) described the xenolithic quartzite inclusions observed in the Rooiberg Group as ranging in size from a few centimetres to more than 100 m. These inclusions were described as white crystalline ortho-quartzites that show sharp contacts with the felsites. Furthermore, these blocks are discontinuous and exhibit differing strikes and slips (Twist and French, 1983), supporting the proposition that they are inclusions and not sedimentary interbeds.

Twist (1985) further subdivided the Rooiberg Group into nine stratigraphic units based on field and petrographic descriptions (texture and phenocryst contents of the massive lavas, and occurrence of pyroclastic and sedimentary interbeds). Twist (1985) described Unit 1 occurring in the lowest part of the Rooiberg stratigraphy as massive, dark red and grey porphyritic felsites. This lava contains hornblende and chlorite with rare flow-banding and layers of minor tuffite, volcanic breccia, and sandstone. Overlying this unit is a layer of massive, crystalline porphyritic, dark brown to dark green felsites, which Twist (1985) described as augite- bearing (Unit 2). Twist (1985) observed that a minor layer composed of sandstones, sandy shales and tuffites with ripple marks, mud cracks, and crossbeds occur between Units 1 and 2. A similar layer, with the absence of sandy shale, was also seen between Unit 2 and the overlying Unit 3 (Twist, 1985). Unit 3 is described as dense, dark-brown, grey and black porphyritic felsites that are spherulitic towards the top and often exhibit amygdales. Unit 4 exhibits dark brown felsites with prominent flow-banding and is typically bearing amygdales and lithophysae with interbeds of sandstones and volcanic breccias. The overlying Unit 5 is described as brick-red to purple felsites with prominent flow banding. Also prominently visible in this unit are ash-flow tuffs overlain by siltstone, tuffite and tuff in the centre of the unit. Just above Unit 5 is a thin layer composed of very prominent and cross-bedded medium-grained quartzite. This thin unit of quartzite is overlain by a layer of massive porphyritic red felsites (Unit 6), that exhibit localized flow-banding and

amygdales, along with prominent ash-flow tuffs in the upper part. Twist (1985) described Unit 7 as a relatively small interlayer of ash-flows and red porphyritic to non-porphyritic lavas. Above Unit 7 is a layer of sandstone that separates it from Unit 8. Unit 8 is described as an interbed of sandstones and tuffites within sparsely porphyritic pinkish-red felsites. These sandstones are described as occuring at the base of Unit 8. The topmost Unit 9 is separated from the underlying Unit 8 by a thick sequence of pyroclastic and sedimentary rocks consisting of tuffs and volcanic breccias in the lower part of this sequence. Tuffs and lava are also observed inter-layered between sandstones and shales in the upper part, indicating a lahar deposit (Twist, 1985). Unit 9 constitutes porphyritic to non-porphyritic pinkish-red felsites that exhibit flow banding with a thin layer of tuff and ash-flow tuff marking the top of the unit. Table 1 below shows a better illustration of these sequences.

Table 1: Field textures used by Twist (1985) to divide the Rooiberg Group into units and the formation each unit represents (Lenhardt and Eriksson, 2012)

Unit (Twist, 1985)	Description	Formation (Lenhardt and Eriksson, 2012)
9	Sparsely porphyritic to non-porphyritic pinkish-red felsites. Generally flow-banded , feldspars invariably sericitized. A thin layer of tuff and ash-flow tuff mark the top of the unit.	Schrikkloof Formation
8	Very sparsely porphyritic and very flaggy pinkish-red felsite. Commonly flow-banded. Sandstones and Tuffites towards the base.	Kwaggasnek Formation
7	Zone of interlayered ash-flows and red porphyritic and non-porphyritic lavas.	
6	Generally mass porphyritic red felsite with local flow-banding and amygdaloidal layers. Sometimes light greyish to greenish. A prominent ash-flow tuff occurs within the upper portion.	Damwal Formation
5	Brick red to purple, slightly porphyritic felsite. Very flaggy and commonly flow-banded. Prominent ash-flow tuffs overlain siltstone, tuffite and tuff in centre of unit.	
4	Typically amygdaloidal and lithophysal dark brown felsites, sometimes with coarse, prominent flow-banding. Impersistent to fairly persistent sandstones, hyaloclastites and volcanic breccias.	
3	Dense, dark brown, grey and black porphyritic felsites, often with glassy strong conchoidal fracture. Strongly spherulitic towards the top. Often amygdaloidal.Local hyaloclastites, sandstones, tuffites and tuffs.	
2	Massive, crystalline microporphyritic black, dark brown and dark green felsites. Sometimes amygdaloidal and flow-banded. Augite phenocrysts are abundant. Impersistent sandstone horizon.	Dullstroom Formation
1	Massive, dark red and grey porphyritic felsites, rarely amygdaloidal or flow-banded. Typically hornblende- and chlorite-bearing, becoming more pervasively altered downwards. Contains layers of jet-black porphyritic felsite, minor tuffite, volcanic breccia and sandstone.	

The use of physical properties such as the colour, texture, and layers of volcaniclastic sediments for the Rooiberg Group classification by Twist (1985) was soon criticized by Eriksson et al. (1993) and Schweitzer and Hatton (1995). This method of classification by Twist (1985) was criticised due to primary differences in style of deposition and processes of

alteration occurring in these depositional settings (Schweitzer et al., 1995). As a result, Schweitzer et al. (1995) employed lithological and geochemical properties to subdivide the Rooiberg Group. Schweitzer et al. (1995) correlated lithological characteristics of the Rooiberg Group with its geochemical signatures. Immobile elements such as TiO_2 and Zr were used in subdividing the Rooiberg Group as its different formations exhibit distinct geochemical signatures. Subsequently, the Dullstroom Formation was described as exhibiting four different magma types; these include the low titanium basaltic andesite (LTI_{ba}), high titanium basalt (HTI_{ba}), high magnesium felsites (HMF) and basal rhyolite. Similar compositions for the HMF above and below the mafic rocks of the Bushveld Complex are the basis for including the Dullstroom Formation below the Bushveld Complex as part of the Rooiberg Group (Schweitzer et al., 1995). A unique magma type, the high Fe-Ti-P magma, occurs in the upper part of the Dullstroom Formation above the mafic/ultramafic cumulates of the Rustenburg Layered Suite (Schweitzer et al., 1995).

Schweitzer et al. (1995) and Schweitzer and Hatton (1995) identified the major different lava types in these volcanic rocks. The Dullstroom Formation at the base of the Rooiberg Group is proposed to have the highest number of different lava types, with six different types identified. Hatton and Schweitzer (1995) described the Dullstroom Formation as consisting of low-Ti (LTI) basaltic andesite, basal rhyolite, high-Ti (HTI) basalt, high-Mg felsites (HMF), high-Fe-Ti-P andesite and low-Mg felsites (LMF). The Damwal, Kwaggasnek and Schrikkloof formations are composed majorly of the LMF (Hatton and Schweitzer, 1995). Little explanation, however, has been given on why there is such a distinct difference between the basal Dullstroom formation and the overlying upper Damwal as compared with the Kwaggasnek and Schrikkloof formations.

Three main theories have been postulated for the origin of the volcanic rocks of the Bushveld Complex. Due to closely spaced ring features observed in the Bushveld Magmatic Province, Rhodes (1975), Elston and Twist (1989) and Elston (1992) originally proposed multiple impacts of large comets and asteroids for the formation of this province, including the Rooiberg Group. This hypothesis was later opposed by Buchanan and Reimold (1998). These authors stated that quartz paramorph (tridymite) observed in the Rooiberg Group and interpreted as a product of superheated impact melt, an indication for meteoric impacts, is also observed in terrestrial volcanic provinces. Furthermore, Buchanan and Reimold (1998) stated that the lobate shape of the entire Bushveld province, exhibiting features of several closely-spaced rings, may be the result of post-Rooiberg Group deformation. Using

geochemical data, Hatton (1988, 1995) proposed an origin for the Rooiberg Group due to the melting of detrital material during subduction under the Kaapvaal Craton. More recently, Hatton (1995) suggested an origin from the partial melting of the mantle and lower crust by a mantle plume, a hypothesis most researchers (Schweitzer et al., 1995; Hatton and Schweitzer, 1995; Buchanan et al., 2002, 2004) nowadays agree on. Although the part of the mantle melted is not ascertained, Hatton (1995), however, proposed melting of the lower mantle.

Schweitzer and Hatton (1995) described evidence for simultaneous emplacement of the Rooiberg Group volcanics and mafic-ultramafics of the Rustenburg Layered Suite (RLS), representing the extrusive and intrusive phases of the Bushveld magmatism. Evidence described by Schweitzer and Hatton (1995) include close spatial association of the Rooiberg Group with the mafic intrusions of the Rustenburg Layered Suite. This is indicated by the localised occurrence of the lower part of the Rooiberg Group (Dullstroom Formation), whereas the upper parts that include the Damwal, Kwaggasnek and Schrikkloof formations cover much larger areas. Other evidence to support the synchronous extrusive and intrusive magmatism of the Bushveld province is the age similarity between the Rooiberg Group and the Rustenburg Layered Suite. For example, a zircon age from the Kwaggasnek Formation of 2061 ±2 Ma (Walraven, 1997) is similar to the 2061 ±27 Ma age of the Rustenburg Layered Suite (Cawthorn and Walraven, 1998) (2058.9±0.8 Ma, Buick et al., 2001).

Schweitzer and Hatton (1995) also stated that the majority of the granophyres do not represent re-melted felsites but intrusive equivalents of the Rooiberg Group. These authors hypothesised that the granophyres compare well to the compositions of the younger part of the Rooiberg Group succession. These authors also described differences in composition between the granophyres and the lower part of the Rooiberg Group. With such above mentioned evidence, Schweitzer and Hatton (1995) proposed the exclusion of the Rooiberg Group from the Transvaal Supergroup and subsequent inclusion in the Bushveld Magmatic Province.

1.2. SLIPs around the world

Significant questions about SLIPs include: Are SLIPs explosively or effusively erupted and why? How are these voluminous SLIPs emplaced in relatively short time periods? Do SLIPs form from fractional crystallization of a mantle-derived liquid or assimilation/contamination of crustal material by such crystallizing liquid, and how much contamination occurs? Are SLIPs similar across the earth?

In this study, focus is set on the crystallization history of the Rooiberg Group. Furthermore, the effect of crustal contamination is determined through modeling, which further helps to improve the understanding of the petro-genetic evolution of the Rooiberg Group and, hence, other SLIPs around the world.

Other SLIPs from around the world are used for comparison with the Rooiberg Group volcanics (Table 2). SLIPs used for comparison are selected on the basis of detailed studies conducted and available on these SLIPs; however, effort is made to select different SLIPs from different continents around the world (including LIPs with substantial volume of silicic rocks), independent of their composition (large igneous provinces dominated by or with minor volumes of rocks of silicic composition) and size (area covered and volume). This further helps to decide whether SLIPs have similar origins or not. Selected silicic provinces used in comparison include the Snake River Plain and Gawler Range Volcanics (GRV), as well as LIPs, containing felsic volcanics such as the Central Atlantic Magmatic Province (Keweenawan), the Paraná-Etendeka Province, and the Karoo-Ferrar Province.

The Rogerson Graben of the Snake River Plain (USA) is a ~10-17 Ma (Pierce and Morgan, 1992) rhyolitic volcanic succession consisting of ignimbrites/ash-flow tuffs and other volcaniclastic deposits (Andrews et al., 2008), visible between the Bruneau-Jarbidge and Twin Falls eruptive centres (Pierce and Morgan, 1992). This volcanic province is described as hosting some of the youngest and best exposed lava-like, highly-welded ignimbrites (Bonnichsen and Citron, 1982; Ekren et al., 1984; Branney and Kokelaar, 1992). Ignimbrites of this volcanic succession are crystal-poor, having <20% phenocrysts (Christiansen and McCurry, 2008). Phenocrysts observed include plagioclase, quartz, Fe-Ti oxides, Fe-rich pyroxenes and sanidine with rare secondary minerals such as biotite and hornblende (Christiansen, 2001; Wright et al. 2002; Cathey and Nash, 2004). Christiansen and McCurry (2008) further described the volcanic rocks of the Snake River plain as calc-alkaline with compositions ranging mainly from basalt to rhyolite with only a few basaltic andesites and andesitic rocks.

The ~1591-1592 Ma Gawler Range Volcanics in Australia (Creaser, 1995; Agangi et al., 2012) is described as voluminous (25,000 km^3) and extensive (>200 km) extrusion of felsic lavas and ignimbrites (Allen et al., 2008; Agangi et al., 2012) with minor mafic to intermediate units. Betts et al. (2009) interpreted that the Gawler Range Volcanics (GRV) emplaced as a result of a hotspot-related igneous event that affected the central part of

Australia. The GRV is divided into an upper and lower part. The lower part is a thick (3 km) succession composed mainly of dacite and rhyolite with interbeds of ignimbrites and mafic lava (Stewart, 1994; Ferris, 2003) whereas the upper part is >1000 km^3 of extensive, homogenous, massive lavas having a composition of dacite to rhyolite (Allen et al., 2008; McPhie et al., 2008). Major mineral phases observed in the GRV are a quartz-feldspar groundmass with phenocrysts of plagioclase, K-feldspar, orthopyroxene, and Fe-Ti oxide. Rocks in the GRV range in composition from dacite to rhyolite with SiO_2 >90%.

The Keweenawan Province of the Midcontinental Rift System (2×10^6 km^3) (Cannon, 1992) is a ~1.1 Ga volcanic succession. This province is about 4 km thick (Zartmann et al., 1996) and is described as having a lateral extent of 40 km and a volume of about 600 km^3 (~25% of the entire Midcontinental Rift System; MRS) (Green and Fitz, 1993). The Keweenawan volcanics range from andesite to rhyolite in composition with the latter having high SiO_2 contents >80% (Vervoort and Green, 1997).

The Karoo volcanic province, located in the southern part of Africa, is a ~182 Ma volcanic succession that Duncan et al. (1997) described as covering an area of 3×10^6 km^2 with an original estimated volume of 2×10^6 km^3 (Catuneanu et al., 2005; Jourdan et al., 2007b). The Karoo lavas are composed of two main magma types (Duncan et al., 1990; Sweeney et al., 1994); a high Ti-Zr and low Ti-Zr flood basalts. The Karoo volcanics range in composition mainly between dacites and rhyolites with some minor trachytes (Melluso et al., 2008). Minerals observed include plagioclase, augite, pigeonite, and Fe-Ti oxides.

Lastly, the ~134 Ma Paraná-Etendeka magmatic province occupies southern South America and Southwest Africa. This province have an estimated exposure of 1×10^6 km^2 (Janasi et al., 2011). Volcanic rocks of this province are composed of low-Ti basalts at the base, then low-Ti dacites and rhyolites, and finally high-Ti basalt, observed in the northern and western portion of the Paraná basin (Peate et al., 1992; Peate, 1997). The Paraná is divided into two petrographically distinct groups (Belleini et al., 1986; Garland et al., 1995), namely the high-Ti rhyolites that are plagioclase-rich and the low-Ti rhyolites described by Belleini et al. (1986) and Milner et al. (1992) as including plagioclase, pyroxene, and titanomagnetite with rare ilmenite. Figure 2 shows the location of the different SLIPs used in comparison to the Rooiberg Group and Table 2 shows a summary of these SLIPs.

Table 2: Selected SLIPs from around the world. * indicates value for only the silicic volcanics in the province.

Province	Region	Age	Area (km^2)	Volume (km^3)	Reference
Paraná	Brazil	134 Ma[(a)]	1×10^6 km^2 [(a)]	35 000 km^3 [(b)]	Thiede and Vasconcelos, 2010 [(a)]; Kirsten et al., 2000 [(b)]
Gawler Range Volcanics	Australia	1592 Ma[(c)]	25 000 km^2 [(d)]	25 000 km^3 [(c)]	Blissett et al., 1993 [(c)]; McPhie et al., 2008 [(d)]
Karoo	Southern Africa	182 Ma[(e)]	3×10^6 km^2 [(f)]	2×10^6 km^3 [(f)]	Duncan et al., 1997 [(e)] ; Catuneanu et al., 2005 [(f)]
Keweenawan *	USA-Canada	1.1 Ga		600 km^3	Zartmann et al., 1996
Snake River Plain	USA	17 Ma[(g)]		2.3×10^5 km^3 [(h)]	Pierce and Morgan, 1992 [(g)], Pierce and Morgan, 2009 [(h)]

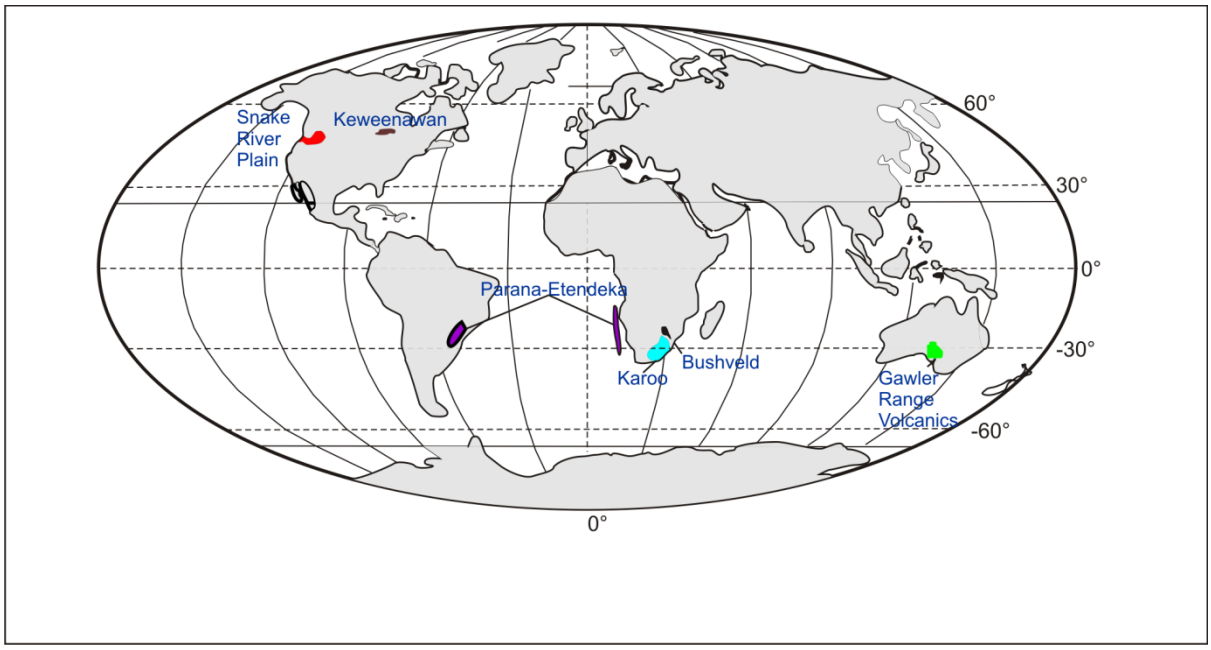

Figure 2: Map showing the Location of other SLIPs around the world.

Aims and objectives

This project aims to describe the detailed petrographic signatures of the different formations within the 2.06 Ga Rooiberg Group sampled at different type localities in South Africa. This study also aims to present detailed analysis of major and trace element composition of the magma that gave rise to these volcanic rocks, as well as their isotopic signatures. Major, trace

and rare earth elements are used to decipher the crystallization history of the Rooiberg Group and evaluate whether these rocks formed from fractional crystallization of magma, magma mixing, crustal contamination, or a combination of two or more of these processes. Modelling is conducted to investigate which of the major processes mentioned above is involved in the evolution of the Rooiberg Group rocks, or possibly propose a new mechanism of evolution.

Field mapping and sampling of the Rooiberg Group volcanics is carried out in three different locations. These locations include the area north-east of Loskop Dam, north of Modimolle (the former Nylstroom), and north-west of Dullstroom (From 2011-2013). The exposed Rooiberg Group was mapped and sampled in these locations. A geological map of each area is produced using the field, petrographic and geochemical characteristics of the rocks sampled. Petrographic descriptions of thin sections are conducted to determine the major mineral phases occurring as the groundmass and phenocrysts, as well as their relative abundances across the different formations of the Rooiberg Group from the different type localities mapped and sampled. Petrography of these rocks is not only used to decipher the origin of these rocks, but also to estimate the degree of alteration undergone by these rocks.

Geochemical analyses conducted in this project include major, trace and rare element analyses as well as isotopic signatures. Major elements differentiate the formations within sampled localities as well as establish the chemostratigraphy of the rocks in the area north of Loskop Dam (area with the highest number of Rooiberg formations). Trace and rare earth elements are used predominantly to decipher the origin of the Rooiberg Group as either mantle-derived melts or crustal sources (assimilation/contamination). Furthermore, some trace elements are used to identify the most likely geotectonic settings of these rocks which are used to support their origin.

Finally, isotope data is used to determine the possible origin of these rocks and the main formational processes of the Rooiberg Group. Processes such as contamination, if any, during the formation of these rocks is evaluated using a modelling program called Petromodeler (Ersoy, 2013).

CHAPTER 2

METHODOLGY

Areas exposing the Rooiberg Group are mapped and sampled. These areas include the Dullstroom, Nylstroom/Modimolle and the area north of Loskop Dam. Lava flows are sampled, based on location and apparent freshness, for petrographic and geochemical analysis. Of the 69 samples collected, one part is used for thin-sections and the remaining, amygdale-free material is used for geochemical analysis. 28 samples representing the Dullstroom Formation are selected, 19 from the Damwal Formation, 16 from the Kwaggasnek Formation and 6 from the Schrikkloof Formation. The lower number of samples of the upper formations is due to the exposures of altered/weathered outcrops. The degree of weathering and quality of the samples used are accounted for based on the calculation of the chemical index of alteration (CIA) according to Nesbitt and Young (1982).

Analysis for major element oxides is carried out by the Stoneman Laboratory technican at the University of Pretoria, using x-ray fluorescence (XRF) according to Loubser and Verryn (2008). Analysis for trace elements (Rb, Ba, Sr, Pb, Th, U, Zr, Hf, Ta, Y, Nb, Sc, Cr, Ni, Co, V, Zn, Cu, S) and REE is conducted using a Thermo Fisher Xseries2 by the AEON EarthLAB of the University of Cape Town (Table 6). The analyses are executed by the dissolution of 50 mg of sample powder in a 4:1 HF/HNO3 acid mixture in sealed Savilex beakers on a hotplate for 48 hours, followed by evaporation to incipient dryness and two treatments of 2 ml of concentrated HNO_3. The final dried product is then taken up in 5% HNO_3 solutions containing 10 ppb Re, Rh, In and Bi as internal standards. Standardisation is against artificial multi-element standards.

Input of major, trace and isotope data into a modelling program, Petromodeller, is executed to model and further assist in identifying the mode evolution of the Rooiberg Group. Ersoy (2013) describes all the formulae utilized in the modeller. Though this modelling program may not be as widely recognised, it can model numerous magmatic processes such as melting, crystallization and mixing, and all results can be displayed on a bivariate graphical diagram similar to the more recognised MELTs (Ghiorso et al., 2002) or PELE (Boudreau, 1999). The Petromodeller has previously and successfully been employed to model the calc-alkaline lamprophyres in Turkey (Karsli et al., 2014) and Kashmar granitoids in Iran (Moghadam et al., 2015), further attesting to the credibility of the program.

Isotope data used in this project include data from Buchanan et al. (2004), Schneiderhan (2007) and Toulkeridis et al. (1998). Estimates of pressure, temperature and water content of the Rooiberg Group are accounted for using the thermobarometry spreadsheet modified after Putirka (2008). Putirka (personal communication, 2014), however, stated that of the three parameters measured, pressure, temperature and water content, only the temperature values are accurate and reliable, due to the fact that the program does not work well for all rock types.

CHAPTER 3

FIELD MAPPING AND TYPE LOCALITIES

This section includes a description of the geological maps of each studied area where the Rooiberg Group rocks is sampled for this study. The map of the Loskop dam area (Fig. 3) shows the Damwal, Kwaggasnek and Schrikkloof formations. The Nylstroom (Modimolle) map (Fig. 4) contains only one of the Rooiberg formations, the Schrikkloof Formation. Similar to the Nylstroom area, the Dullstroom area contains only one formation as well, namely the Dullstroom Formation. However, different lava types are observed within this study area, leading to the map shown in Figure 5.

The methodology for field mapping mainly utilized the field and petrographic characteristics as defined by Lenhardt and Eriksson (2012), e.g. colour, texture, phenocryst content, internal structure and relationship to intercalated sedimentary units, for assigning the various units of the different formations within the Rooiberg Group. These physical properties assisted in subdividing the Rooiberg Group samples into the geological formations in the field before geochemical analyses are obtained. Table 1 shows the major physical characteristics of the different units (according to Twist, 1985) and the unit to which each of the Dullstroom, Damwal, Kwaggasnek or Schrikkloof formations belong (according to Lenhardt and Eriksson, 2012).

3.1. Loskop Dam

The Loskop Dam study area has a size of ca. 40 km^2 and is situated north-east of Loskop Dam, ca. 120 km east of Pretoria (S 25°24’0”, E 29°31’30”), where three of the four formations (Fig. 3) of the Rooiberg Group is encountered in the field. Elevations within the study area range between 1060 m and 1369 m above sea level (a.s.l.). In the Loskop Dam area, the Rooiberg Group attains an estimated thickness of 3,520 m. This thickness increases towards the east to a maximum of 5,110 m (Twist, 1985; Clubley-Armstrong, 1977). Towards the north of the study area, the intrusive rocks of the Rustenburg Layered Suite are exposed. In the southern part of the area, the Damwal Formation crops out, interbedded with meta-sandstones, and overlying ca. 1000 m of granophyre (Rashoop Granophyre Suite) whose intrusion supposedly accompanied the emplacement of the Rooiberg Group lavas (Walraven, 1985). The Damwal Formation is overlain by the Kwaggasnek and Schrikkloof Formations. The Dullstroom Formation is not present in the study area, as the thick sequence

of mafic intrusive rocks extends further northwards and detaches the Dullstroom Formation from the rest of the Rooiberg Group.

The average strike direction of the Rooiberg Group rocks in this area is 270° with all beds dipping towards the south, away from the centre of the Bushveld province. Dips increase from 15-30° in the north to 55-70° in the south.

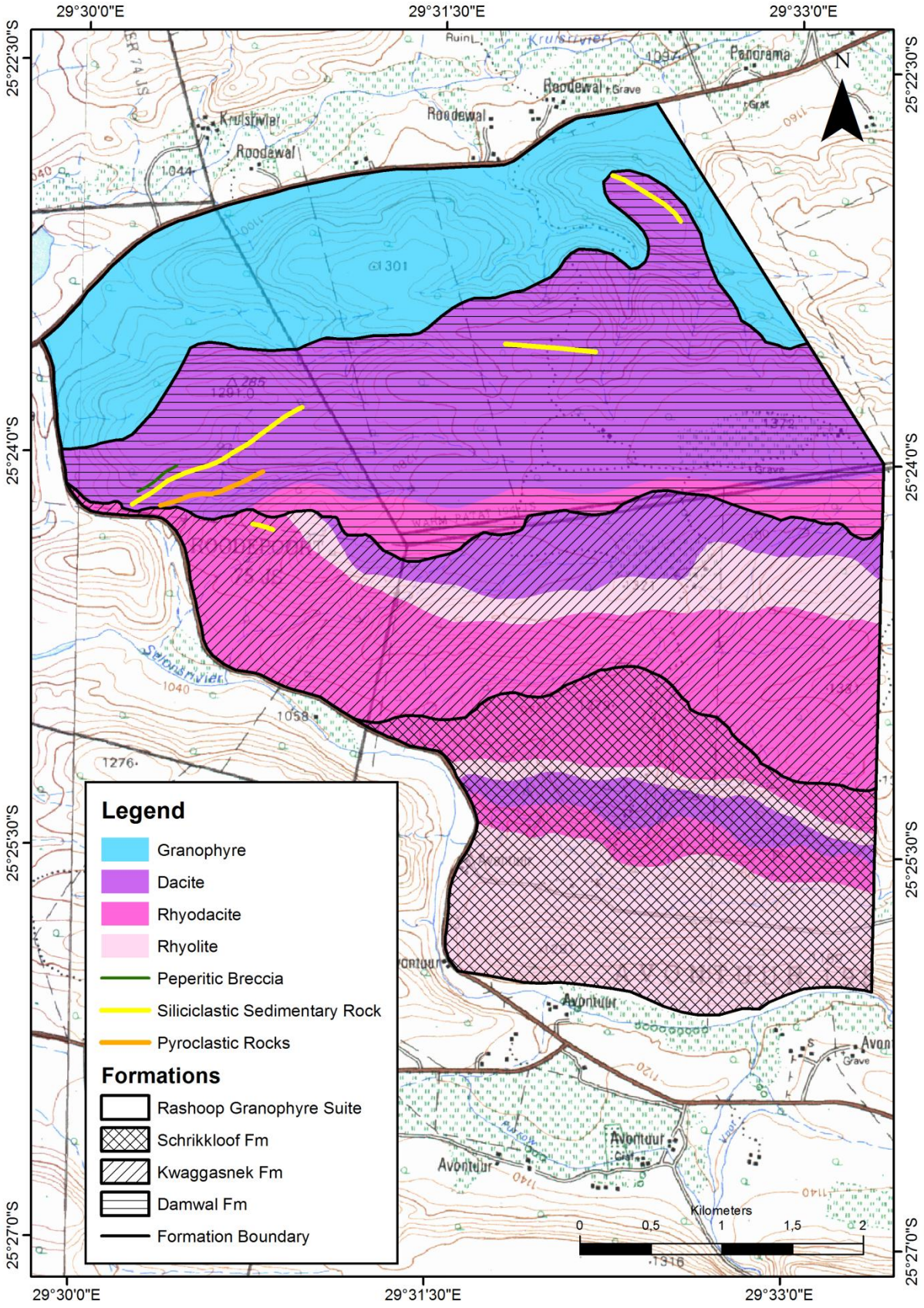

Figure 3a: Geological map of the study area north of Loskop Dam showing the distribution of the Rooiberg Group formations and their major rock types.

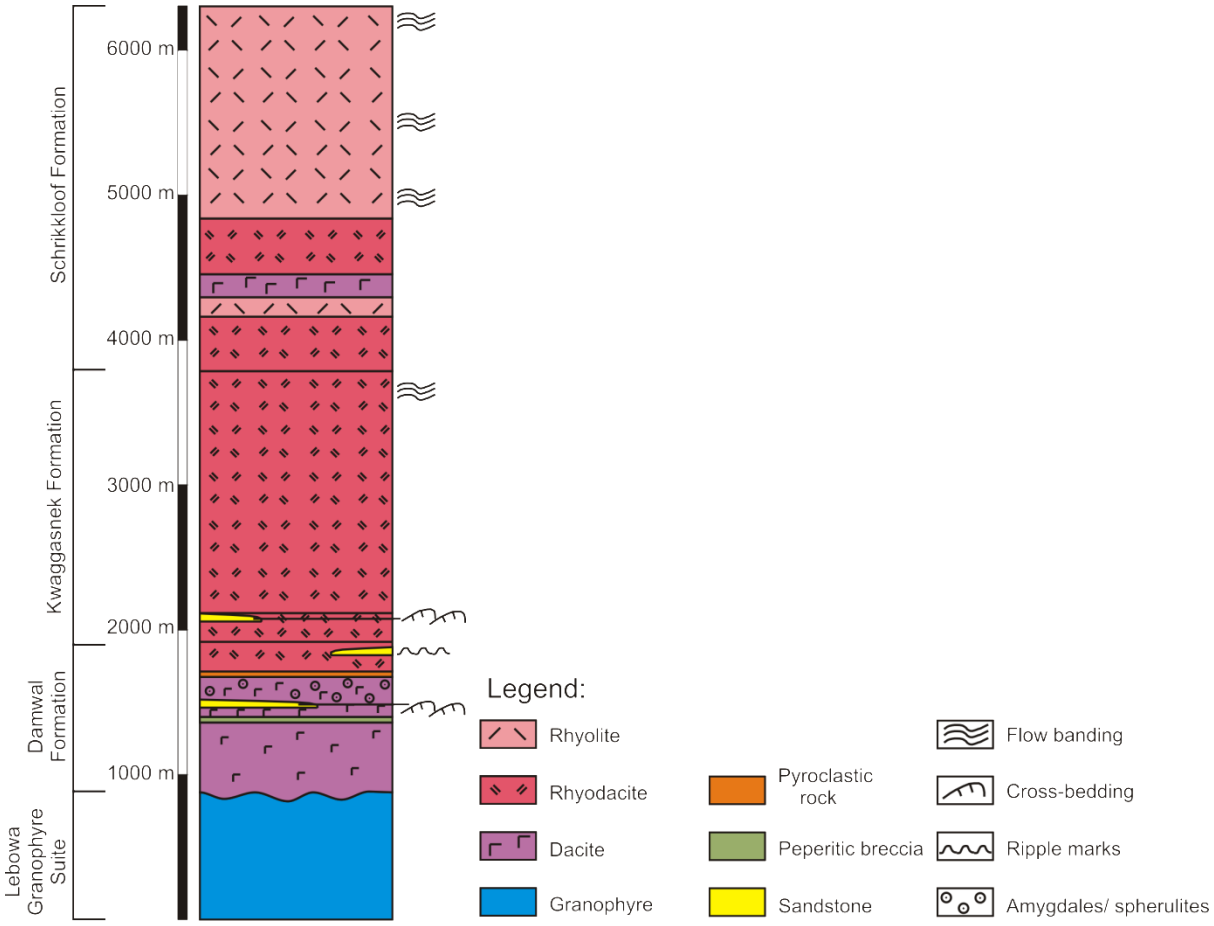

Figure 3b: Stratigraphy of the study area near Loskop Dam showing the rock types in each formation.

3.2. Nylstroom (Modimolle)

The Nylstroom study area north of Nylstroom and ca. 132 km SE of Polokwane, Limpopo Province, South Africa extends from the Khutaba game farm (S 24°36'30", N 28°26'0") north-eastwards into the neighboring farm along Driefontein Road. This study area has an aerial extent of about 37 km^2, exhibiting a topography that ranges from mountainous areas and deep valleys to minor flat lying areas with altitudes ranging from 1312 m to 1565 m a.s.l.. The rocks of this study comprise mainly of red and grey lavas (predominantly rhyolitic in composition) that make up the Schrikkloof Formation (Fig. 4), the only Rooiberg Group formation in this area. During the rainy season, most of the outcrops are covered by vegetation, making mapping and sampling a difficult task. Outcrops are better exposed after

the rainy season, starting from June onwards. The study area is home to wildlife animals such as zebras, wildebeests, kudus and impalas, with leopards being the only major predators of the area.

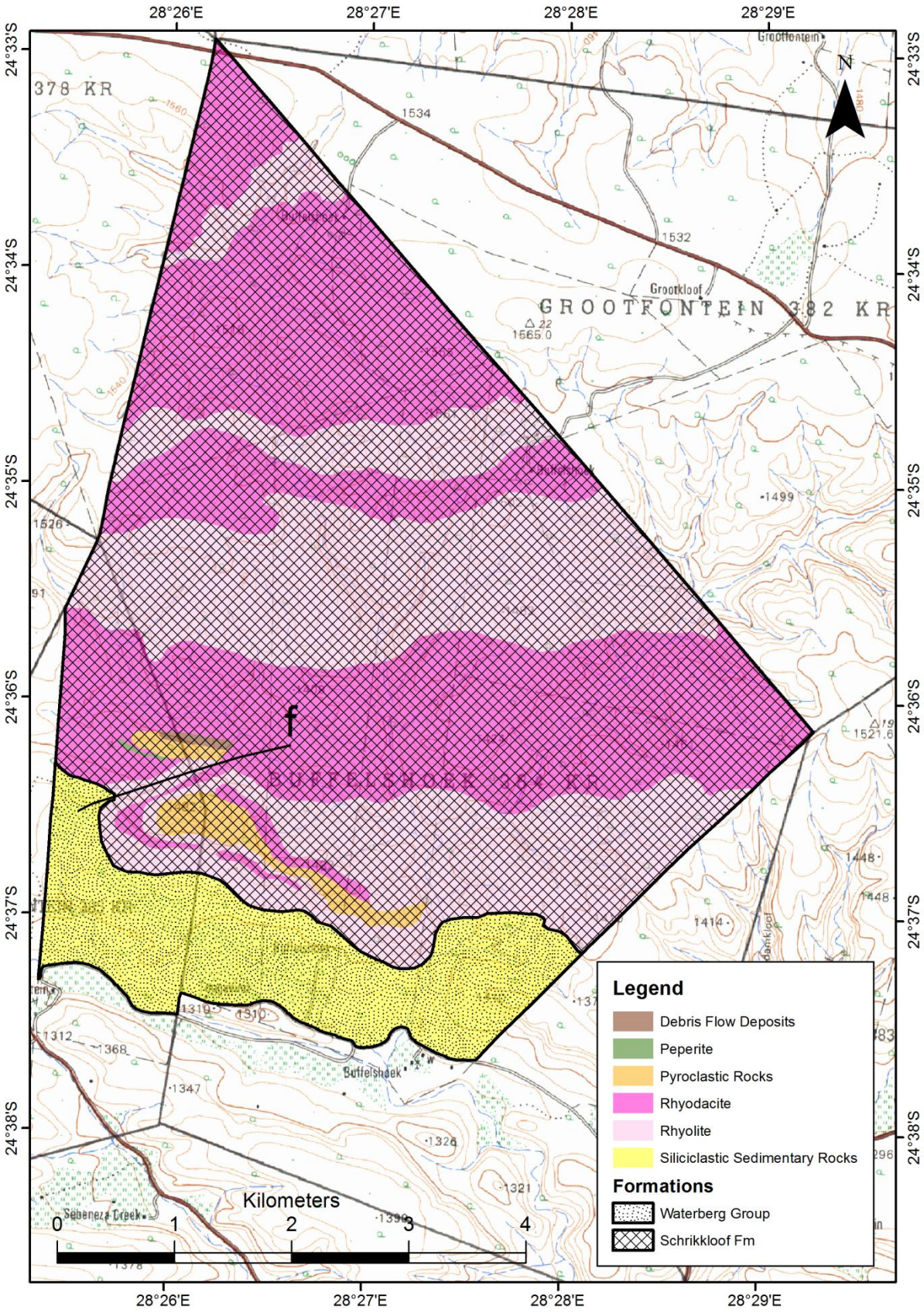

Figure 4a: Geological map of the study area in Nylstroom.

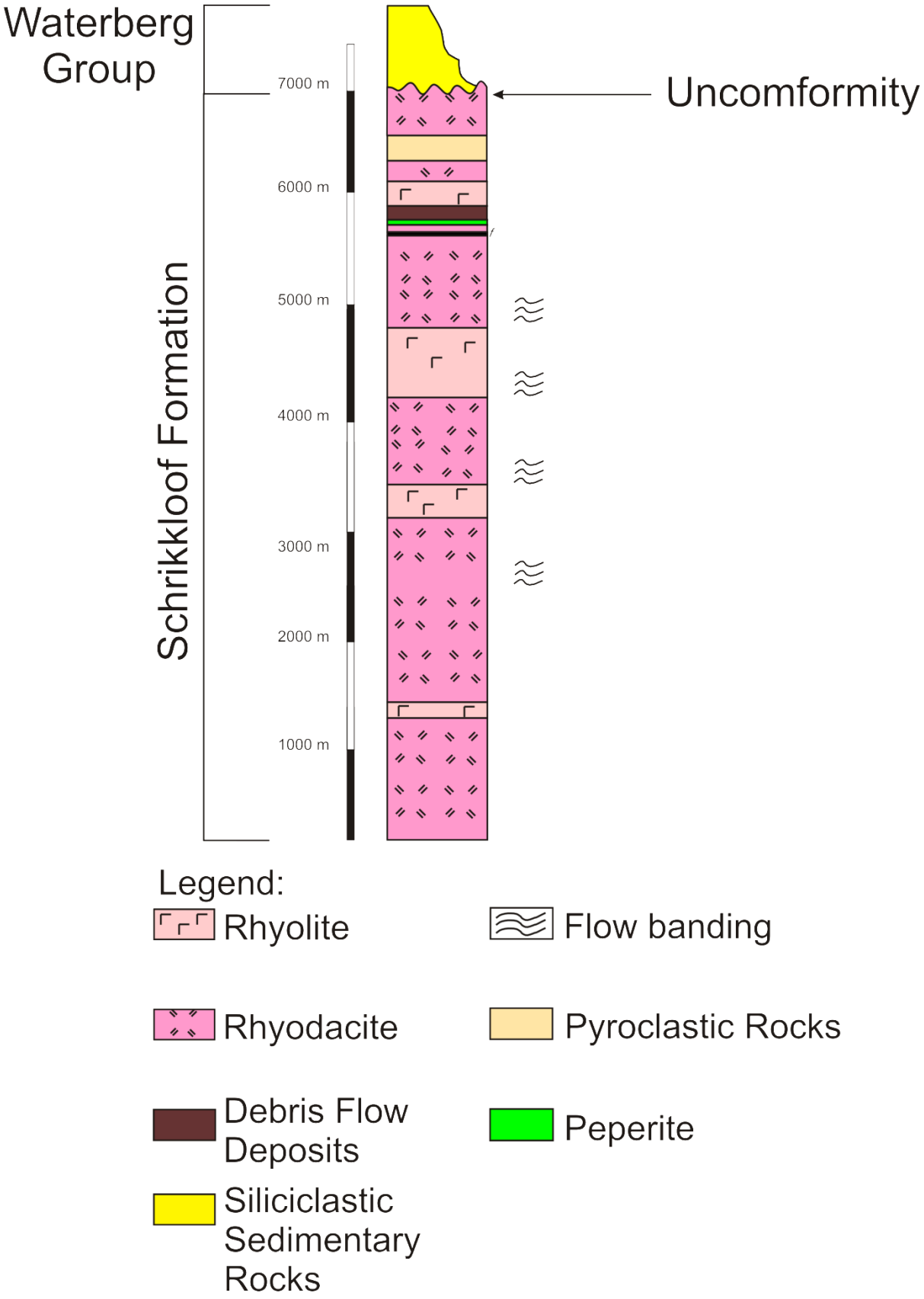

Figure 4b: Stratigraphy of the study area in Nylstroom.

3.3. Dullstroom

This study area is located near Dullstroom (S 25°23'0", E 30°0'0"), 233.5 km northeast of Pretoria. The area has an estimated aerial extent of 52 km^2 and is also fairly mountainous with elevations reaching 2000 m. Ubiquitous in this region is dense dark colored lava (usually grey) with amygdales that represent the Dullstroom Formation. Fresh exposures of the Dullstroom rocks occur not only in the high mountains but also in low-lying areas in some locations, enhancing mapping and sampling of this area.

In the Dullstroom area, neither sedimentary nor pyroclastic units are observed except for the uppermost sandstones of the Pretoria Group as shown in Fig. 5. Also seen in the region is the Rashoop Granophyre Suite of the Bushveld Magmatic Province. Flow-bands are well exhibited by rocks displaying brighter, reddish-brown colours in this area. Alteration in this area (as seen in the field, handsamples and thin-sections) is at a minimum. One cause for these alterations may have been the intrusion of the Rustenburg Layered Suite since the Dullstroom Formation, the basal unit of the Rooiberg Group, sits closest to the intrusion of the Rustenburg Layered Suite. Nevertheless, a clear distinction between alterations caused by an intrusion or other processes (e.g., weathering or metasomatism) is not conducted in this study.

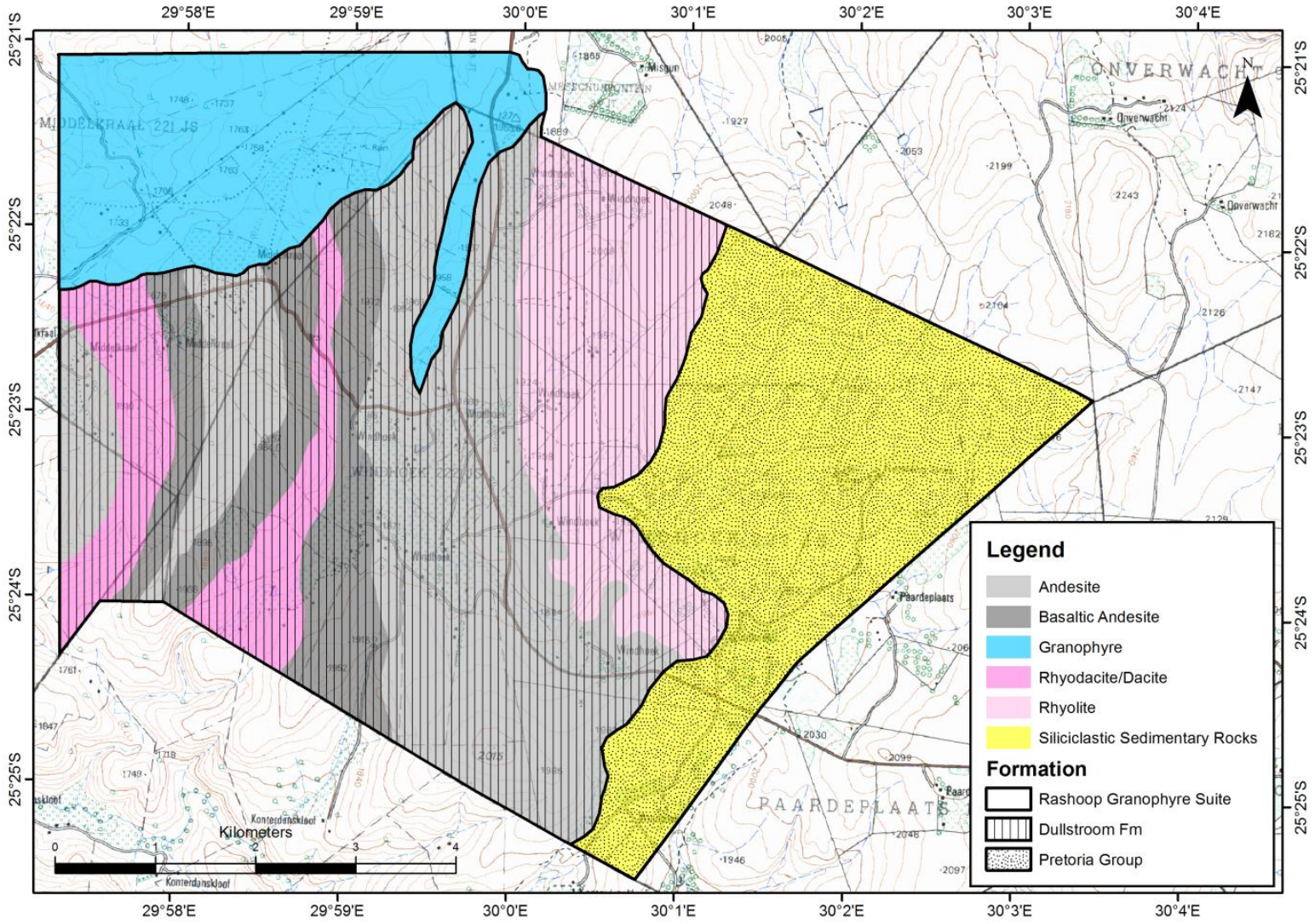

Figure 5a: Geological map of the study area in Dullstroom.

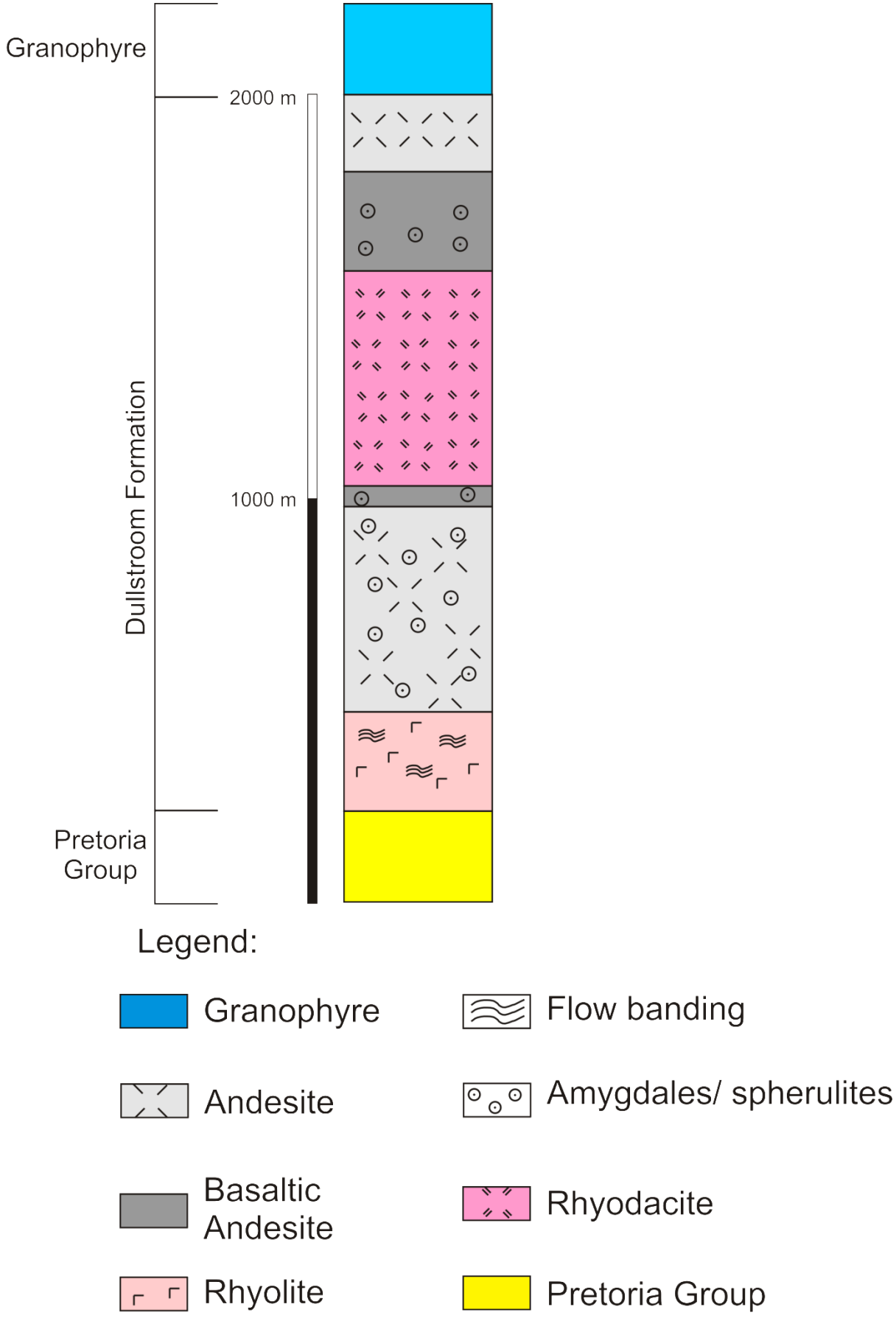

Figure 5b: Stratigraphy of the study area in Dullstroom.

CHAPTER 4

LITHOLOGY AND PETROGRAPHY

4.1 Thin-section description

The total phenocryst content of the Rooiberg Group lava samples is usually <10 vol.%. The phenocrysts are variable in size and predominantly comprise of k-feldspar and plagioclase. Noteworthy is the change in colour of the rocks from predominantly dark-grey rocks in the more mafic Dullstroom Formation to bright red rhyolitic (usually termed low-Mg lava type in this section) rocks in the Schrikkloof Formation. Table 3 shows a summary of the petrographic descriptions.

4.1.1 Dullstroom Formation

Within the Dullstroom area, the Dullstroom Formation consists of a variety of dense lava flows, and no siliciclastic or volcaniclastic rocks are observed in this study. Lava types identified in the Dullstroom Formation in this study include the basal rhyolite, high-Mg felsite and basaltic andesite. The basaltic andesite, high-Mg and basal rhyolite lava samples of the Dullstroom Formation are holocrystalline (Fig 6a). The basal rhyolite exhibit prominent flow-banding in areas where occurring while amygdales (usually filled with quartz), that can be up to 1 cm in diameter, are observed in some basaltic andesite (such as RG 54) and high-Mg lava types (such as RG 13). Phenocrysts in all lava types are usually plagioclase and K-feldspar, occurring as <5 vol.% of the entire sample. The phenocrysts in these rocks are subhedral to anhedral feldspar (ranging from albite to anorthite, with the former less abundant than the latter). Amphibole (± chlorite) is also observed especially in the basaltic andesite lava types such as RG 54, appearing as a secondary mineral formed from mafic minerals such as pyroxene or clay minerals. Other evidence for alteration is exhibited by the presence of clay minerals such as illite. Biotite (about 2 vol.%) as well as quartz (usually <5 vol.%) occurs in minor abundance in all lava types, with quartz occurring along the rims of some of the amygdales. The holocrystalline groundmass consists mainly of albite and anorthite with the former more abundant (about 40 vol.%), minor amounts of quartz (usually <10 vol.% although few samples show high abundance of up to 40 vol.%) and some Fe-Ti-rich minerals (usually <5 vol.%) such as ilmenite (occurring as an alteration product) and some titanomagnetite.

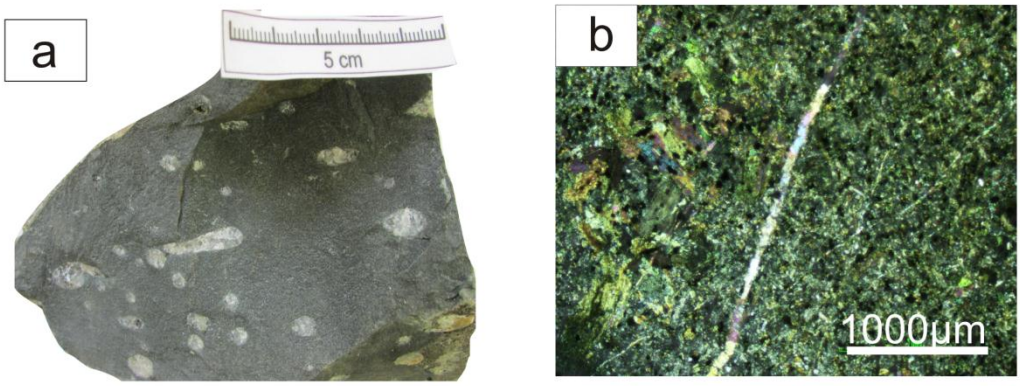

Figure 6: (a) Microcrystalline texture with some amygdales (up to 3cm in diameter) of the Dullstroom Formation (RG 54); the photomicrograph (b) shows groundmass composed mainly of feldspar altering to chlorite

4.1.2 Damwal Formation

Within the Loskop Dam area, the Damwal Formation consists mainly of lava flows with minor units of pyroclastic and siliciclastic origin. All lavas are mainly low-Mg type, appearing as dense and massive but do not exhibit brecciated material that could resemble a carapace. All analyzed samples of the lavas have a microcrystalline texture (SM 45.1, Fig. 7a). Locally, flow-banding and spherulitic textures can be observed. The total phenocryst content is <5 vol.%. Plagioclase is the most abundant phase with subordinate quartz and minor K-feldspar. Accessory phases consist of hornblende, chlorite, ±muscovite, opaque Fe (±Ti)-rich minerals (magnetite and ilmenite, usually subhedral-euhedral) and some clay minerals. The Plagioclase phenocrysts (~0.1-0.5 µm) are subhedral to euhedral, showing no apparent zonation and poor (in some cases none) twining which may be as a result of mobility of some elements such as Na and K or alteration of the minerals (Li et al., 2013). Quartz phenocrysts are subhedral and mostly <0.5 µm in size. In a few samples such as SM 3, SM 41 and SM 51, plagioclase and K-feldspar (mostly 0.3-0.5 µm in size) are altered to muscovite; hornblende is altered to chlorite. Clay minerals such as illite and sericite are further evidence for alteration.

The groundmass exhibits a microcrystalline texture and mainly contains plagioclase, quartz and some minor amounts of K-feldspar. Spherulites that are up to 3 cm in diameter in sample SM 3 are composed mainly of K-feldspar and make up about 5 vol.% of the sample. Vesicles

can form up to 2-3 vol.% of the rocks and are usually <3 cm in diameter. Some of the vesicles filled with secondary minerals such as quartz and chlorite, form amygdales.

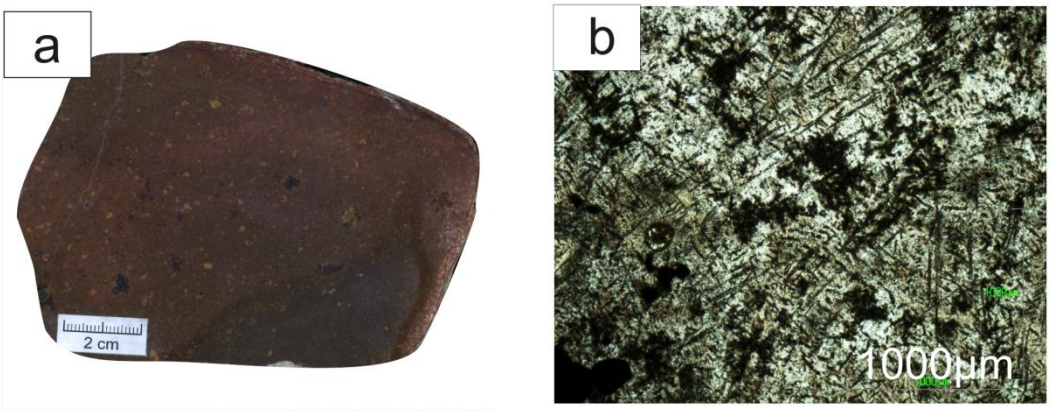

Figure 7: (a) Microcrystalline texture with phenocrysts (<0.5µm) lava of the Damwal formation (SM 45.1); the photomicrograph (b) shows groundmass composed mainly of feldspar altering to chlorite

4.1.3 Kwaggasnek Formation

The Kwaggasnek Formation within the Loskop Dam consists of dense and massive lava flows composed of the low-Mg lava type. These rocks lack any brecciated material but are intercalated by some minor pyroclastic rocks. The pyroclastic rocks (e.g., SM 37) are represented by a massive, matrix-supported tuff, rich in crystals such as quartz, plagioclase, K-feldspar, some secondary sericite replacing K-feldspar and minor Fe-rich minerals.

The lava samples of this formation have a microcrystalline groundmass, exhibiting flow-banding and locally spherulitic textures. Especially the flow-banding, together with an increase in vesicles (~20 vol.%), is more prominent here than in the underlying Damwal Formation. The total phenocryst content ranges from 2-5 vol.%. The most abundant phenocrysts are plagioclase and quartz with hornblende and chlorite (±muscovite) occurring as accessory phases. The plagioclase phenocrysts (~0.5 µm) are euhedral to subhedral. Quartz phenocrysts (<0.5 µm) are subhedral and more abundant here than in the underlying Damwal Formation.

In samples SM 14 and SM 48, plagioclase and K-feldspar are observed to have been altered to clay minerals.

The groundmass shows a microcrystalline texture, comprised of quartz and plagioclase. Some of the vesicles (≤3 cm in diameter) contain secondary minerals such as quartz and chlorite. SM 14 also contains spherulites (up to 3 cm), which are mostly made up of K-feldspar (Fig. 8a). The majority of the spherulites have developed into lithophysae.

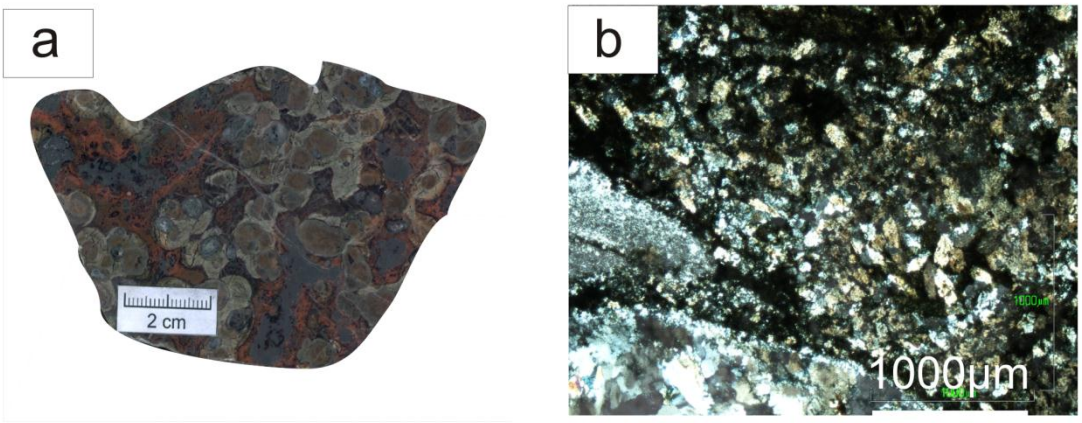

Figure 8: (a) Microcrystalline texture exposing lithophysae (up to 3cm) lava of the Kwaggasnek Formation (SM 14); photomicrograph (b) showing the groundmass composed mainly of quartz and feldspar (indication of silicification compared to (6a)) and infilling of veins with quartz.

4.1.4 Schrikkloof Formation

The Schrikkloof Formation, in the Loskop Dam and Nylstroom areas, exhibit similarities in physical and optical properties. Both localities consist of dense lava flows, exhibiting major flow-bands and composed of a microcrystalline to cryptocrystalline matrix as shown in Fig. 9a, SM 19) and typical of the low-Mg lava types. Although no pyroclastic layer occurs in the Schrikkloof Formation within the Loskop Dam, a small layer is observed in Nylstroom. The lava samples of this formation contain lesser amounts of phenocrysts (<3 vol.%) than the older Rooiberg Group formations. The majority of the samples are microcrystalline, containing up to 3 vol.% volcanic glass with very few vesicles where present. Flow-banding is more pronounced here than in the Kwaggasnek and Damwal formations. Phenocrysts are mainly quartz (<0.1 µm), minor plagioclase (up to 5 mm) and K-feldspar (3-5 mm) with a

groundmass containing mainly quartz and feldspars. Secondary minerals and signs of alteration are more visible and pronounced in these rocks as compared to the Damwal and Kwaggasnek formations.

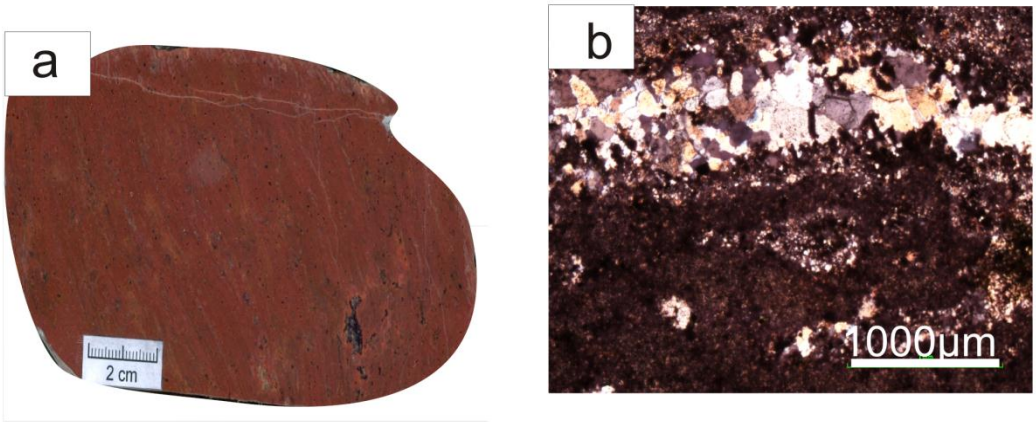

Figure 9: (a) Microcrystalline texture of the Schrikkloof Formation (SM 19); photomicrograph (b) showing quartz dominating micro-cryptocrystalline groundmass and quartz vein containing a lesser amount of feldspar.

Table 3: Petrographic description and rock type classification of the upper part of Rooiberg Group. The preparation of the Dullstroom samples are incomplete at this stage and will be presented in future studies.

Sample No.	***Coordinates***	***Formation***	***Unit after Twist***	***Rock type***	***Groundmass/matrix***	***Phenocryst/Crystals***	***Major mineral phases***	***Flow deformation/other***
SM 23	S 25°25'17,8" E 29°31'39,0"	Damwal	9	Dacitic	microcrystalline, very few vesicles	Moderately abundant, 1-5mm	Pyroxene inclusion, K-feldspar, quartz	-
SM 25	S 25°25'16,1" E 29°31'37,5"	Schrikkloof	7	Rhyolitic	microcrystalline	Highly abundant, ≥5mm	Phenocryst – smoky quartz, K-feldspar, quartz	-
SM 28.2	S 25°25'07,0" E 29°31'32,1"	Schrikkloof	7	Rhyolitic	Microcrystalline and containing some volcanic glass	Highly abundant, ≥5mm	K-feldspar, pyroxene, quartz	-
SM 38.1	S 25°24'10,7" E 29°30'27,8"	Damwal	5	Dacitic	Microcrystalline and highly vesicular	Highly abundant, medium size (1-5mm)	Fractured, olivine, feldspar, pyroxene	Flow banded, filling of vesicles
SM 44.1	S 25°24'14,7" E 29°30'28,7"	Damwal	4	Dacitic	Microcrystalline	Highly abundant, smaller sizes (≤1mm)	Fractured, quartz, plagioclase and pyroxene	-
SM 45.1	S 25°24'13,8" E 29°30'31,5"	Damwal	4	Dacitic	Microcrystalline with few vesicles	Highly abundant (≥5mm)	Thin olivine veins, pyroxene, K-feldspar	Olivine filling vesicles
SM 48	S 25°24'14,6"	Kwaggassnek	7	Rhyolitic	Very fine-grained	Moderate abundance	K-feldspar,	-

Sample No.	*Coordinates*	*Formation*	*Unit after Twist*	*Rock type*	*Groundmass/matrix*	*Phenocryst/Crystals*	*Major mineral phases*	*Flow deformation/other*
	E 29°30’42,3”					(1-5mm)	pyroxene, plagioclase, quartz	
SM 50	S 25°24’13,7” E 29°30’48,4”	Damwal	-	Rhyolitic	Very fine-grained	Moderate abundance (1-5mm)	K-feldspar, quartz, pyroxene	-
SM 51.1	S 25°24’12,0” E 29°30’53,0”	Damwal	1	Rhyolitic	Very fine-grained	Highly abundant (1-5mm)	K-feldspar, quartz, pyroxene	-
SM 4.1	S 25°24’13,1” E 29°30’06,7”	Kwaggassnek	5		Very fine-grained	Highly abundant, medium size (1-5mm)	Quartz, K-feldspar and pyroxene	-
SM RL 1	S 25°23’44,0” E 29°30’30,5”	Damwal	1	Dacitic	Very fine-grained	Highly abundant, smaller size (≤1mm)	K-feldspar, pyroxene	-
SM 3	S 25°24’13,1” E 29°30’06,7”	Damwal	2	Trachydacitic	Very fine-grained	Highly abundant, medium size (1-5mm)	Quartz, K-feldspar and pyroxene	-
SM 5.1	S 25°24’12,4” E 29°30’12,0”	Damwal	-	Dacitic	Microcrystalline	Highly abundant, smaller size (≤1mm)	Quartz, K-feldspar (plagioclase)	-
SM 5.2	S 25°24’12,4” E 29°30’12,0”	Schrikkloof	6	Rhyolitc	Very fine-grained	Moderate abundance, medium size (1-5mm)	Pyroxene, K-feldspar, quartz	-
SM 6	S 25°24’13,0” E 29°30’13,9”	Damwal	3	Dacitic	Very fine-grained	Moderate abundance,	Pyroxene, quartz, K-	-

Sample No.	*Coordinates*	*Formation*	*Unit after Twist*	*Rock type*	*Groundmass/matrix*	*Phenocryst/Crystals*	*Major mineral phases*	*Flow deformation/other*
						medium size (1-5mm)	feldspar	
SM 10	S 25°24’20,7” E 29°30’25,6”	Damwal	7	Rhyolitic	Very fine-grained	Moderate abundance, medium size (1-5mm	K-feldspar, quartz, olivine (veins), pyroxene	Contains some pyroclastic rocks
SM 13	S 25°24’50,8” E 29°30’37,1”	Damwal	2	Rhyolitic	Highly altered, patchy rocks	Highly altered, patchy rocks	Quartz, pyroxene and plagioclase	Flow banded
SM 14	S 25°24’48,8” E 29°30’39,0”	Damwal	1	Dacitic	Very fine-grained, spherulitic with some volcanic glass	Highly altered, patchy rocks	Quartz, K-feldspar, pyroxene	
SM 17	S 25°24’53,8” E 29°30’58,6”	Damwal	4	Dacitic	Very fine-grained, with few vesicles and spherulitic	Highly abundant, medium size (1-5mm)	Pyroxene, K-feldspar, quartz	
SM 18.1	S 25°26’00,0” E 29°31’44,8”	Schrikkloof	9	Rhyolitic	Microcrystalline, few vesicles	Moderate abundance, small sizes (≤1mm)	K-feldspar, quartz, pyroxene	Flow banded
SM 19	S 25°25’59,3” E 29°31’43,8”	Schrikkloof	9	Rhyolitic	Microcrystalline, with very few vesicles	Highly abundant, small size (≤1mm)	Fractures, olivine, pyroxene, K-feldspar	Flow banded
SM 22	S 25°25’19,7” E 29°31’39,8”	Schrikkloof	9	Rhyolitic	Very fine-grained, with some vesicles	Moderate abundance, medium size (1-5mm)	Olivine, quartz, plagioclase	-

Sample No.	*Coordinates*	*Formation*	*Unit after Twist*	*Rock type*	*Groundmass/matrix*	*Phenocryst/Crystals*	*Major mineral phases*	*Flow deformation/other*
SM 40	S 25°23’37.3’’ E 29°59’57.8’’	Dullstroom	1	Andesite	Fine-grained grey lava	Amphibole, quartz and feldspar (k-feldspar and anorthite) phenocrysts	Quartz, amphibole, feldspar	-
RG 10	S 25°23’00.9’’ E 29°58’48.4’’	Dullstroom	2	Basalt	Fine grained grey lava	Plagioclase, K-feldspar	K-feldspar, quartz, pyroxene	Amygdales (2mm-64mm)
RG 54	S 25°23’57.9’’ E 30°00’23.8’’	Dullstroom	2	Andesite	Fine grained green-grey lava	-	Quartz, amphibole, feldspar (k-feldspar) and chlorite	Spherical quartz amygdales (~6mm). Some amygdales have black-brown minerals Amoebal shaped amygdales (3mm) are filled with amphibole which forms the core and has a fine-grained quartz rim.

4.2 Interpretation of petrography and field descriptions

The different rock types of the Rooiberg Group typically display a fine-grained, aphanitic matrix. The fine-grained matrix is usually composed of microcrystalline quartz and feldspar, occurring throughout the Rooiberg formations but is more pronounced in the Damwal, Kwaggasnek and Schrikkloof formations. The microcrystalline nature of most of the rocks used in this study represent quench textures that result from rapid cooling. This is typical of volcanic rocks, although devitrification of original glassy products occurs, as is seen by the presence of spherulites. However, contrary to the microcrystalline nature of the growth of quartz and feldspar, the opaque minerals are subhedral-euhedral and comparatively larger. Semi-quantitative analysis suggests that the opaque minerals are likely to be Fe-Ti-rich minerals. Vesicles in the Dullstroom Formation are filled with secondary minerals such as quartz which suggests a lower viscosity when compared to the Damwal, Kwaggasnek and Schrikkloof lavas. The absence of empty vesicles in the Dullstroom Formation possibly indicates absence of trapped gasses during the initial stages of Rooiberg magmatism. This suggests that a less viscous magma generated the Dullstroom Formation while a more viscous magma generated the Damwal, Kwaggasnek and Schrikkloof formations (Hurwitz and Navon, 1998)

The greater occurrence of vesicles in the upper part of the Rooiberg Group, i.e. the Damwal, Kwaggasnek and Schrikkloof formations than in the Dullstroom Formation therefore indicates a more pronounced presence of gases in this region which suggest a possible increase in the eruption pressure (pressure of overlying magma) from the bottom to the top within the Rooiberg stratigraphy. Also supporting high viscosity in the Damwal, Kwaggasnek and Schrikkloof formations is the occurrence of flow-banding in the upper part of the Rooiberg Group. Flow-banding, which results from the friction between a phenocryst-bearing, flowing magma (composition and texture) and a solid rock interface (wallrock) (Morris, 1992), is most visible in the Schrikkloof Formation. Higher amount of visible flow-bands in the upper part of the Rooiberg Group implies that the viscosity increases from the base upward within stratigraphy.

Minor and thin layers of pyroclastic rocks suggest that (minor) explosions occurred during the emplacement of the Rooiberg Group in the Loskop Dam area. A few thick layers of pyroclastic rocks are also observed in areas such as Modimolle, which suggests that explosive eruptions were also present and alternated with effusive eruptions (as also interpreted by

Lenhardt and Eriksson, 2012). Other volcanic provinces that exhibit thick layers of pyroclastics such as the Snake River Plain are more explosive (Andrews et al., 2008). It, therefore, suggests that during the formation of the Rooiberg Group there was a rapid accumulation of a protective cover of either reworked or additional primary volcanic material that resulted in the localized thin layers of pyroclastic fall deposits. The occurence of peperites in the Loskop Dam area show that Rooiberg Group in the Loskop Dam area experienced minor explosive eruption due to contact with wet sediments. The presence of sedimentary interbeds also suggest that during the volcanic eruption of the Rooiberg Group, there were periods of quiescence or very little activity which led to the deposition of sediments. These sediments are transported along streams, which when in contact with lava can result in peperites as observed in this study (Lenhardt and Eriksson, 2012). The minor amounts of both pyroclastic and sedimentary interbeds in the area of study further suggest that there were short periods of quiescence.

The occurrences of secondary minerals in igneous rocks are usually the results of two processes. First is the alteration of pre-existing mineral assemblages and secondly through metamorphism. In the Rooiberg Group, there are secondary minerals present in relative abundance (~40%), and as such could either be due to alteration processes such as weathering or metamorphism (if close to a heat source such as an intrusion). However, secondary minerals (including those filling vesicles to form amygdales) are observed to increase upward through the Rooiberg stratigraphy from the Dullstroom Formation to the Schrikkloof Formation. Secondary minerals such as chlorite in the lower parts of the Rooiberg Group, the Dullstroom and lower Damwal formations, are suggested to be mainly due to the proximity of these regions to the intrusion of the Rustenburg Layered Suite. Low levels of alteration in the Dullstroom Formation are further supported by the relatively low abundance of secondary minerals when compared to the upper parts of the Rooiberg Group. Since the Rustenburg Layered Suite intruded the Rooiberg within the Dullstroom Formation, the high amount of secondary minerals in the upper Damwal, Kwaggasnek and Schrikkloof formations is attributed mainly to alteration processes such as weathering and hydrothermal activities.

CHAPTER 5

GEOCHEMISTRY

This chapter focuses on describing the major and trace element signatures of the Rooiberg Group as well as on the identification, characterization and interpretation of the different formations within this volcanic succession. Emphasis was put on rock samples from the Loskop Dam as well as the Modimolle area. Until the time of submission, no trace element data were available for the Dullstroom area, which is the reason why the Dullstroom Formation is excluded in most of the descriptions. Nevertheless, these data will be included in future studies.

The identification of different formations within the Rooiberg Group was done by means of chemostratigraphy using major and trace element characteristics. Furthermore, a comparison of isotope signatures of the Rooiberg Group with the surrounding rocks such as the Rustenburg Layered Suite and rocks of the Kaapvaal Craton was carried out in order to to find out more about the source of the Rooiberg volcanics. The petrographic investigations of Chapter 4 reveal that most samples have been subjected to varying (but minor) degrees of alteration, which is also evident from their LOI (loss on ignition) values, ranging from 0.84 to 4.93 wt.% (average of 1.93 wt.%). The effect of weathering can further be estimated by using Gresen's (1967) equation (2Ca+Na+K)/Al vs K/Al. Figure 10 shows that most of the samples have undergoneminor alteration. This result is similar to that of the volcanics of the Taupo Volcanic Zone (Warren et al., 2007). As shown in the result, the closer the samples plot to the 1.0 and 1.1 lines, the less altered (fresher) the samples are. The Rooiberg Group, as shown in Fig. 10, plot close to the line (line 1.0 and 1.1, representing a range of feldspar compositions and biotite) and have therefore undergone minor alteration. However, the Rooiberg rhyolites exhibit more probable potassium mobility than in the Taupo volcanics as the Rooiberg samples plot closer to the K-feldpar (K-feldspar and biotite) phase and having a slightly higher K/Al than rocks of the Taupo Volcanic Zone. It is therefore suggested that the samples closest to the line 1.0 and 1.1 and within the dotted ellipsoid are most probably least altered. Noteworthy is the occurrence of Schrikkloof samples further away from the ellipsoid. This supports the suggestion of more alteration occurring in the Schrikkloof Formation, which could be observed in thin sections. Due to the mobility of potassium in the feldspars, the equation of Nesbitt and Young (1982)- Al_2O_3 / (Al_2O_3 + CaO + Na_2O + K_2O) x100 termed the chemical index of alteration (CIA), was further used to decipher the degree of

alteration, as the CIA measures the extent to which feldspars have been altered to aluminous clays.

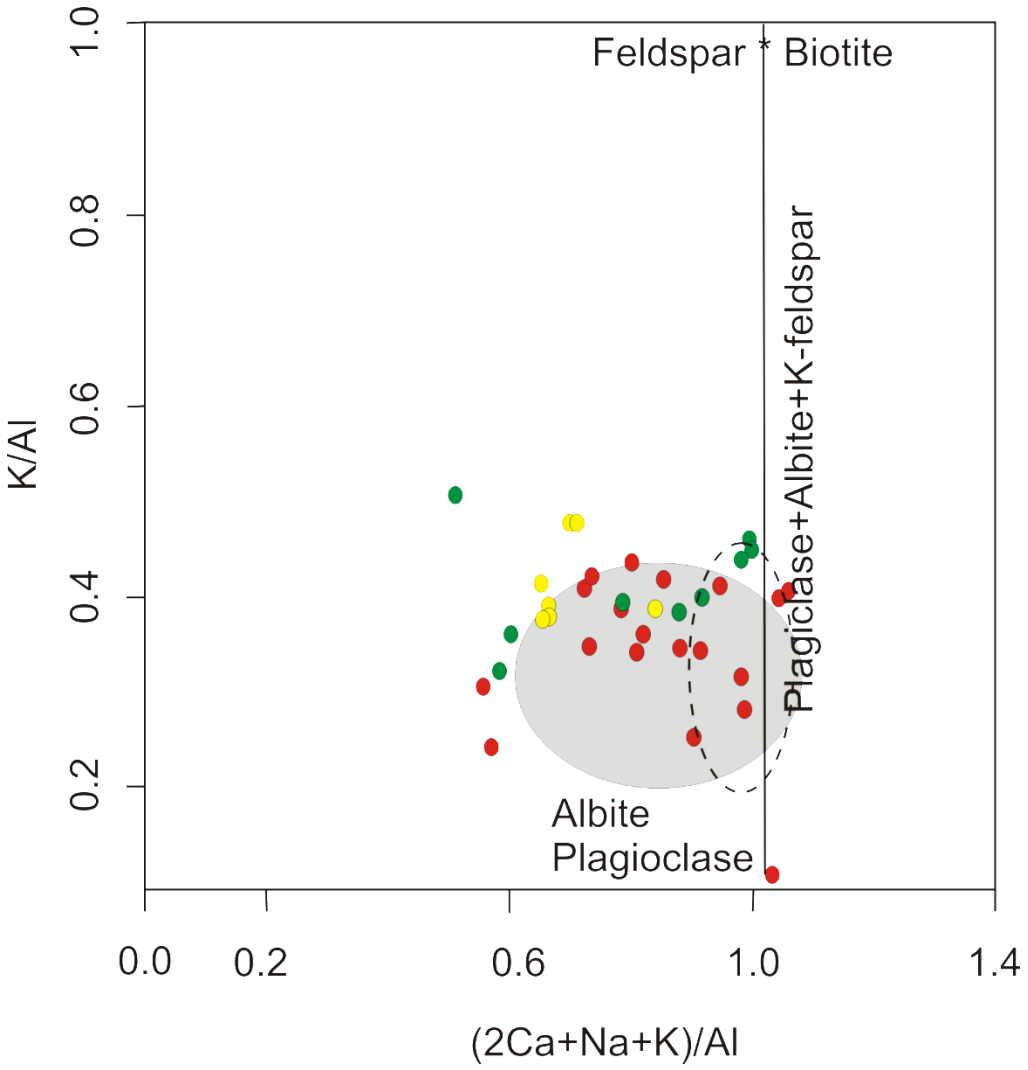

Figure 10: Comparison between the volcanics of the Rooiberg Group and the Taupo Volcanic Zone (shaded grey area), showing the degree of alteration. The dotted elipsoid represent the region of samples that are probably least affected by alteration. Yellow dots- Schrikkloof samples; Green circles- Kwaggasnek samples; Red circles- Damwal samples.

The chemical index of alteration (CIA; Nesbitt and Young, 1982) for the samples used in this study ranges between 52 and 64. High CIA values (value ≥90) due to the removal of alkali or alkali earth elements indicate intense chemical weathering. Unaltered basaltic rocks usually have CIA values between 30 and 45. Illite and montmorillonite have CIA values that range

between 75 and 85, indicating a more intense weathering. However, kaolinite and chlorite show the highest CIA values close to 100. The CIA values for the Rooiberg Group lava samples, therefore, indicate that the lavas have undergone minor alteration, with chlorite, sericite and muscovite as the main alteration products and, thus, proving the credibility of these samples. The lavas of the Rooiberg Group near Loskop Dam are predominantly silicic in composition. The silicic composition is reflected by the varying compositions from rhyolite and rhyodacite to dacite (Fig. 11). It should be noted that the fields in the classification scheme does not indicate the exact composition of the Rooiberg Group but suggests the most probable composition of these rocks, as a result classification is conducted with utmost caution.. The Rooiberg samples constitute low Mg (MgO) content with Mg# ranging from 0.003 to 0.128 (Table 4).

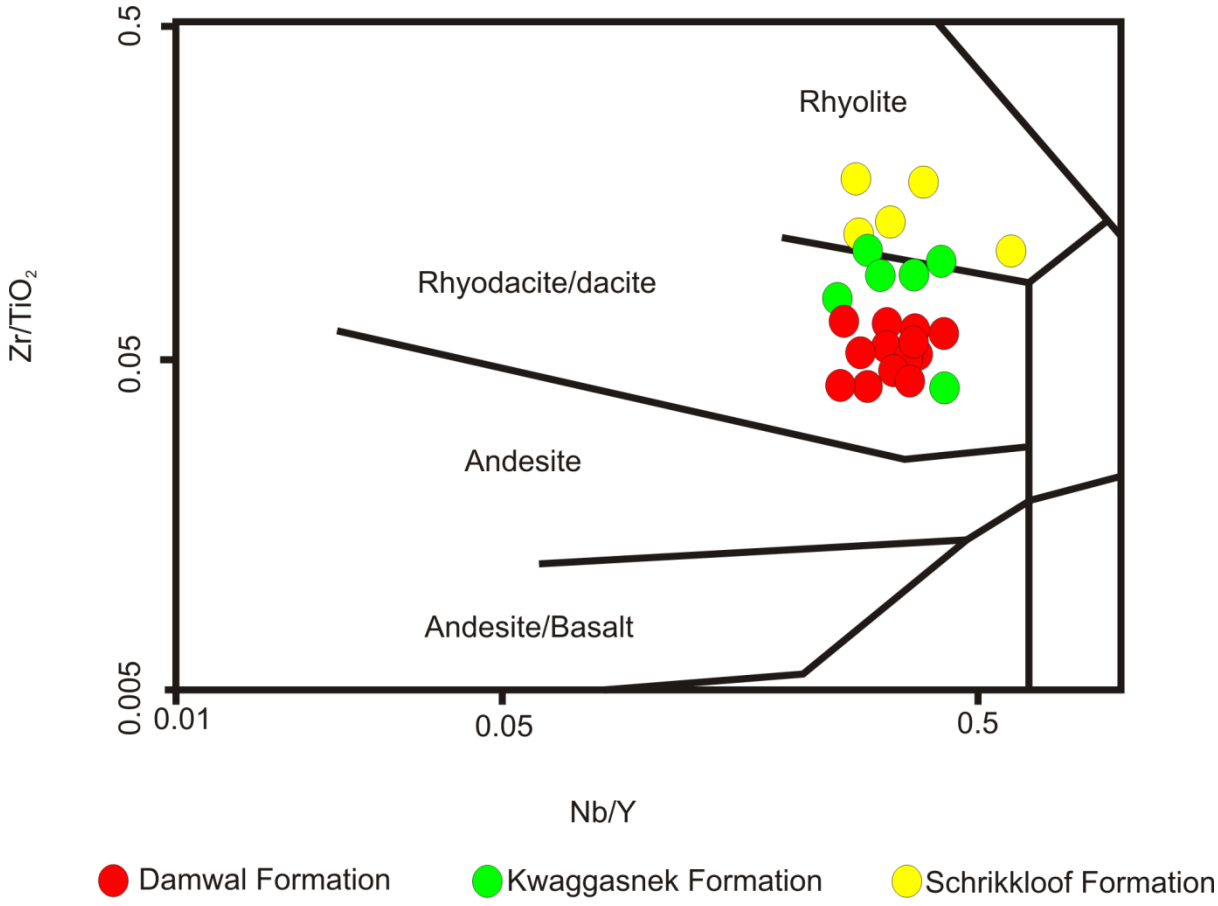

Figure 11: Geochemical classification of the Upper Rooiberg Group volcanic rocks in the Loskop Dam area (compositional boundaries according to Winchester and Floyd, 1977).

5.1 MAJOR ELEMENT CHEMOSTRATIGRAPHY

Major element oxide compositional analysis (Table 4) was employed to describe the chemostratigraphy of the Rooiberg Group (established for the area north of Loskop Dam due to the good exposure of the Damwal, Kwaggasnek and Schrikkloof formations within this area). Geochemical composition is used to distinguish the three main formations of the Rooiberg Group in the Loskop Dam area. Geochemical properties such as major element oxides and ratios, and trace elements were used to establish a chemostratigraphy for this area (following the suggestion of Schweitzer et al., 1995, and Schweitzer and Hatton, 1995): TiO_2, SiO_2, TiO_2/SiO_2, Na_2O, K_2O, P_2O_2, MgO, Fe_2O_3, and Lu. Figure 12 shows a clear decrease in Ti-content up-section (0.64-0.21 wt.%) for the Rooiberg Group rocks within the study area from the Damwal to the Schrikkloof Formation. However, distinction between the rhyolites of the Dullstroom Formation and those of the Damwal, Kwaggasnek and Schrikkloof formations is almost imposible. This implies that the basal and more mafic magma of the Dullstroom Formation (the high-magnesium felsite, low-Ti basaltic andesite, high-Ti basalt and high-Fe-Ti-P lava types described by Schweitzer et al., 1995) can be easily differentiated from the typical low-magnesuim felsites/rhyolites of the Damwal, Kwaggasnek and Schrikkloof formations. On the other hand, SiO_2, also a major constituent of these rocks, shows an increase up-section (66.07-77.08 wt.%). The TiO_2/SiO_2 ratio shows a decrease from the base to the top of the stratigraphic section. Na_2O and K_2O only show a slight decreasing trend in the Damwal Formation but otherwise exhibit a relatively random distribution. The random distribution of Na_2O and K_2O across the stratigraphy is due to these elements being the major constituents of feldspars (Na is a constituent of albite while K is a constituent of K-feldspar), which are major mineral phases in all Rooiberg Group rocks. The AFM composition exhibited by the Rooiberg Group (Hatton and Schweitzer, 1995) also show that Na and K_2O are major constituents of these rocks, especially in the Damwal, Kwaggasnek and Schrikkloof formations. P_2O_5 first shows a slight increase throughout the Damwal Formation, but a decrease throughout the Kwaggasnek to the Schrikkloof Formation. MgO shows a decreasing trend within the Damwal Formation, followed by steady low values within the Kwaggasnek and Schrikkloof formations. $Fe_2O_{3(total)}$ shows an enrichment in the lower part of the stratigraphy, the Damwal Formation, having a composition of 5.85-9.87 wt.% compared to the lower 1.11-6.78 wt.% in the Kwaggasnek and Schrikkloof Formations. Lutetium, a compatible trace element in mafic minerals such as

amphiboles, first shows a decrease throughout the Damwal Formation, then an increase in the Kwaggasnek Formation and a relatively random distribution in the Schrikkloof Formation.

Table 4: Major element oxides data of the Rooiberg Group samples.

Sample name	Formation	Height (m)	SiO_2	TiO_2	Al_2O_3	Fe_2O_3	MnO	MgO	CaO	Na_2O	K_2O	P_2O_5	Cr_2O_3	NiO	V_2O_5	ZrO_2	LOI	CIA	Mg#	Eu/Eu*
SM-23	Damwal	1097	69.11	0.58	11.62	7.14	0.14	0.26	2.62	2.23	4.60	0.12	0.01	0.00	0.00	0.04	1.60	55.15	3.51	0.51
SM-25	Schrikkloof	1097	73.93	0.25	11.73	3.50	0.06	0.05	0.00	3.24	4.52	0.01	0.01	0.01	0.00	0.06	1.58	60.18	1.41	0.51
SM-28.2	Schrikkloof	1100	74.28	0.29	12.13	3.94	0.08	0.30	0.00	3.39	4.54	0.02	0.01	0.00	0.00	0.06	1.08	60.47	7.08	0.47
SM-38.1	Damwal	1120	70.12	0.56	11.43	7.33	0.07	0.07	3.63	3.34	1.23	0.13	0.00	0.01	0.00	0.04	1.81	58.23	0.95	0.51
SM-44.1	Damwal	1132	67.08	0.66	12.04	7.80	0.14	0.68	2.10	3.59	3.05	0.17	0.00	0.00	0.01	0.04	1.73	57.94	8.02	0.52
SM-45.1	Damwal	1147	68.27	0.65	12.38	7.52	0.11	0.40	2.56	3.59	3.47	0.17	0.00	0.00	0.00	0.04	1.65	56.27	5.05	0.51
SM-48	Kwaggasnek	1209	70.11	0.41	11.59	6.78	0.14	0.12	1.04	2.47	4.58	0.05	0.01	0.01	0.00	0.05	1.91	58.89	1.74	0.54
SM-50	Damwal	1240	69.06	0.53	11.83	7.39	0.12	0.17	1.19	2.74	4.97	0.11	0.00	0.00	0.00	0.04	1.80	57.07	2.25	0.59
SM-51.1	Damwal	1259	69.67	0.57	12.09	7.37	0.13	0.19	0.89	2.95	4.69	0.12	0.00	0.00	0.00	0.04	1.75	58.63	2.51	0.51
SM-4.1	Kwaggasnek	1140	80.84	0.40	7.13	5.35	0.05	0.13	0.00	0.01	3.61	0.07	0.01	0.00	0.01	0.03	1.94	66.32	2.37	0.57
SM-RL1	Damwal	1280	68.78	0.64	12.17	8.26	0.10	0.32	0.09	2.92	3.69	0.13	0.00	0.00	0.00	0.04	2.39	64.49	3.73	0.51
SM-3	Damwal	1140	67.40	0.69	12.94	7.94	0.12	0.48	2.18	2.54	5.31	0.17	0.00	0.00	0.00	0.04	0.84	56.33	5.70	0.58
SM-5.1	Damwal	1134	66.07	0.65	11.94	9.77	0.16	0.44	2.55	2.82	3.75	0.23	0.00	0.00	0.00	0.04	1.29	56.70	4.31	0.53
SM-5.2	Schrikkloof	1134	73.47	0.21	12.90	3.48	0.02	0.03	0.00	2.99	5.35	0.03	0.00	0.00	0.00	0.03	1.57	60.73	0.85	0.52
SM-6	Damwal	1131	67.63	0.60	12.03	9.03	0.13	0.32	1.74	2.92	4.16	0.17	0.00	0.00	0.00	0.04	1.08	57.70	3.42	0.67
SM-10	Damwal	1085	71.89	0.44	11.40	5.85	0.06	0.11	0.91	2.33	4.99	0.07	0.00	0.00	0.00	0.05	1.81	58.07	1.85	0.52
SM-13	Damwal	1116	72.86	0.64	11.22	6.21	0.12	0.91	0.59	2.44	2.73	0.13	0.02	0.01	0.01	0.06	1.86	66.08	12.78	0.51
SM-14	Damwal	1074	66.96	0.61	11.96	9.10	0.14	0.33	1.91	2.93	4.08	0.18	0.00	0.00	0.00	0.04	1.66	59.69	3.50	0.59

Sample name	Formation	Height (m)	SiO_2	TiO_2	Al_2O_3	Fe_2O_3	MnO	MgO	CaO	Na_2O	K_2O	P_2O_5	Cr_2O_3	NiO	V_2O_5	ZrO_2	LOI	CIA	Mg#	Eu/Eu*
SM-18.1	Schrikkloof	1090	76.37	0.24	10.92	3.37	0.04	0.04	0.12	2.33	5.19	0.01	0.00	0.00	0.00	0.06	0.86	58.84	1.17	0.55
SM-19	Schrikkloof	1103	73.72	0.27	12.08	3.70	0.03	0.02	0.06	2.54	5.73	0.01	0.00	0.00	0.00	0.06	1.21	59.89	0.54	0.55
SM-22	Schrikkloof	1094	79.54	0.26	7.70	4.38	0.07	0.08	0.74	1.98	2.97	0.05	0.02	0.01	0.00	0.04	1.31	57.51	1.79	0.64
LD016	Kwaggasnek	1092	69.44	0.37	11.12	5.64	0.09	<0.01	2.07	1.96	5.00	0.03	<0.01	<0.01	<0.01	0.05	2.97	55.19	na	0.55
LD07	Kwaggasnek	1173	69.86	0.40	12.40	6.61	0.06	0.07	0.59	2.00	4.01	0.08	0.01	<0.01	<0.01	0.06	2.46	65.26	1.05	0.53
LD018	Kwaggasnek	1134	70.74	0.41	11.75	6.57	0.09	0.06	0.14	2.58	4.22	0.04	<0.01	<0.01	<0.01	0.05	1.85	62.87	0.90	0.65
LD04	Kwaggasnek	1135	74.19	0.39	12.21	5.75	0.03	0.04	<0.01	1.54	5.24	0.03	<0.01	<0.01	<0.01	0.04	1.85	na	0.69	0.51
LD02	Kwaggasnek	1134	71.24	0.37	11.32	7.37	0.12	<0.01	<0.01	2.76	4.10	0.03	<0.01	<0.01	<0.01	0.05	1.61	na	na	0.43
LD015	Kwaggasnek	1061	77.08	0.36	11.41	1.49	<0.01	<0.01	<0.01	1.68	5.30	0.02	<0.01	<0.01	<0.01	0.05	1.55	na	na	0.52
LD012A	Kwaggasnek	1058	69.80	0.38	11.47	5.94	0.11	0.10	2.49	1.23	5.10	0.03	<0.01	<0.01	<0.01	0.04	4.93	56.53	1.66	0.5
LD012B	Kwaggasnek	1058	68.94	0.37	11.14	5.76	0.13	0.02	2.08	1.83	5.07	0.03	0.01	<0.01	<0.01	0.05	3.05	56.37	0.35	0.59
LD028	Damwal	1248	68.93	0.59	11.83	7.74	0.10	0.57	1.02	2.44	4.12	0.15	<0.01	<0.01	<0.01	0.03	2.13	60.95	6.86	0.61
LD026	Damwal	1234	65.65	0.50	11.42	8.05	0.12	0.25	2.80	1.86	4.56	0.10	<0.01	<0.01	<0.01	0.04	3.43	55.33	3.01	0.59
LD09	Kwaggasnek	1089	69.34	0.39	12.58	6.15	0.10	0.05	2.01	2.40	5.05	0.03	<0.01	<0.01	<0.01	0.04	3.06	na	0.81	0.6
LD019	Damwal	1142	69.03	0.66	12.20	9.98	0.06	0.03	0.63	2.50	5.04	0.21	<0.01	<0.01	<0.01	0.04	1.34	59.89	0.30	0.48
LD017	Kwaggasnek	1111	70.88	0.39	13.21	5.18	0.01	0.10	<0.01	2.99	4.69	0.05	<0.01	<0.01	<0.01	0.05	1.90	na	1.89	0.49
LD08	Kwaggasnek	1063	76.18	0.37	13.28	1.11	0.01	0.01	<0.01	0.42	6.21	0.02	<0.01	<0.01	<0.01	0.05	1.91	na	0.89	0.55
LD010	Kwaggasnek	1101	71.91	0.39	11.79	5.96	0.04	0.02	<0.01	1.57	4.81	0.06	<0.01	<0.01	<0.01	0.06	2.04	na	0.33	0.57
LD011	Kwaggasnek	1101	71.97	0.42	11.26	6.17	0.03	<0.01	<0.01	2.38	4.90	0.03	<0.01	<0.01	<0.01	0.05	1.48	na	na	0.51

Sample name	Formation	Height (m)	SiO_2	TiO_2	Al_2O_3	Fe_2O_3	MnO	MgO	CaO	Na_2O	K_2O	P_2O_5	Cr_2O_3	NiO	V_2O_5	ZrO_2	LOI	CIA	Mg#	Eu/Eu*
LD013	Kwaggasnek	1066	73.81	0.39	11.27	3.65	0.05	<0.01	1.56	2.41	4.31	0.04	<0.01	<0.01	<0.01	0.05	2.33	57.65	na	0.51
LD014	Damwal	1127	67.19	0.64	11.77	9.87	0.06	0.03	0.61	2.41	4.93	0.21	<0.01	<0.01	<0.01	0.04	2.06	59.69	0.30	0.53
LD020	Damwal	1144	68.64	0.56	11.59	7.77	0.11	0.25	1.71	1.99	4.13	0.16	<0.01	<0.01	<0.01	0.04	3.02	59.68	3.12	0.46
LD021	Damwal	1156	68.27	0.61	11.74	7.25	0.13	0.49	1.74	2.03	4.00	0.18	<0.01	<0.01	0.01	0.04	3.13	60.17	6.33	0.59
RG7	Dullstroom	1903	67.02	0.61	13.47	6.34	0.09	1.83	4.01	3.04	2.76	0.13	0.02	<0.01	0.02	0.03	1.18	58.08	22.40	na
RG8	Dullstroom	1907	56.15	0.63	14.87	9.78	0.14	5.24	8.16	2.3	1.44	0.11	0.04	0.02	0.03	0.01	1.89	58.7	34.89	na
RG10	Dullstroom	1908	53.97	1.42	11.29	11.81	0.25	5.66	8.44	2.77	1.9	0.14	0.07	0.03	0.04	0.02	0.97	46.27	32.40	na
RG13	Dullstroom	1871	64.27	0.64	13.3	6.98	0.12	1.8	4.2	2.9	2.55	0.12	0.02	<0.01	0.02	0.03	1.79	52.44	20.50	na
RG23	Dullstroom	1968	75.26	0.29	11.22	3.94	0.08	1.41	2.53	0.98	4.34	0.07	0.02	0.01	0.01	0.03	1.05	58.81	26.36	na
RG24	Dullstroom	1969	55.97	0.61	14.99	9.07	0.18	5.06	9.26	2.3	0.9	0.12	0.02	0.01	0.03	0.02	1.05	56.04	35.81	na
RG25	Dullstroom	1808	57.99	1.62	13.32	11.28	0.15	3.86	7.54	2.53	1.35	0.17	0.02	0.01	0.04	0.02	1.16	55.91	25.50	na
RG34	Dullstroom	1960	68.81	0.5	12.71	5.13	0.08	1.52	3.95	1.81	3.4	0.11	0.07	0.01	0.02	0.03	1.58	57.47	22.86	na
RG40	Dullstroom	1912	61.66	0.71	14.52	9.74	0.16	3	6.3	2.6	1.73	0.17	0.02	0.01	0.03	0.02	1.18	54.61	23.55	na
RG41	Dullstroom	1949	57.92	0.64	14.20	10.00	0.19	3.96	6.89	2.75	1.55	0.15	0.02	0.01	0.03	0.02	1.55	57.75	28.37	na
RG42	Dullstroom	1940	42.25	0.46	11.08	7.82	0.15	3.69	6.58	1.37	0.8	0.09	0.01	0.01	0.02	0.01	25.67	57.85	32.06	na
RG47	Dullstroom	1949	72.63	0.31	10.92	3.86	0.06	1.69	2.52	1.33	3.99	0.08	0.03	0.01	0.01	0.03	1.15	54.67	30.45	na
RG49	Dullstroom	1965	53.9	0.59	15.02	9.47	0.14	5.6	9.16	1.86	1.47	0.11	0.02	0.01	0.03	0.01	2.48	55.53	37.16	na
RG50	Dullstroom	1975	59.05	0.41	13.28	9.84	0.19	4.23	8.72	2.77	0.56	0.06	0.03	0.01	0.03	0.01	0.99	55.86	30.06	na
RG51	Dullstroom	1976	57.73	0.46	14.37	9.61	0.17	5.88	8.41	1.8	1.25	0.07	0.04	0.02	0.03	0.01	2.08	53.86	37.96	na

Sample name	Formation	Height (m)	SiO_2	TiO_2	Al_2O_3	Fe_2O_3	MnO	MgO	CaO	Na_2O	K_2O	P_2O_5	Cr_2O_3	NiO	V_2O_5	ZrO_2	LOI	CIA	Mg#	Eu/Eu*
RG52	Dullstroom	1969	55.57	0.45	14.05	9.52	0.16	6.17	8.51	1.93	1.25	0.06	0.04	0.02	0.03	0.01	1.89	58.53	39.32	na
RG54	Dullstroom	1905	56.62	0.58	14.46	9.91	0.18	4.73	8.68	1.8	1.31	0.13	0.03	0.02	0.03	0.02	1.05	54.62	32.31	na
RG55	Dullstroom	1935	57.83	0.54	14.53	10.12	0.2	4.86	7.42	1.79	1.27	0.13	0.03	0.01	0.03	0.02	1.76	58.13	32.44	na
RG60	Dullstroom	1699	65.31	0.62	13.49	7.19	0.08	1.86	4.33	2.83	2.82	0.14	0.01	<0.01	0.02	0.03	1.28	55.61	20.55	na
RG62	Dullstroom	1807	56.37	1.75	13.98	13.6	0.08	2.62	4.98	3.37	2.32	0.21	0.01	0.01	0.04	0.04	0.71	58.83	16.15	na
RG63	Dullstroom	1898	55.38	0.75	14.72	10.1	0.19	4.83	8.45	2.25	1.51	0.13	0.03	0.01	0.03	0.02	1.69	57.97	32.35	na

The sign and degree of any Eu anomaly is quantified by the Eu/Eu* value, where Eu is the chondrite-normalized Eu concentration ($2*Eu_N$), and Eu* is ($Sm_N + Gd_N$) according to Sun and McDonough (1989). Chemical index of alteration (CIA) calculated according to Nesbitt and Young (1982). CIA columns without values are due to the CaO below the detection limit. Mg#= MgO/(MgO+FeO)*100.

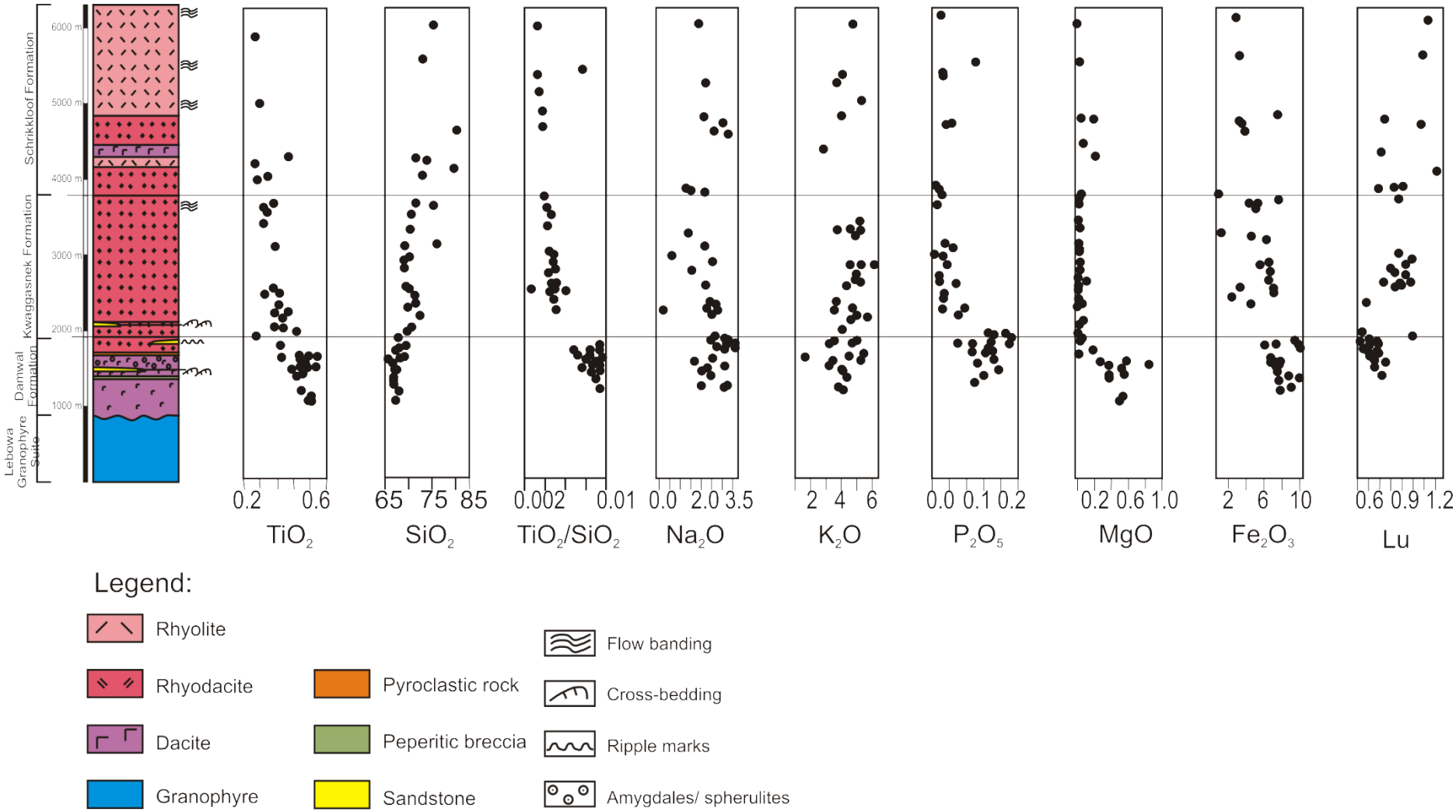

Figure 12: Chemostratigraphy of the Rooiberg Group rocks in the northeast area of Loskop Dam displaying the variations in compositions across the stratigraphy.

The chemostratigraphy for the Rooiberg Group and the importance of the elements used is even more obvious when looking at Fig. 13. All plots (Figs. 13a-d) show clearly defined clusters of samples in the coloured formational fields, defined by Schweitzer and Hatton (1995), by means of which discrimination into the different formations is possible as shown in Table 5.

Table 5: Major element concentrations used for chemostratigraphy of the Loskop Dam. The Dullstroom samples in this table are obtained from the Dullstroom area in this project (showing the change in major elements across the Rooiberg Formations).

Name of Formation	**TiO_2 wt.%**	**SiO_2 wt.%**	**MgO wt.%**	**P_2O_5 wt.%**	**Fe_2O_3 wt.%**
Dullstroom	0.29-1.75	37.13-80.14	1.41-6.17	0.06-0.21	3.72-13.6
Damwal	0.44-0.69	66.07-72.86	0.03-0.91	0.07-0.21	5.85-9.98
Kwaggasnekk	0.36-0.42	68.94-77.08	0.01-0.13	0.02-0.08	1.11-7.37
Schrikkloof	0.21-0.29	73.47-79.54	0.02-0.30	0.01-0.05	3.37-4.38

The relationship between MgO, P_2O_5, Fe_2O_3 and TiO_2 suggests compatibility between these elements during crystallization. MgO and Fe_2O_3 are compatible in mafic minerals such as clinopyroxene as observed in the Dullstroom and lower Damwal formations (Buchanan et al., 2002, 2004). P_2O_5 is compatible with apatite which was also observed in the Dullstroom and lower Damwal formations (Twist, 1983; Lenhardt and Eriksson, 2012) while TiO_2 is compatible with crystallization of Fe-Ti minerals such as ilmenite observed only in the Dullstroom Formation. Noteworthy is that the Mg (MgO) content described for the Damwal Formation in the area north of Loskop Dam (0.01-0.91 wt.%) in this study is lower than that described by Schweitzer et al. (1995) and Schweitzer and Hatton (1995), with MgO usually ~1.0 wt.%. Also, the TiO_2 concentration reported by Schweitzer et al. (1995) and Schweitzer and Hatton (1995) especially for the high-Fe-Ti-P lava displayed higher values (TiO_2 usually >1.0 wt.%) than those reported for the Loskop Dam area in this study (0.21-0.69 wt.%).

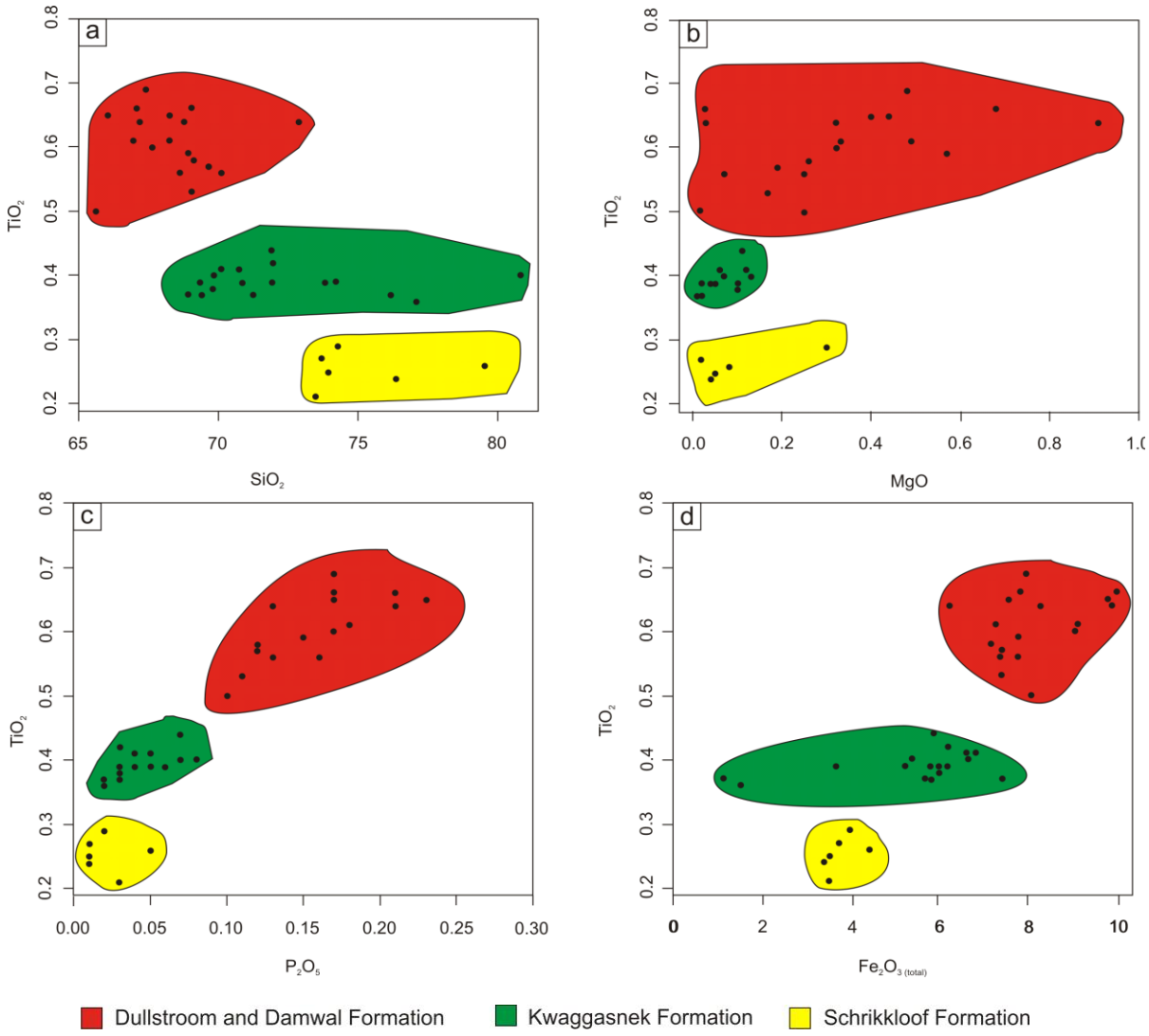

Figure 13: Major element distribution used in the classification of the Rooiberg Group into Dullstroom, Damwal, Kwaggasnek and Schrikkloof formations.(a) plot of TiO_2 against SiO_2; (b) plot of TiO_2 against MgO; (c) plot of TiO_2 against P_2O_5; (d) plot of TiO_2 against Fe_2O_3. Field boundaries are from Hatton and Schweitzer (1995).

In Fig. 13a, the Dullstroom and Damwal samples exhibit the lowest SiO_2 but the highest TiO_2 content. The high TiO_2 content decreases in the Kwaggasnek Formation and is lowest in the Schrikkloof Formation but with increasing SiO_2 content. However, a positive trend is observed when crystallising mafic mineral phases such as Fe-Ti bearing minerals (for example ilmenite and titanomagnetite as observed by Twist (1985) in the Dullstroom Formation) that crystallize Mg (as MgO) and FeO (as in Fe_2O_3) as shown in Fig. 13b and d as well as compatible suits of crystallizing elements such as P (as in P_2O_5) as shown in Fig.

13c. P_2O_5 is observed to decrease from the Dullstroom and Damwal formations along with TiO_2 to the Schrikkloof Formation. The occurrence of Fe-Ti minerals in the Dullstroom and Damwal formations is suggested as one of the main reasons in the decline in TiO_2 upward the Rooiberg Stratigraphy.

However, Fig. 13b shows that some of the Schrikkloof and Kwaggasnek samples have similar MgO contents to those of the Dullstroom and Damwal formations, representing similar compositions between the magma types that evolved these formations. The similarities exhibited in elemental composition across the different formations in the Rooiberg Group provides evidence that a more accurate, precise and statistical approach is required for dividing the samples into different formations. For this study, clusters of samples in Fig. 13 are employed as the basis of division into the different formation, though may not be accurate, but show the probability to which formation each sample belongs. Further improved methods of classification will be presented in subsequent studies.

5.2 THE ORIGIN OF THE UPPER PART OF THE ROOIBERG GROUP, NORTH EAST OF LOSKOP DAM: TRACE AND RARE EARTH GEOCHEMISTRY

The trace element variation diagram (Fig. 14a) shows negative spikes for Nb, Ba, Sr and Ti, a trend which is similar in the three formations. In Fig. 14b, an enrichment of the light rare earth elements (LREEs) with slight depletion of the heavy rare earth elements (HREEs) and a negative Eu anomaly is exhibited. Trace and rare earth element abundances are normalized to chondritic composition in Fig. 14 as they are observed to have a more constant set of values than the crustal composition. The negative spikes of Ba, Sr and Ti can be explained by the compatibility of these elements with the crystallization of feldspar (White et al., 2003), thereby increasing the relative concentrations of incompatible elements such as Rb, Th and Ta as exhibited in (Fig. 14a). Furthermore, the depleted amount of Ti suggests the formation of the upper part of the Rooiberg Group from low-Ti magma. Buchanan et al. (2002) also described that the Damwal, Kwagassnek and Schrikkloof formations evolved from a low-Ti that bear lower abundances of incompatible elements than the high-Ti magma. The enriched LREEs, together with the negative Eu anomaly, are characteristic for an upper crustal signature (White, 2013), suggesting that a particular amount of the upper crust was involved during the formation of the Rooiberg Group and played an important role in the evolution of these volcanics. It is important to note that the Eu anomaly is absent in the Dullstroom Formation as compared with the Damwal, Kwaggasnek and Schrikkloof formations. This

comparison is made using the Dullstroom data in Buchanan et al. (1999, 2002), due to the absence of the Dullstroom Formation samples in area northeast of Loskop Dam.

The negative Eu anomaly is observed to be greater in the Damwal, Kwaggasnek and Schrikkloof formations than in the Dullstroom Formation (when Eu in this study is compared to that of Buchanan et al., 2002). This further indicates that the processes responsible for the formation of the Dullstroom Formation may not be identical to the ones that formed the Damwal, Kwaggasnek and Schrikkloof formations. Some samples such as SM4.1 (Kwaggasnek Formation) as shown in Fig. 14 occur within the Damwal Formation, and thus suggest a certain extent of magma mixing during the evolution of these rocks. Furthermore, trace elements such as Nb and Ta, ranging between 5.83-24.2 ppm and 0.45-1.86 ppm respectively, for the Damwal, Kwaggasnek and Schrikkloof formations are similar to crustal and not mantle compositions. The Nb and Ta values of the Damwal, Kwaggasnek and Schrikkloof formations are also observed to exhibit higher values when compared to the Dullstroom Formation (comparison between the Damwal, Kwaggasnek and Schrikkloof formations in this study and the Dullstroom samples from Buchanan et al., 2002), further indicating a possible difference between the processes that evolved the Dullstroom Formation and the Damwal, Kwaggasnek and Schrikkloof formations. The similarity between the trace elements composition of the Rooiberg Group and crustal compositions indicate a possible process of crustal melting for the formation of the Rooiberg Group.

Table 6: Trace element data of the Rooiberg Group samples north of Loskop Dam

Sample name	Li	Sc	V	Cr	Co	Ni	Cu	Zn	Rb	Sr	Y	Zr	Nb	Ba	La	Ce
SM-23	24.6	11.6	1.77	0.57	113	< d.l.	34.9	149	132	114	49.5	313	16.2	869	62.3	123
SM-25	7.22	< d.l.	1.15	1.38	303	3.35	11.8	133	158	54.5	74.2	312	23.1	877	107	156
SM-28.2	13.5	< d.l.	1.54	2.78	107	1.74	9.23	126	158	61.9	87.2	328	24.2	963	117	181
SM-38.1	11.2	8.99	15.1	2.53	128	< d.l.	61.2	73.9	54.2	353	40.4	269	13.8	198	61.4	107
SM-44.1	13.5	10.6	20.4	0.96	101	< d.l.	19.3	119	91	125	39.6	290	14.3	737	57	111
SM-45.1	5.24	9.88	14.4	2.57	182	< d.l.	7.22	100	103	253	41.6	287	14.4	512	59.9	118
SM-48	16.1	4.27	0.3	0.7	240	0.64	15.4	164	154	80.7	57.7	368	18	971	72.1	138
SM-50	8.28	7.12	2.12	0.54	120	< d.l.	28.1	165	167	105	44.9	323	16	985	62.4	121
SM-51.1	7.06	7.39	2.42	0.64	153	0.11	25.8	216	146	104	45.6	316	15.8	997	63.4	138
SM-4.1	59.2	3.96	29.1	57.9	99	23.5	10.9	28	140	57.7	12.6	170	5.38	900	43.6	40.6
SM-RL1	9.05	7.28	7.09	1.06	107	1.44	39.4	162	116	60.3	45.4	328	15.9	814	61.2	124
SM-3	12.4	9.29	13.7	1.64	88.7	< d.l.	24.4	160	144	138	44.8	322	16.4	1216	58.9	116
SM-5.1	20.4	13.8	2.18	0.92	55.3	< d.l.	35.7	149	122	154	51	296	16.5	852	60.1	120
SM-5.2	9.05	0.78	8.91	3.4	135	5.48	21.2	62.7	184	101	34.9	226	20.8	571	22.1	54.8
SM-6	21.3	11.1	1.7	0.39	54.1	< d.l.	36.1	145	136	117	53.2	319	17	897	62.3	124
SM-10	5.33	4.48	0.38	0.75	532	1.81	25.3	73.9	186	90.5	69	355	18.2	997	82.5	150
SM-13	74.7	4.9	46.2	60.7	135	16	25.7	206	107	110	32.1	385	12.9	1063	61.9	121
SM-14	18.2	8.28	3.65	4.43	145	< d.l.	26.2	99.8	180	116	52.7	341	17.5	1088	64.3	125
SM-18.1	11.1	< d.l.	0.19	0.61	128	0.6	22.8	68.2	184	68.6	71	427	20.1	1149	80.7	155
SM-19	17.6	< d.l	0.62	0.93	322	2.13	21.3	104	207	82.7	62.2	480	23.7	1269	78.3	140
SM-22	6.51	1.63	0.58	2.38	131	0.7	42	111	103	53	46.2	268	13.5	679	49.2	90.9
LD016	7.79	2.47	0.28	0.17	103	< d.l.	5.67	87	189	69	60.7	352	16.5	1953	82.7	138
LD07	26.3	3.56	0.75	1.77	107	0.86	19.8	146	147	62	67.6	372	18	1197	91.4	144
LD018	27.3	1.89	0.24	0.72	91	0.81	17.2	179	134	32.2	60.3	369	17.2	1197	84.2	146
LD04	7.15	1.59	1.1	0.38	100	2.54	12.7	130	192	16	42.6	373	17.2	861	60.3	140
LD02	5.75	2.85	0.84	1.35	123	1.44	11.7	180	147	28.1	55.3	360	16.9	811	67	129

Sample name	Li	Sc	V	Cr	Co	Ni	Cu	Zn	Rb	Sr	Y	Zr	Nb	Ba	La	Ce
LD015	5.93	1.88	1.7	0.28	120	1.65	31.1	34.6	172	19.7	50.9	347	15.8	639	85	157
LD012A	7.98	1.75	0.38	0.37	138	< d.l.	19.8	126	199	48.2	54.2	354	17	724	68.8	134
LD012B	8.04	2.75	0.31	0.24	83.6	< d.l.	10.6	80.5	201	69.4	62	348	16.7	2077	91.8	143
LD028	27.7	9.11	9.67	13.8	91.2	1.27	27.6	114	126	103	41.1	282	13.1	1016	53.9	107
LD026	37.5	8.08	0.88	0.27	72.2	< d.l.	27.4	144	162	111	52.1	307	14.9	1006	61.5	121
LD09	10.1	2.47	0.24	0.25	125	< d.l.	10.1	115	175	65.5	56.3	349	16.5	1158	78.8	135
LD019	4.76	9.78	3.02	0.96	92.4	0.26	11	59.2	172	57.5	43	288	14.6	1353	51.5	109
LD017	15.9	2.19	0.45	0.42	102	1.02	27.3	111	140	30.8	46	352	16.4	978	79.2	191
LD08	6.68	1.87	1.03	1.44	159	2.18	7.91	46.6	212	23.3	54.6	358	16.3	2370	99.3	186
LD010	6.91	1.62	0.76	0.71	122	1.57	16.5	149	175	25	63.9	378	17.6	1054	98.4	143
LD011	6.28	2.42	0.48	0.65	152	1.92	7.43	150	171	30.2	57.2	378	18.4	875	72	144
LD013	4.6	2.51	0.27	0.66	119	< d.l.	8	119	164	54.6	60.1	343	15.3	728	70.6	133
LD014	32.6	10.7	24.1	14.3	69.5	3.67	37.8	155	137	124	41.7	276	12.3	1289	49.9	97.5
LD020	6.09	8.01	10.6	12.2	93.3	< d.l.	9.11	144	158	51.2	39.5	272	12.6	651	54.4	108
LD021	28.3	9.32	9.98	11	114	0.37	37.3	149	138	88.3	45.8	269	12.4	1798	56.1	108

Sample name	Pr	Nd	Sm	Eu	Tb	Gd	Dy	Ho	Er	Tm	Yb	Lu	Hf	Ta	Pb	Th	U
SM-23	13.7	52.6	10	2.01	1.48	9.68	9.33	1.88	5.46	0.8	5.23	0.78	8.11	1.1	24.7	18.5	4.72
SM-25	22.5	87.3	15.8	2.54	2.26	14.6	14.1	2.84	8.17	1.19	7.75	1.15	8.99	1.67	11	26.1	6.26
SM-28.2	22.9	88.7	16.3	2.88	2.63	17.6	16.3	3.27	9.25	1.31	8.36	1.22	9.33	1.6	11.6	24.7	5.17
SM-38.1	12.2	45.3	8.16	1.85	1.27	8.31	7.8	1.55	4.38	0.62	4	0.59	6.97	1.03	56.5	15.8	3.78
SM-44.1	12.6	47.3	8.77	1.57	1.18	7.71	7.26	1.47	4.22	0.62	4.07	0.61	7.64	1.05	19	18.2	4.62
SM-45.1	13.2	50.4	9.43	1.76	1.23	8.14	7.62	1.52	4.31	0.62	4.12	0.61	7.55	1.32	137	18.1	4.7
SM-48	15.5	60.6	11.3	1.94	1.59	10.2	10.2	2.09	6.11	0.9	5.93	0.89	9.53	1.27	33.9	21.7	5.59
SM-50	13.5	52.5	9.75	1.6	1.28	8.35	8.02	1.62	4.69	0.69	4.6	0.69	8.42	1.13	46.4	21.2	5.31
SM-51.1	14.1	53.8	10.1	1.62	1.29	8.32	8.17	1.65	4.77	0.7	4.68	0.69	8.29	1.21	71.3	20.5	5.21
SM-4.1	7.74	25.4	4.28	0.73	0.44	3.04	2.53	0.47	1.31	0.19	1.31	0.2	4.56	0.45	20.9	9.68	2.17
SM-RL1	14.4	54.8	10.4	1.63	1.29	8.41	8.1	1.64	4.72	0.69	4.6	0.69	8.7	1.18	27.3	19.5	4.55
SM-3	12.9	48.9	8.9	1.61	1.31	8.58	8.01	1.62	4.77	0.69	4.49	0.67	8.38	1.12	56.2	19.9	5.05
SM-5.1	13	49.5	9.08	2.25	1.54	10.1	9.36	1.89	5.48	0.77	5.08	0.75	7.52	1.03	23.2	16.7	4.24
SM-5.2	6.63	25.9	5.27	1.04	0.92	5.64	5.94	1.25	3.93	0.61	4.17	0.61	6.69	1.86	53.1	35.1	7
SM-6	13.3	50.4	9.27	2.22	1.58	10.6	9.83	1.97	5.7	0.81	5.35	0.79	8.11	1.11	20.9	17.8	4.48
SM-10	17.7	66.3	12.3	2.22	1.84	12	11.6	2.38	6.96	0.99	6.46	0.98	9.25	1.59	12.8	20.3	5.18
SM-13	13	48	8.08	1.19	1.02	7.12	5.91	1.18	3.52	0.51	3.43	0.52	10.1	0.94	56.4	22.7	4.76
SM-14	13.5	51.4	9.55	1.95	1.48	9.62	9.22	1.89	5.62	0.81	5.35	0.79	8.84	1.18	19.5	20.5	5.17
SM-18.1	17.6	66.1	12.2	1.8	1.93	12.1	12.5	2.56	7.67	1.11	7.21	1.07	10.9	1.36	36.7	23.4	4.15
SM-19	17	63.7	11.7	1.99	1.77	11.4	11.2	2.31	6.93	1.02	6.81	1.02	12.1	1.73	26.9	25.6	4.17
SM-22	10.5	39.9	7.72	1.5	1.25	7.96	7.95	1.62	4.83	0.7	4.51	0.66	6.83	0.88	35.4	15	3.47
LD016	16.8	62.7	11.9	2.06	1.67	11.3	10	2.04	6.12	0.88	5.8	0.86	9.27	1.14	50.3	21.5	5.73
LD07	18.2	68.9	12.9	2.39	1.89	13	11.3	2.31	6.85	0.97	6.46	0.96	9.77	1.25	35.7	21	5.73
LD018	17.6	66.7	12.6	2.17	1.72	11.9	10.3	2.09	6.2	0.87	5.87	0.88	9.71	1.2	17.8	20.6	5.51
LD04	14	52.3	10.2	1.68	1.36	9.09	8.31	1.67	4.98	0.73	4.88	0.73	9.78	1.19	16.2	21.5	5.97
LD02	14.9	56	11	1.84	1.58	9.96	9.85	2.01	5.99	0.86	5.78	0.86	9.51	1.17	12.9	22.6	6.06
LD015	21.7	80.7	15.3	2.33	1.78	13.3	9.8	1.88	5.45	0.76	5.06	0.77	9.25	1.15	59.6	20.1	5.11

Sample name	Pr	Nd	Sm	Eu	Tb	Gd	Dy	Ho	Er	Tm	Yb	Lu	Hf	Ta	Pb	Th	U
LD012A	14.9	55.6	10.7	1.87	1.61	10.2	9.85	2.05	6.06	0.89	5.82	0.88	9.28	1.24	14	21.9	5.34
LD012B	17.7	65.8	12.2	2.1	1.73	11.8	10.4	2.1	6.27	0.9	5.89	0.89	9.12	1.18	36.2	21.6	5.59
LD028	11.7	43.9	8.38	1.62	1.23	7.99	7.5	1.53	4.5	0.66	4.29	0.65	7.4	0.95	34.2	17.5	4.41
LD026	13.4	50.7	9.8	1.91	1.46	9.41	9.13	1.86	5.56	0.79	5.31	0.79	8.09	1.05	14.9	19	4.82
LD09	16.1	60.5	11.5	1.98	1.62	10.9	9.92	2.02	6	0.87	5.76	0.85	9.2	1.17	18.5	21.7	5.33
LD019	12.2	46.9	9.32	1.84	1.29	8.65	8.01	1.63	4.79	0.69	4.6	0.69	7.48	1.02	19.4	16.7	4.78
LD017	19.1	74.3	14.5	2.41	1.64	12.8	9.28	1.84	5.56	0.82	5.65	0.85	9.07	1.15	11.9	17.1	5.3
LD08	23.2	87.4	15.6	2.56	1.77	13.2	10.1	1.97	5.72	0.79	5.2	0.75	9.36	1.17	45.8	21.5	4.84
LD010	21.7	81	14.8	2.55	1.97	14.1	11.7	2.3	6.86	0.98	6.38	0.94	9.82	1.24	17	21.6	5.4
LD011	15.9	59.4	11.4	2.13	1.69	11.2	10.3	2.15	6.67	0.97	6.42	0.97	9.84	1.34	20	21.3	5.79
LD013	15.2	56.5	10.7	2.05	1.66	10.8	10.1	2.05	6.05	0.87	5.66	0.84	8.93	1.12	21.3	20	4.54
LD014	12.5	49.4	9.86	2.04	1.34	9.54	7.94	1.56	4.52	0.63	4.2	0.62	7.13	0.84	20.1	13.2	3.4
LD020	12.2	45.4	8.72	1.74	1.23	8.4	7.37	1.46	4.36	0.63	4.19	0.62	7.12	0.87	66.6	16.4	4.03
LD021	12.8	48.7	9.65	2.01	1.39	9.56	8.3	1.64	4.89	0.67	4.38	0.65	7.03	0.86	16.5	15.8	3.89

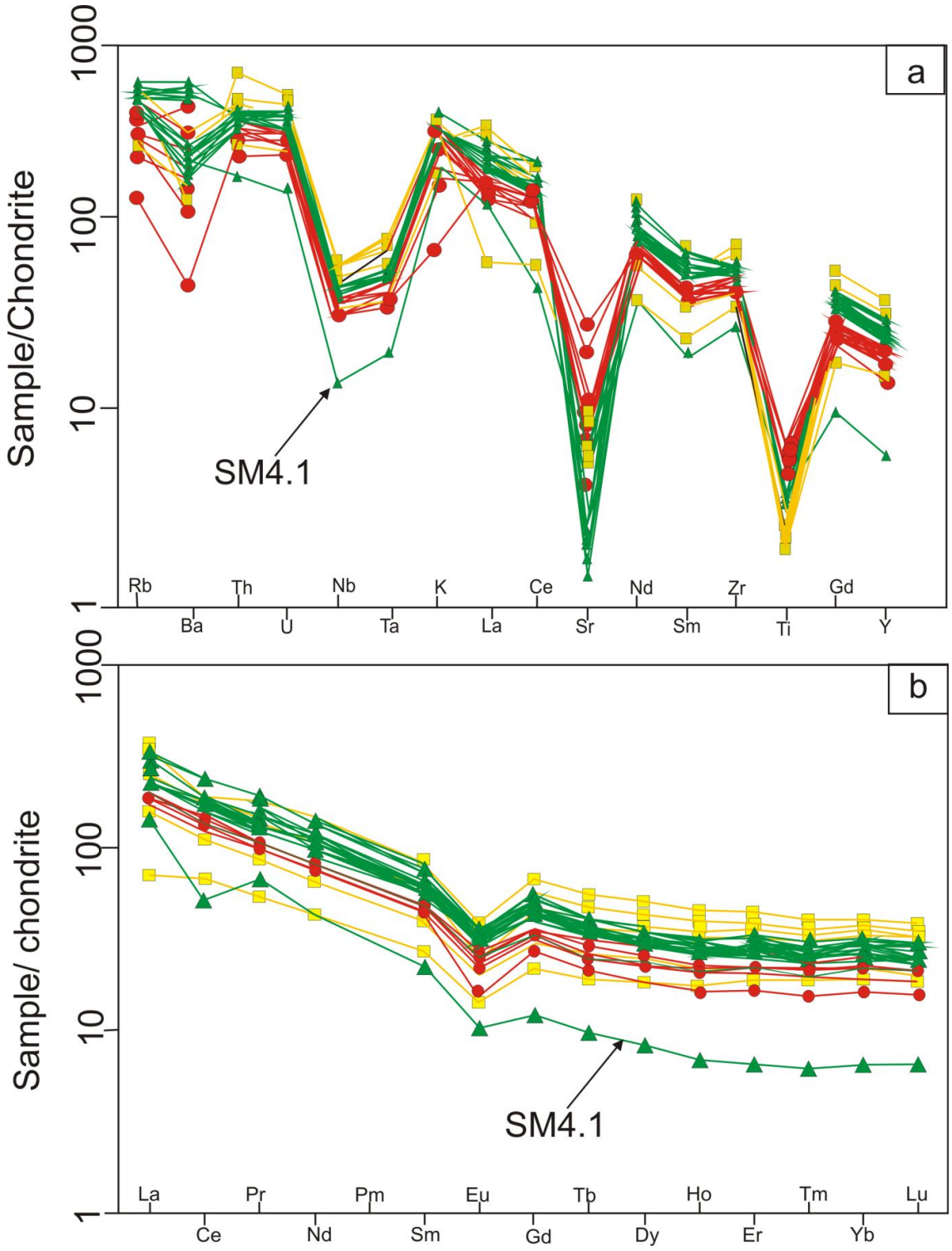

Figure 14: Spider diagrams showing the trace and rare earth (REE) element distribution of the Rooiberg Group rocks in the Loskop Dam area. (a) Trace element distribution normalized according to Sun et al. (1980); (b) REE distribution normalized according to Boynton (1984). Colours indicate the Damwal, Kwaggasnek and Schrikkloof Formations as in Figure 10.

In both Yb vs. Ta (Fig. 15a) and Y vs. Nb (Fig. 15b) plots according to Pearce et al. (1984) the majority of the Rooiberg Group samples plot in the within-plate granitoid field (WPG).

Only few samples (SM13, SM38.1, SM44.1, LD14, LD21, LD28, LD20) plot within the volcanic-arc granitoids (VAG) region (Fig. 15a). Similarly, in Fig. 15b, only few samples plot along the boundary to (SM13, LD14 and LD20) or into (SM4.1) the VAG+syn-COLG field, further suggesting a potential crustal contamination.

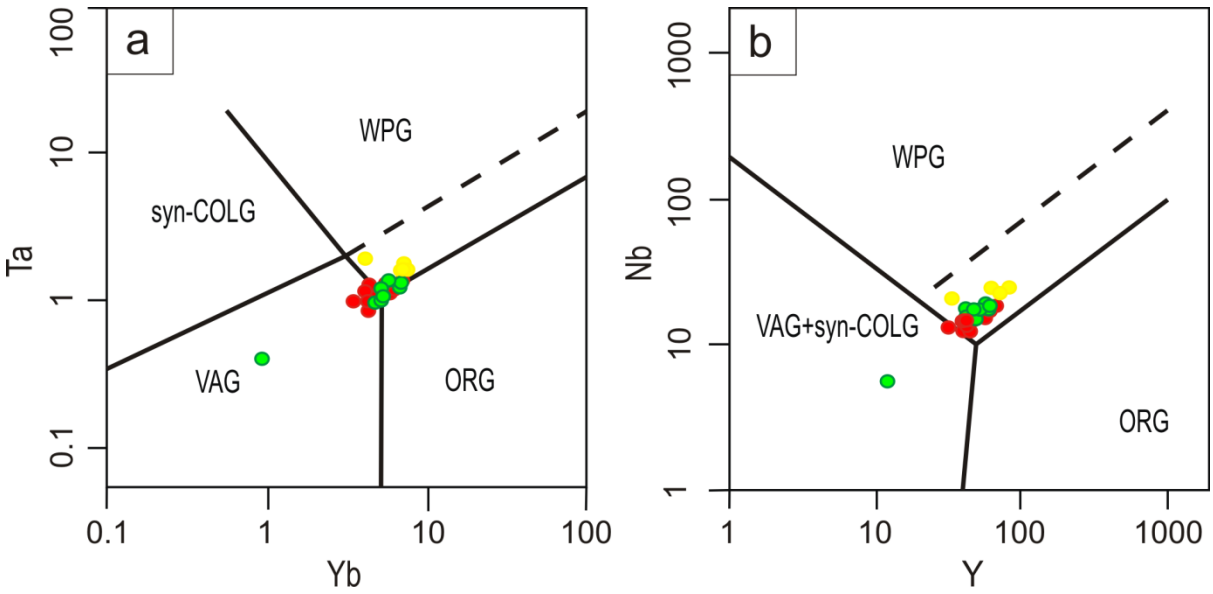

Figure 15: Trace element discrimination diagram of the tectonic setting of the Rooiberg Group according to Pearce et al. (1984). (a) Yb vs. Ta discrimination diagram for granitoids; (b) Y vs. Nb discrimination diagram for granitoids. VAG, volcanic-arc granitoids; ORG, ocean-ridge granitoids; WPG, within-plate granitoids; Syn-COLG, syn-collisional granitoids. Colours represent different formations as indicated in Fig. 13.

It is noteworthy to point out that the samples in Fig. 15a appear in two groups with about half of the samples plotting in the WPG field while the other half plot along the WPG and VAG boundary and within the VAG field. The Schrikkloof and about half of the Kwaggasnek samples plot in the WPG field in Fig. 15a while most of the Damwal samples as well as the other half of the Kwaggasnek samples plot transitionally between the WPG and VAG fields. In Fig. 15b, the majority of the Rooiberg samples plot in the WPG. The samples that plot distinctively in the WPG field are samples from the Schrikkloof and Kwaggasnek formations while the majority of those that plot along the boundary between the WPG and VAG are Damwal samples. However, few samples from the Kwaggasnek Formation such as SM 4.1 plot in the VAG field. The classification scheme by Pearce et al. (1984) is still in wide use

(Chen et al., 2000; Li, 2000; Zhou et al., 2002) and is selected as an important way to decipher the tectonic enviroment of granitoid rocks whose tectonic setting is not preserved, as the trace element compositions of granitoids can reflect their sources and crystallization history of the melt (Frost et al., 2001). However, the scheme according to Pearce et al. (1984) shows that the chemical composition of each tectonic group in the plot is influenced by a range of source components, making samples plot over a range of fields. For this reason, this classification scheme may not show the exact source of rock samples but give an indication of the probable source of the samples plotted.

Figure 16 shows similar but a more recent, and what the writer believes, more accurate plots according to the scheme designed by Verma et al. (2013). In these diagrams, the majority of the Rooiberg Group samples plot within the continental ridge (CR) + ocean island (OI) field. Verma et al. (2013) related these two fields to Pearce et al.'s (1984) within-plate granite (WPG) field. Furthermore, similar to Pearce et al. (1984), few samples (SM4.1, SM13, SM38.1, SM44.1, LD14, LD21, LD28, LD20) plot transitional between the collision (COL) and the continental arc (CA) fields in the diagram according to Verma et al. (2013) (Figs. 16 b, c, e). It is noteworthy that, in contrast to the plots according to Pearce et al. (1984), SM 4.1 does not plot in the CA or Col field of Verma et al. (2013). Similar to the plots in Fig. 15a, a clearer division is exhibited in Fig. 16a, b and e, with the two groups as indicated in Fig. 15. The samples in the dark circle represent the Kwaggasnek and Schrikkloof formations while the red circles include samples from the Damwal Formation.

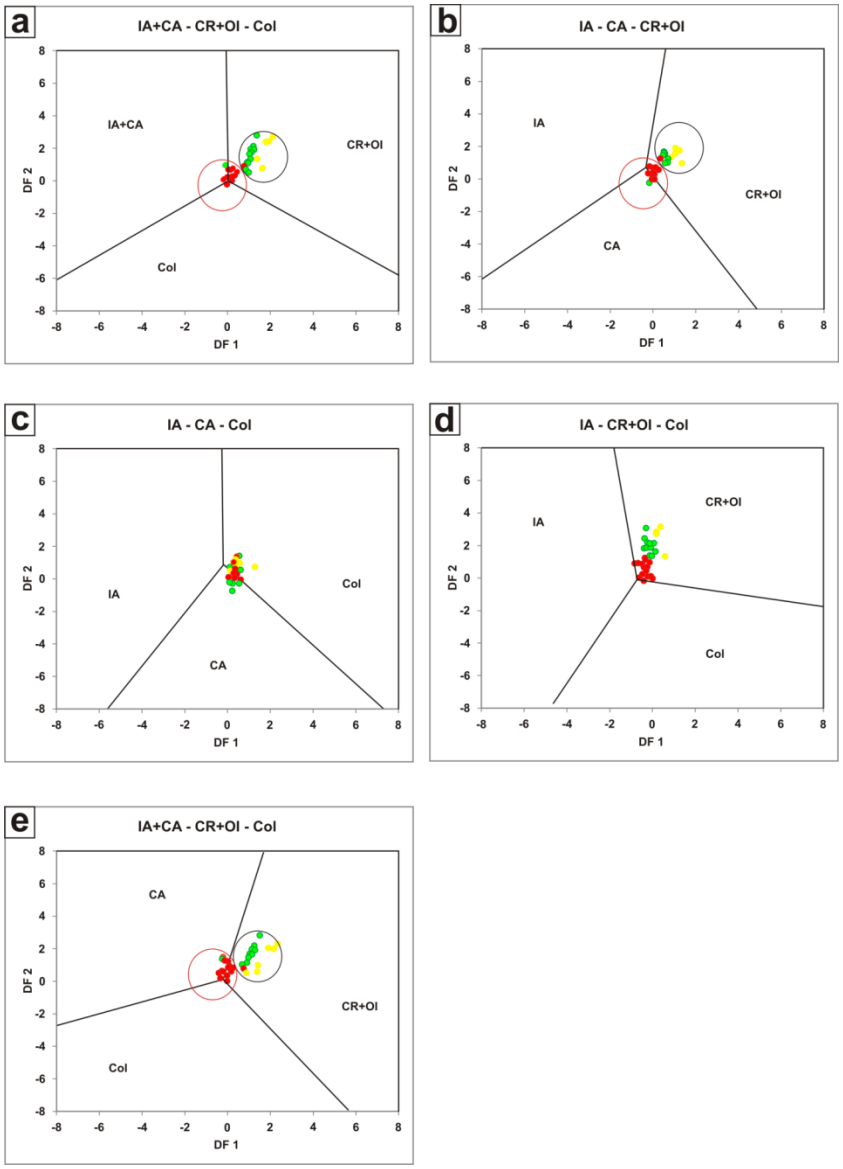

Figure 16: Acid rock discrimination plots of the upper part of the Rooiberg Group according to Verma et al. (2013). IA- island arc; CA- continental arc; CR- continental ridge; OI- ocean island; Col- collision. Note: CR+OI= within plate granite and IA+CA= arc setting. The axes are based on logarithms of both major and trace elements according to Verma et al. (2013).Dark circles represent the Schrikkloof and Kwaggassnek formations while the red circles represent the Damwal Formation. Noteworthy is the similarity in results between the rhyolites occurring in the area north of Loskop Dam and the Nylstroom area and as such results of these two areas are identical and comparable.

5.3 ISOTOPE GEOCHEMISTRY

Silicic large igneous provinces (SLIPs) have been proposed to evolve from mantle-derived melts that is contaminated by crustal material (e.g. Watts et al., 2011; Bryan et al., 2002;

Bryan, 2007). In this section, Dullstroom Formation samples are included since the data used here are obtained from Buchanan et al. (2004). Hence the term Rooiberg Group will be used in this section.

Tegner et al. (1998) described an increase in $^{87}Sr/^{86}Sr$ and subsequent decrease in ε_{Nd} upward in stratigraphy as evidence for assimilation and fractional crystallization. A similar trend is observed in the Rooiberg Group from the basal Dullstroom Formation to the Kwaggasnek Formation. However, due to the presence of different lava types in the Rooiberg Group and especially the Dullstroom Formation, the increase in $^{87}Sr/^{86}Sr$ and subsequent decrease in ε_{Nd} upward the Rooiberg stratigraphy is observed in each lava type. It is important to state that samples of the Schrikkloof Formation are excluded from this study due to a large variation in isotopic values (Table 7) which is proposed to be due to alteration or hydrothermal processes.

Table 7: Isotopic data used for analysis and modelling.

Sample name	Formation	Magma type	$^{87}Sr/^{86}Sr$	Rb/Sr	Nd/Nd	Epsilon Nd	Sr (ppm)
kk10	Dullstroom	Low Ti Dullstroom Formation	0.7068	0.3227	0.5096	-8.1800	290.0
kk12-1	Dullstroom	Low Ti Dullstroom Formation	0.7053	0.4207	0.5096	-7.7300	261.0
kk12-3	Dullstroom	Low Ti Dullstroom Formation	0.7059	0.4155	0.5095	-8.9600	265.0
kk16	Dullstroom	Low Ti Dullstroom Formation	0.7082	0.3649	0.5095	-8.7600	216.0
kk18	Dullstroom	Low Ti Dullstroom Formation	0.7083	0.2380	0.5095	-8.5800	235.0
hs14	Dullstroom	Low Ti Dullstroom Formation	0.7065	0.1011	0.5095	-9.6100	301.0
kk24	Dullstroom	High Ti Dullstroom Formation	0.7071	0.4926	0.5096	-7.4100	397.0
kk25	Dullstroom	High Ti Dullstroom Formation	0.7067	0.3456	0.5096	-7.5100	415.0
kk31	Dullstroom	High Ti Dullstroom Formation	0.7060	0.6517	0.5096	-7.8100	389.0
kk33	Dullstroom	High Ti Dullstroom Formation	0.7063	0.2593	0.5095	-8.9500	333.0
hs6	Dullstroom	High Ti Dullstroom Formation	0.7059	0.5031	0.5096	-9.8600	425.0
kk23	Dullstroom	Upper Dullstroom Formation	0.7084	0.7547	0.5096	-7.1900	248.0
hs1	Dullstroom	Upper Dullstroom Formation	0.7068	0.9299	0.5096	-7.3700	258.0
hs2	Dullstroom	Upper Dullstroom Formation	0.7058	0.7804	0.5096	-8.2200	248.0
hs8	Dullstroom	Upper Dullstroom Formation	0.7073	1.1190	0.5095	-9.1200	264.0
hs16	Dullstroom	Upper Dullstroom Formation	0.7077	0.8848	0.5095	-8.7500	260.0

kk21	Damwal	Damwal Formation	0.7073	3.0020	0.5096	-8.0100	139.0
nk2	Damwal	Damwal Formation	0.7108	2.8140	0.5096	-8.0000	138.0
nk8	Damwal	Damwal Formation	0.7052	2.5760	0.5096	-10.0000	153.0
nk11	Damwal	Damwal Formation	0.7061	2.2320	0.5096	-7.1400	161.0
nk14	Damwal	Damwal Formation	0.7131	2.6500	0.5096	-10.1200	164.0
nk15	Damwal	Damwal Formation	0.7042	2.9590	0.5095	-9.9600	141.0
m3	Kwaggasnek	Kwaggasnek Formation	0.7080	11.4100	0.5095	-9.1800	41.9
m10	Kwaggasnek	Kwaggasnek Formation	0.6625	10.2800	0.5096	-9.0600	46.5
l1	Kwaggasnek	Kwaggasnek Formation	0.6959	12.4300	0.5096	-6.4600	33.1
ig3	Kwaggasnek	Kwaggasnek Formation	0.6446	15.8400	0.5096	-7.8900	39.7
SM19	Schrikkloof	Schrikkloof	0.8981	-	0.5086	-26.7433	87.2
SM22	Schrikkloof	Schrikkloof	0.8549	-	0.5086	-25.7230	53.0
SM28-2	Schrikkloof	Schrikkloof	0.8898	-	0.5086	-26.2796	61.9
BD24	Schrikkloof	Schrikkloof	2.7214	-	0.5086	-26.4371	14.0
KT207	Schrikkloof	Schrikkloof	2.5692	-	0.5086	-26.7260	5.2
Kaapvaal 1	Kaapvaal	Kaapvaal 1	0.7395	20.2400	-	-	17.8
Kaapvaal 2	Kaapvaal	Kaapvaal 1	0.6949	18.8000	-	-	7.2
Kaapvaal 3	Kaapvaal	Kaapvaal 1	0.7127	9.9230	-	-	17.9

Kaapvaal 4	Kaapvaal	Kaapvaal 1	0.7100	2.0290	-	-	69.5
Kaapvaal 5	Kaapvaal	Kaapvaal 1	0.7193	0.6110	-	-	123.4
Kaapvaal 6	Kaapvaal	Kaapvaal 1	0.7248	1.8920	-	-	179.5
FTG 1	Kaapvaal	Kaapvaal	0.7159	0.3691	-	-	102.4
FTG 2	Kaapvaal	Kaapvaal	0.8188	2.9784	-	-	108.0
FTG 3	Kaapvaal	Kaapvaal	0.8169	2.9242	-	-	92.3
FTG 4	Kaapvaal	Kaapvaal	0.8081	2.6639	-	-	101.4

*** A**ll Rooiberg samples are from Buchanan et al. (2004). Kaapvaal 1-6 samples are from the published Ph.D. thesis by Schneiderhan (2007) and FTG 1-4 from Toulkeridis et al. (1998).

In Fig. 17a, there is a slight observable increase in $^{87}Sr/^{86}Sr$ towards the top of each group of samples (as suggested to represent the different lava types in this study, Fig. 17) in the Dullstroom Formation. The increase in the $^{87}Sr/^{86}Sr$ is seen to form a scatter of sample points in the Damwal Formation which becomes greater in the Kwaggasnek Formation. Similarly, the ε_{Nd} in the lava types of the Dullstroom formation show a decrease towards the top of each flow. The decrease in the ε_{Nd} values from the base upwards the Damwal Formation is not as obvious as described for the Dullstroom Formation and again, becomes least visible in the Kwaggasnek Formation (Fig. 17b).

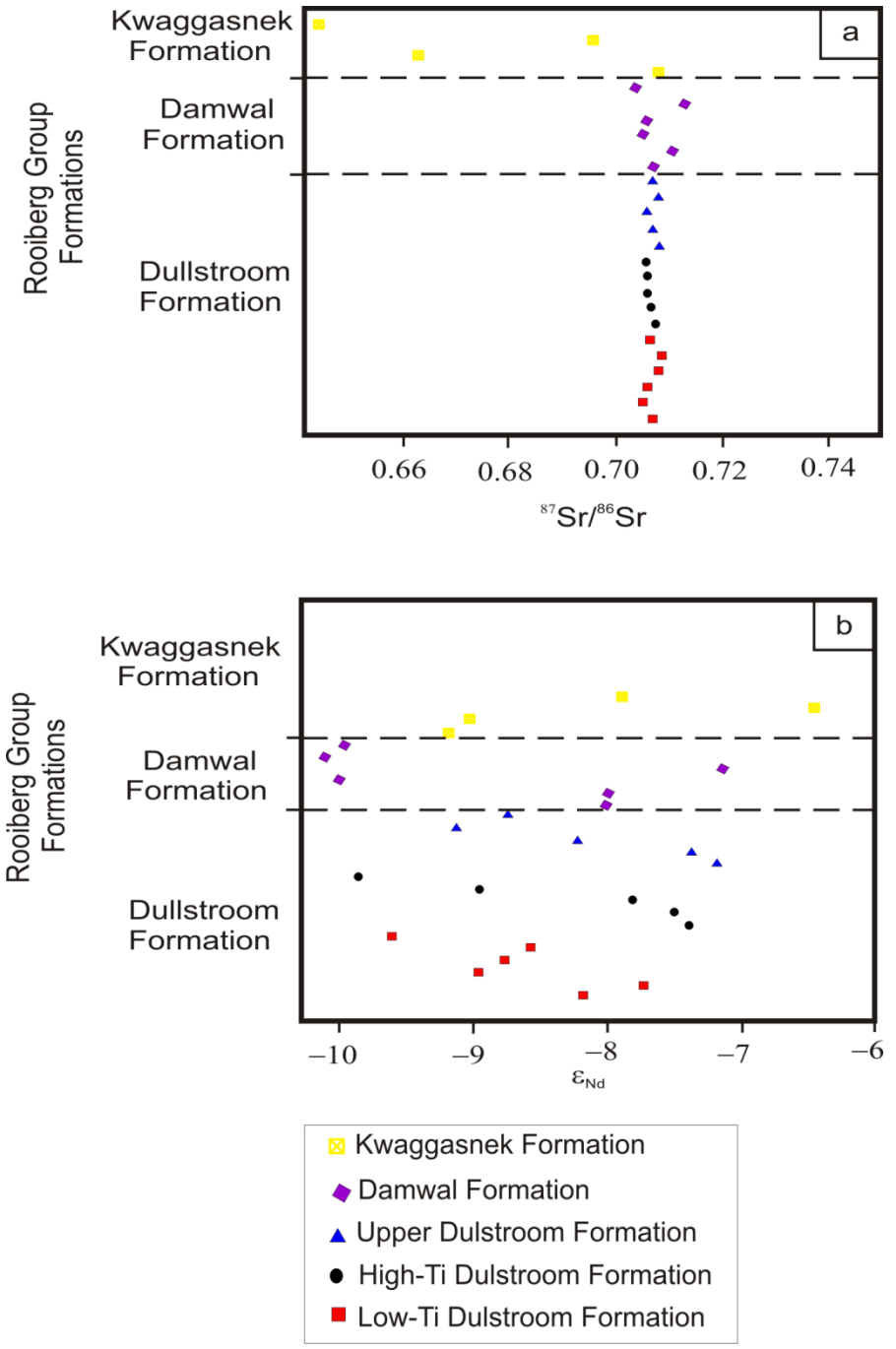

Figure 17: Compositional variation in $^{87}Sr/^{86}Sr$ (Fig. 17a) and ε_{Nd} (Fig. 17b) upward the stratigraphic section of the Rooiberg Group. Samples used in this figure are data obtained from Buchanan et al. (2004) for the Dullstroom, Damwal and Kwaggasnek formations.

However, due to the absence of information on exact stratigraphic level where these samples had been obtained, debates may arise on the stratigraphic height used in Fig. 17, therefore statistical box plots (Fig. 18) were also employed to further support the up-section increase in

$^{87}Sr/^{86}Sr$ with a decrease in ε_{Nd}. Fig. 18a shows the scatter of plots for each lava type and each formation in the Rooiberg Group similar to Fig. 17. The scatter of data as shown increases with an increase in stratigraphy from Dullstroom Formation to Kwaggasnek Formation with a significant increase commencing at the Damwal Formation and then becoming much more increased in the Kwaggasnek Formations. The increase in the scatter of data points, as interpreted for Fig. 17a, suggests that mixing or contamination commenced in the Damwal Formation before becoming more pronounced in the Kwaggasnek Formations. Similarly, Fig. 18b shows increase in the scatter of data from the lowest value to the highest value. The increase in the scatter is observed from the Dullstroom Formation to the Kwaggasnek Formation with a significant increase in the scatter observed in the Damwal Formation and then becoming more visible in the Kwaggasnek Formations. The increase in scatter of data points herein is also interpreted as mixing or contamination that commenced in the Damwal Formation upward into the Kwaggasnek Formations. At this point it is noteworthy to state that the plots shown in Fig. 18 should be interpreted with caution as some of the plots overlap maximum and minimum point values of both $^{87}Sr/^{86}Sr$ and ε_{Nd}. The values exhibited by each sample in Fig. 18 therefore reflect the probability and not the certainty that mixing and contamination commenced in the Damwal Formation.

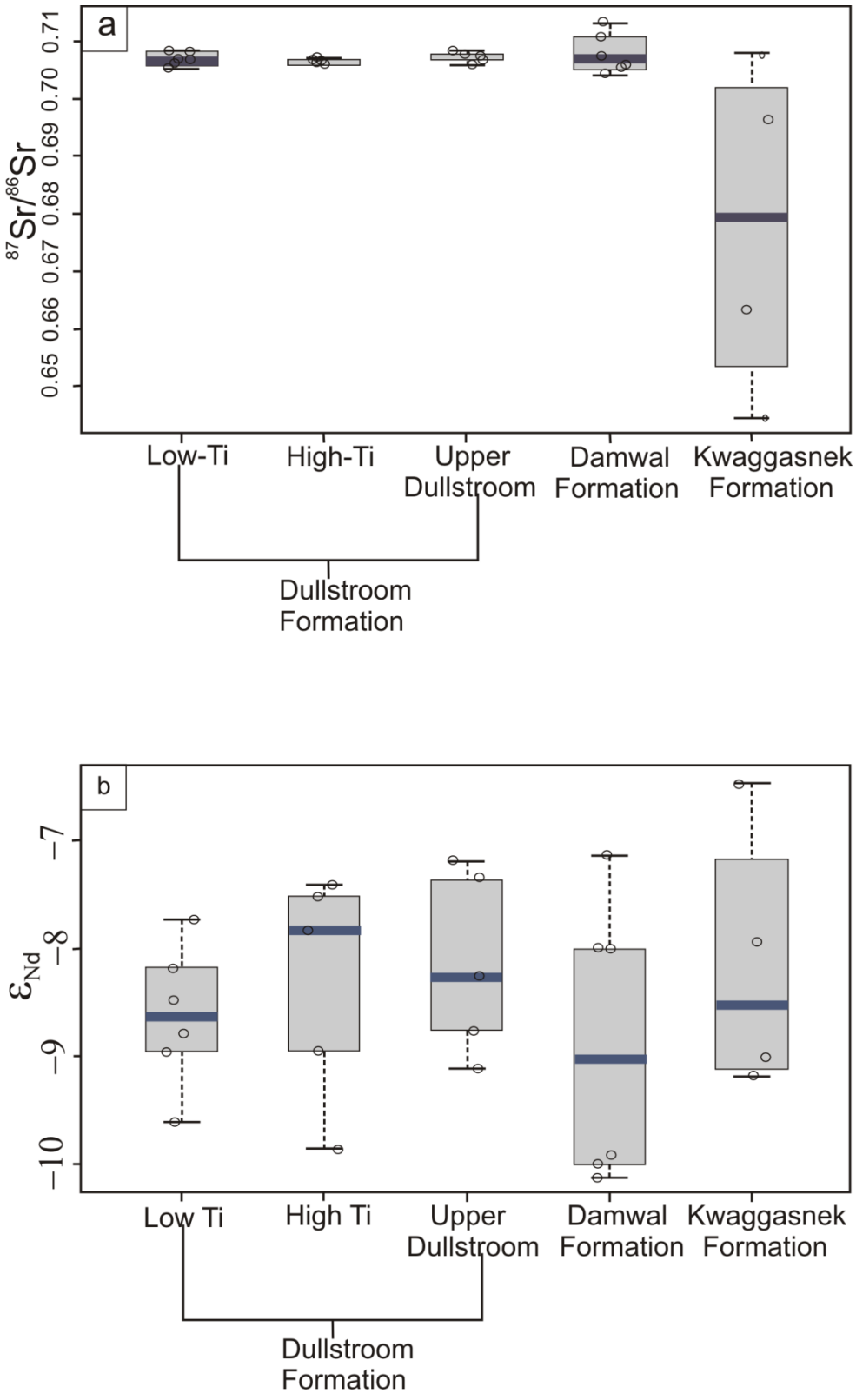

Figure 18: Box plots of the different lava types and formations of the Rooiberg Group Showing the scatter of data sets from the Dullstroom Formation to the Kwaggasnek Formation further supporting Fig. 17, suggesting fractional crystallization in the Dullstroom Formation and mixing/assimilation in the Damwal and Kwaggasnek formations.

Furthermore, plots of $^{87}Sr/^{86}Sr$ vs Rb/Sr and $^{87}Sr/^{86}Sr$ vs Sr (ppm) (Fig. 19) show a deviation of the trend of sample plots from the Dullstroom Formation to the Kwaggasnek Formation within the Rooiberg Group stratigraphy. In Fig. 19a, the Dullstroom Formation lava types show similar $^{87}Sr/^{86}Sr$ and Rb/Sr compositions. However, the Damwal Formation shows higher Rb/Sr values over a small range of $^{87}Sr/^{86}Sr$ values compared to the Dullstroom samples. This deviation is more visible in the samples of the Kwaggasnek Formation exhibiting higher Rb/Sr and $^{87}Sr/^{86}Sr$ values than those of the Damwal Formation. In Fig. 19b, Sris observed to decrease with increasing stratigraphic height. In this plot, the deviation of similar$^{87}Sr/^{86}Sr$ values with increasing stratigraphic height is also observed in the Damwal Formation and the Kwaggasnek Formation, with the latter showing the greatest$^{87}Sr/^{86}Sr$ variation.

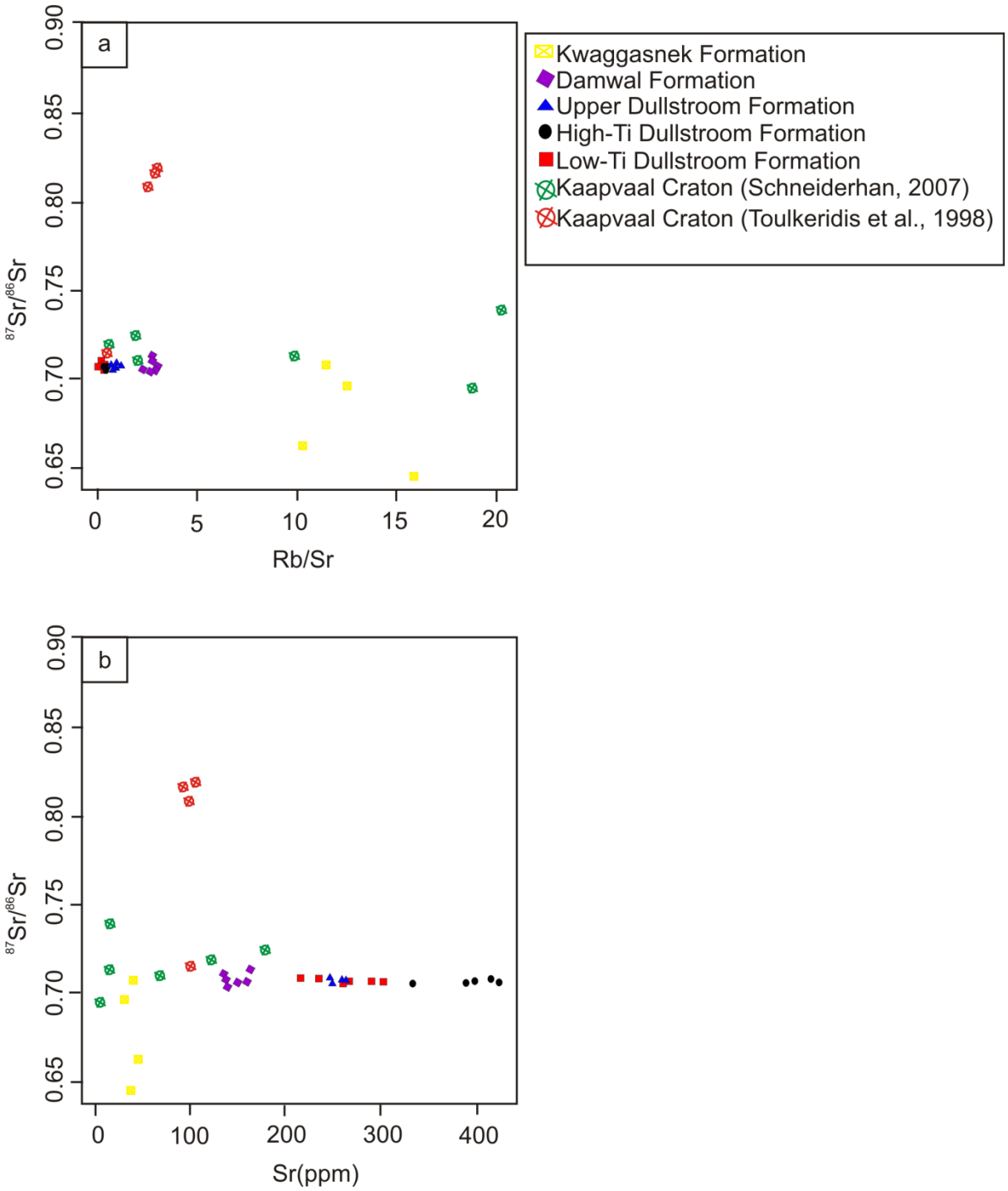

Figure 19: Variations in the $^{87}Sr/^{86}Sr$ and Rb/Sr (Fig. 19a) and $^{87}Sr/^{86}Sr$ and Sr (ppm) (Fig. 19b) between the Rooiberg Group rocks and the sediments from the Kaapvaal Craton. Rooiberg Group samples are same as in Fig. 17, Kaapvaal samples are from Toulkeridis et al. (1998) and the published Ph.D. thesis by Schneiderhan (2007).

Despite isotopic evidence for crustal involvement in the evolution of the Rooiberg Group (especially the upper parts) as presented in Figs. 17 and 19 where there is a deviation from constant $^{87}Sr/^{86}Sr$ values, comparison between the isotopic signatures of the Rooiberg Group

with the mafic rocks of the Rustenburg Layered Suite (RLS) and the Kaapvaal rocks as shown in Fig. 20 exhibit no crustal signatures. The isotopic signatures of the Rooiberg Group and the RLS plot slightly off the mantle array of the bulk silicate earth (BSE) and close to each other, suggesting an origin of mantle source. However the Kaapvaal Craton samples have a high ε_{Nd} isotopic signature and plots away from the mantle array and bulk silicate earth and thus imply that the Kaapvaal Craton did not evolve from the mantle (as expected). The significant difference in isotopic signature between the Rooiberg Group and the Kaapvaal Craton however poses a significant question as the Kaapvaal Craton sediments are the possible crustal contaminant of the mantle-derived melt or the sediments that partially melted to evolve the Rooiberg Group.

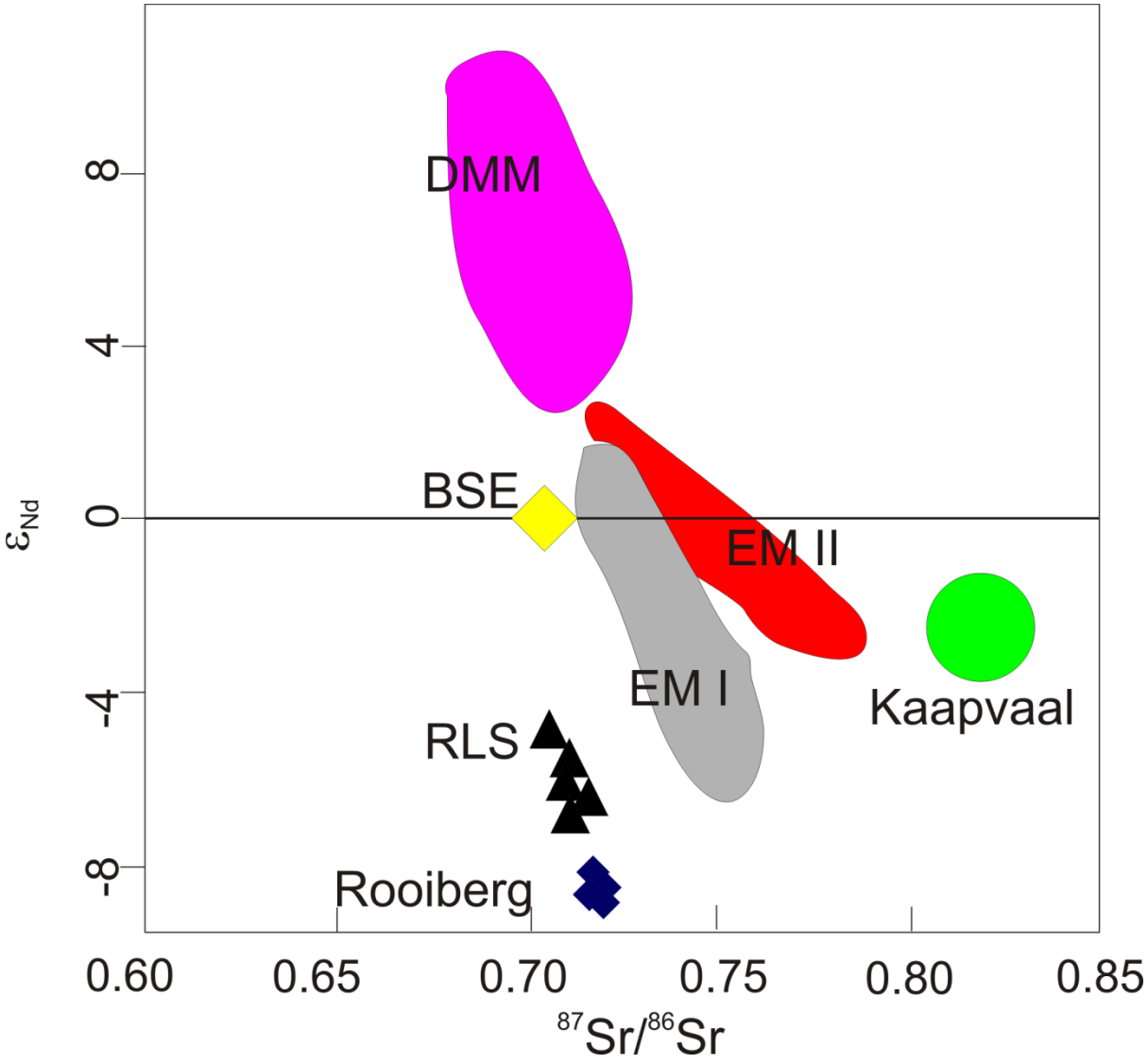

Figure 20: Variations in the initial ε_{Nd} (2.06Ga) and $^{87}Sr/^{86}Sr$ (2.06Ga) among the rocks of the Kaapvaal Craton (Toulkeridis et al., 1998), Rustenburg Layered Suite (RLS) (Pronost et al., 2008) and Rooiberg Group (Buchanan et al. 2004). Also shown is the isotopic composition of the bulk-silicate-earth (BSE) at 2.06 Ga (Workman and Hart, 2005). EM 1- Enriched Mantle I; EM II- Enriched Mantle II; DMM- Depleted Mantle Melt.

Further studies into why there is no initial isotopic evidence for crustal melting as shown in Fig. 20 despite strong evidence provided by trace elements will be conducted in the nearest future. To further ascertain the mode of formation of the Rooiberg Group, modelling the assimilation and fractional crystallization was conducted. Results of the model are presented below.

CHAPTER 6

6.1 MOTIVATION FOR MODELLING

The Rooiberg Group rocks within the Loskop Dam area show evidence of alteration, thereby inducing some degree of uncertainty for the geochemical interpretation. However, LOI and CIA show that alteration has not significantly (comparable to the LOI and CIA values of Altermann and Lehnhardt, 2012) modified the whole-rock composition, therefore attesting to the credibility of the results of this study. As the results of this study have shown, the concentrations of major elements could be useful for regional comparison as already proposed by Schweitzer et al. (1995) and Schweitzer and Hatton (1995). Nevertheless, as long as no detailed geochronological framework for the Rooiberg Group formations exists, any regional correlation is executed with utmost caution. Fractional crystallization and crustal melting as suggested by the trace element and some isotope data shown in this study are proposed as the dominant processes in the evolution of the Rooiberg Group.

Fractional crystallization is also expressed by the varying compositions of these rocks from a mafic suite (high- and low-Ti basalts) in the lower to middle Dullstroom Formation through andesites (and basaltic andesites) and dacites of intermediate composition in the upper Dullstroom Formation to rhyolites in the Damwal, Kwaggasnek and Schrikkloof formations (Buchanan et al., 2002). Examples of compositional change include a decrease in TiO_2 from the lower part of the Rooiberg group, i.e. the Dullstroom and Damwal formations, to the upper parts that include the Schrikkloof Formation and thus suggest a TiO_2-rich magma as the possible parent magma that evolved the Rooiberg volcanics (Figs. 12 and 13). Similarly, MgO, P_2O_5 and Fe_2O_3 in Figs. 13 b, c, and d, respectively, also show a decrease in their concentration up the Rooiberg succession with a simultaneous increase in SiO_2, indicating the occurrence of more mafic rocks in the lower part of the Rooiberg Group and more silicic composition in the upper part of the succession. Fig. 13a shows an increase in SiO_2 from the Dullstroom Formation to the Schrikkloof Formation.The (relatively) high concentration of Ti and Fe in the lower part of the Rooiberg Group is due to the presence of Ti- and Fe-rich minerals such as ilmenite and magnetite observed in the Dullstroom and Damwal formations (as mentioned in the petrography), similar to the findings of Buchanan et al. (1999). These minerals are, however, more abundant in the former than in the latter formation.

Also, apatite is observed by Twist (1985), Buchanan (2002) and Lenhardt and Eriksson (2012), which crystallizes P_2O_5 in the Dullstroom and Damwal formations. Apatite is,

however, absent in the upper part of the Rooiberg succession, i.e. Kwaggasnek and Schrikkloof formations. The reduction of these elements with increase in K_2O (Table 4) and increase in stratigraphy further supports evidence of feldspar as the dominant mineral phase in these studied rocks. Buchanan et al. (2002) described feldspar crystallization as evidence for fractional crystallization. Similar to Buchanan et al. (2002), Sc concentration decrease with decreasing MgO and increasing Zr and with an increase in stratigraphic height.Sc is therefore compatible with the suite of crystallizing minerals in the lower part of the Rooiberg Group, particularly the Dullstroom and Damwal formations. Such crystallizing minerals may include pyroxene as described and observed by Twist (1985) in the Dullstroom Formation.
The Damwal, Kwaggasnek and Schrikkloof formations are more alkaline than the lower Dullstroom Formation and further supports fractional crystallization as the mechanism responsible for the reduction of alkalinity with increase in stratigraphic height.

Low concentrations of trace elements such as Ba, Nb and Sr (Fig. 14a) also support fractional crystallization of residual mantle melt (c.f., Agangi et al., 2012). The depletion of Ba points to the fractionation of alkali feldspar similar to the description of Xu et al. (2010) for the rhyolites of the Emeishan large igneous province (LIP). The role of fractional crystallization in the evolution of the studied rocks can be further expressed by the constant range of Ce/Yb ratio over a wide range of Ce concentration (Fig. 21) (modified after the plot of Xu et al., 2010) as proposed for most silicic rocks. However, the occurrence of Schrikkloof samples (yellow dots) lower than the other formations is suggested as resulting from weathering/alterations of these samples.

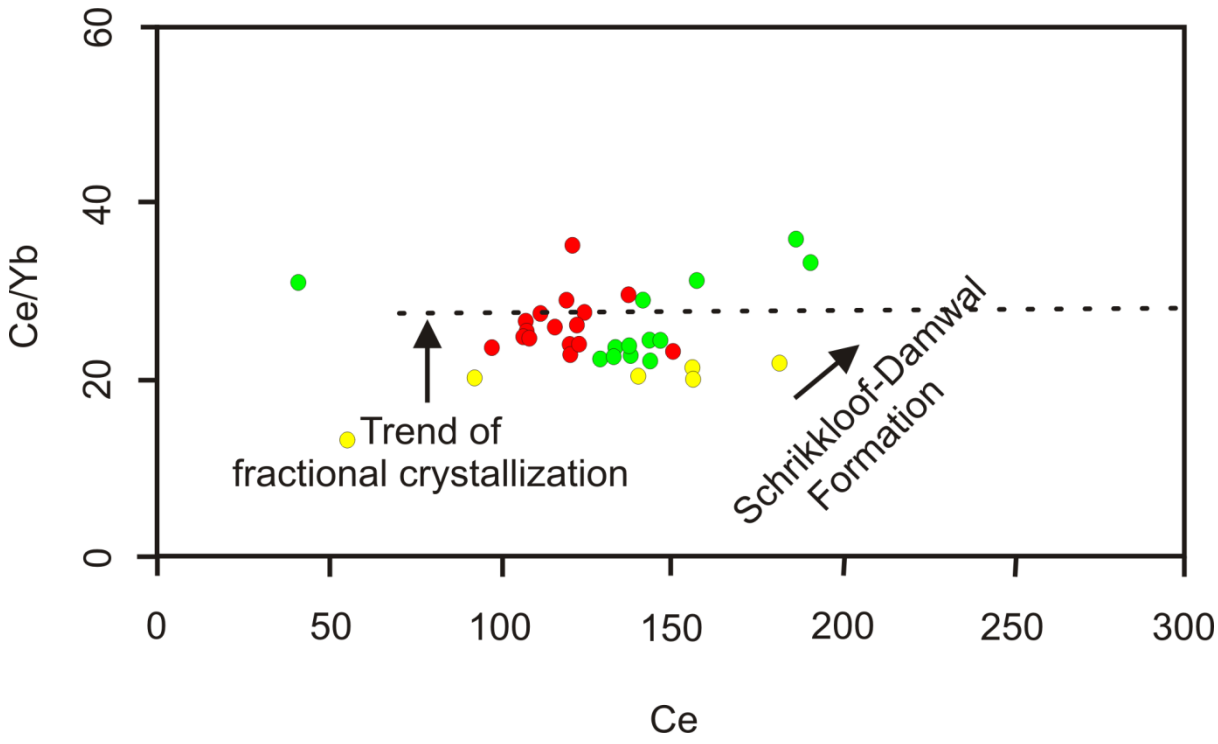

Figure 21: Ce/Yb against Ce of the Rooiberg Group rhyolites modified after Xu et al. (2010). Colours indicate the different formations as shown in Fig. 13. Samples plotted here are from the northeast Loskop Dam used in this study and comprising of Damwal, Kwaggasnek and Schrikkloof formations.

The negative Eu anomaly as shown in Fig. 14b also argues for this hypothesis, supporting fractional crystallization of plagioclase. However, the negative Eu anomaly, shown by the Damwal Formation samples, is not as pronounced as in the Kwaggasnek and Schrikkloof formations and Buchanan et al. (2002) described a complete absence of the negative Eu anomaly from the Dullstroom Formation, i.e. the oldest formation of the Rooiberg Group. VanTongeren and Mathez (2012) further interpreted this characteristic development of the negative Eu anomaly with fractional crystallization that commenced with the crystallization of an Fe-rich fluid to a Si-rich fluid that resulted in the rhyolites in the upper parts of the Rooiberg Group. Furthermore and more recently, Mathez et al. (2013) described the Fe- and Si- enrichment of the upper parts of the Rooiberg Group (the Damwal, Kwaggasnek and Schrikkloof formations) as a result of fractional crystallization of basaltic liquids that formed the older Dullstroom Formation, in which elements such as Ba, Nb, Sr, Ti (Fig 14a) and Sc, V, Cr, Co and Ni (Mathez et al., 2013) are compatible during differentiation.

Despite the strong evidence for fractional crystallization as the dominant process during the crystallization history of the Rooiberg Group, a certain degree of crustal contamination or possibly partial melting of the crust cannot be ignored. Evidence of crustal contamination or melting is shown by the pattern of depleted LREEs together with an enrichment of HREEs that is identical to the composition of the upper crust (crustal composition c.f., White, 2013), cannot be ignored. Buchanan et al. (1999) and Thompson et al. (1983, 1984) described the enrichment in incompatible trace elements as a familiar occurrence in other continental volcanic rocks formed from partial melting of enriched source areas or assimilation of continental crust. The suggestion of crustal assimilation/melting is expressed by the plots of Rooiberg samples in Fig. 15 (according to Pearce et al., 1984) where most samples plot in the WPG field, indicating a mantle-derived melt while few plot transitionally between the WPG and the syn-COLG and VAG field described to represent contamination by continental crust. In Fig. 14a, 8 of the 41 samples plot between the WPG and the syn-COLG and VAG field, representing some contamination and thus suggesting ~19% contamination. On the other hand, Fig. 15b suggests ~10% of contamination as about only 4 samples plot between the WPG and the syn-COLG and VAG field. This discrepancy between the amount of contamination/assimilation between Figs. 14a and b could be one of the errors of plots according to Pearce et al. (1984) which was improved on by Verma et al. (2013).

Similar to Fig. 15, samples in Fig. 16 plot in the CR+OI field which shows increase in the probability that these rocks represent mantle melt while datafor crustal assimilation is shown by samples, about 8 samples as shown in the red circles of Fig. 16a, b and d, plotting transitionally between the CR+OI and CA(+IA) fields. Considering that 8 of the 41 samples represent the contamination, ~19% of contamination during the evolution of the Rooiberg Group is proposed. This further iterates that fractional crystallization is one of the main processes that evolved the Rooiberg Group. Therefore, it is proposed that the percentage of assimilation suggested for the Rooiberg Group could be the result of the upper part of the Rooiberg Group (Damwal, Kwaggasnek and Schrikkloof formations) having trace elements signatures that are identical to crustal compositions. In summary and based on the discriminant plots of acidic rocks in this study, the amount of contamination/assimilation range between ~10% and ~20% indicating the dominance of fractional crystallization during the evolution of the Rooiberg Group.

It cantherefore be suggested that fractional crystallization commenced the formation of the Rooiberg Group rocks in the Dullstroom Formation after which contamination and mixing occurred with continued fractional crystallization in the Damwal Formation which

eventually formed the Kwaggasnek and Schrikkloof formations. Furthermore, from the differences observed in trace and rare earth element characteristics as well as isotope signatures between the Dullstroom Formation and the Damwal, Kwaggasnek and Schrikkloof formations in this study, it is suggested that the main lava types described for the Dullstroom Formation (Hatton and Schweitzer, 1995), i.e. the LTI basaltic andesite, basal rhyolite, HTI basalt and high-Mg felsites, were the original (starting) composition of the crystallizing magma forming the Rooiberg Group and in the Dullstroom Formation. This is supported by the presence of mafic mineral phases such as pyroxene in this region as observed by Twist (1985) and apatite (Twist, 1985; Buchanan et al., 2002). The high-Fe-Ti-P described mainly in the Damwal Formation is proposedto result from the mixing of the earlier described lava types within the Dullstroom Formation while the low-Mg felsites ubiquitous in the Damwal, Kwaggasnek and Schrikkloof formations is suggested to be the result of crustal contamination.

Isotope plots of $^{87}Sr/^{86}Sr$ and ε_{Nd} against height, on the other hand, strongly suggest a crustal origin for the Rooiberg Group, especially the upper part. As displayed in Fig. 17a showing $^{87}Sr/^{86}Sr$ against height, samples represented by different lava types are seen to display an almost linear trend within the Dullstroom Formation. This linear trend becomes less prominent in the Damwal Formation and disappears in the Kwaggasnek Formation. It is therefore suggested that fractional crystallization commenced evolution of the Rooiberg Group within the Dullstroom Formation while mixing and contamination commenced in the Damwal Formation and later evolved the Kwaggasnek Formation. In Figure 17b, a decrease in the ε_{Nd} values is observed in the different lava types of the Dullstroom Formation with increase in stratigraphy. This decrease in ε_{Nd} values within the Damwal Formation begin to form an irregular pattern which is much more visible in the Kwaggasnek Formation. Here, it is proposedthat crustal meltingis responsible for the Damwal and Kwaggasnek formations while fractional crystallization of a mafic liquid (and assimilation of crustal material) is the lone process that evolved the Dullstroom Formation samples. The increase in $^{87}Sr/^{86}Sr$ values and subsequent decrease in ε_{Nd} values as exhibited by the Rooiberg samples strongly support assimilation during fractional crystallization during as suggested by Tegner et al. (1998).

Further investigations to ascertain assimilation during fractional crystallization of the Rooiberg Group included isotopic plots according to DePaolo (1981) in Fig. 19. Figure 19a shows a constant $^{87}Sr/^{86}Sr$ values with increasing Rb/Sr values for the different lava types of the Dullstroom Formation thereby suggesting fractional crystallization as the main process in this formation. This constant $^{87}Sr/^{86}Sr$ values start to form a spread in the Damwal Formation and becomes more pronounced and reduced in the Kwaggasnek Formation with increasing Rb/Sr values. The reduction of the $^{87}Sr/^{86}Sr$ values with increasing Rb/Sr suggests contamination that commenced within the Damwal Formation and became more pronounced in the Kwaggasnek Formation. Similarly, Fig.18b exhibits more clearly, a similar increase in the $^{87}Sr/^{86}Sr$ values with decrease in Sr (ppm) as exhibited by the different lava types of the Dullstroom Formation, suggesting fractional crystallization as the lone process in this formation. Again, the Damwal Formation starts to form a spread which is more pronounced in the Kwaggasnek Formation and thus suggest a process of assimilation during fractional crystallization of these formations. Noteworthy at this point is that most of the signatures, especially isotope values, of the rocks in this study are identical to crustal compositions. For example, the ε_{Nd}values of the Rooiberg Group formations range between -10 and -7 which aresimilar to the values of crustal composition. This further supports that the crust plays a major role in the formation of the Rooiberg Group, contradicting the idea of fractional crystallization of mantle-derived melt. The significant involvement of the crust in the evolution of the Rooiberg Group from partial melting of the crust could also be the major reason why the upsection increase in $^{87}Sr/^{86}Sr$ values as displayed in Figs. 17a and 18a are not very well exhibited, especially when comparing the Dullstroom Formation with the Damwal and Kwaggasnek formations. At this juncture, it is important to state that though crustal melting and or assimilation played a major role in the formation of the Rooiberg Group, the processes involved in the evolution of the Dullstroom Formation is not exactly identical as the processes that crystallized the Damwal and Kwaggasnek formations. This is supported by the markedly different trends exhibited in Figs. 17 (and 18) and 19.Also, as exhibited in Fig. 16, majority of the Rooiberg samples plot in areas with crustal signatures such as the CR+OI, Col, CA and CA+IA and thus further impressing that partial melting of the crust during the Rooiberg Group formation cannot be ignored.

6.2 ASSIMILATION AND FRACTIONAL CRYSTALLIZATION MODELLING

In recent time, crustal contamination has been described as a process that occurs during fractional crystallization and evolution of SLIPs (including the Rooiberg Group) (Huppert et al., 1985; Wade et al., 2012). To determine the occurrence of these processes and their amount, the assimilation and fractional crystallization of the Rooiberg Group rocks was determined using Petromodeler (according to Ersoy, 2013). This program is used because it models magmatic processes such as melting, crystallization, assimilation and mixing. For the process of crystallization, the purpose for which it is used in this study, models such as perfect equilibrium, perfect fractional crystallization (PFC), equilibrium crystallization-imperfect fractional crystallization (EC-IFC), zoned crystallization-imperfect fractional crystallization (ZC-IFC) and combined assimilation and fractional crystallization (AFC) can be conducted. The Petromodeler AFC trend for the Rooiberg Group was conducted using major and trace elements as well as isotopic ratios.

The results of the modeller are shown in Fig. 22. Here mixing of a possible mafic magma, the Rustenburg Layered Suite (RLS) composition (Voordouw et al., 2009) is conducted with a contaminant which is represented by sediments from the Kaapvaal Craton (data obtained from Toulkeridis et al., 1998 and Schneiderhan, 2007). The RLS is used as the crystallizing mafic liquid since it is the possible mantle source in the Bushveld province while sediments of the Kaapvaal Craton are selected as the possible contaminats because these are the crustal rocks surrounding or into which the Bushveld Magmatic Province intruded (the Rustenburg Layered Suite) or extruded (the Rooiberg Group).

The mixing line generated by mixing the starting composition represented by the RLS sample with the contaminant (FTG 2, Fig. 22a) is similar to the starting mafic composition, although not as mafic. Furthermore, the composition generated by the mixture is dissimilar to any of the Rooiberg samples, and suggesting that contamination of mafic magma by crustal source may not result in compositions as shown by the Rooiberg. To ascertain this, a Rooiberg sample (SM 23) sample is mixed with the crustal contaminant (FTG2, Fig. 22b) and a mixing line similar to the original composition is observed. FTG 2 (obtained from Toulkeridis et al., 1998) represents a sample of crustal composition (Kaapvaal Craton) that is most likely to be the Rooiberg contaminant. It is interpreted in this study that if the Rooiberg sample and the crustal contaminant though having similar composition, evolved from different sources, the line of mixing should reflect a different composition as shown in Fig. 22a. The line of mixing

produced from contamination the Rooiberg sample with crustal material is same as the Rooiberg sample composition thereby suggesting similar sources for the two rock types.

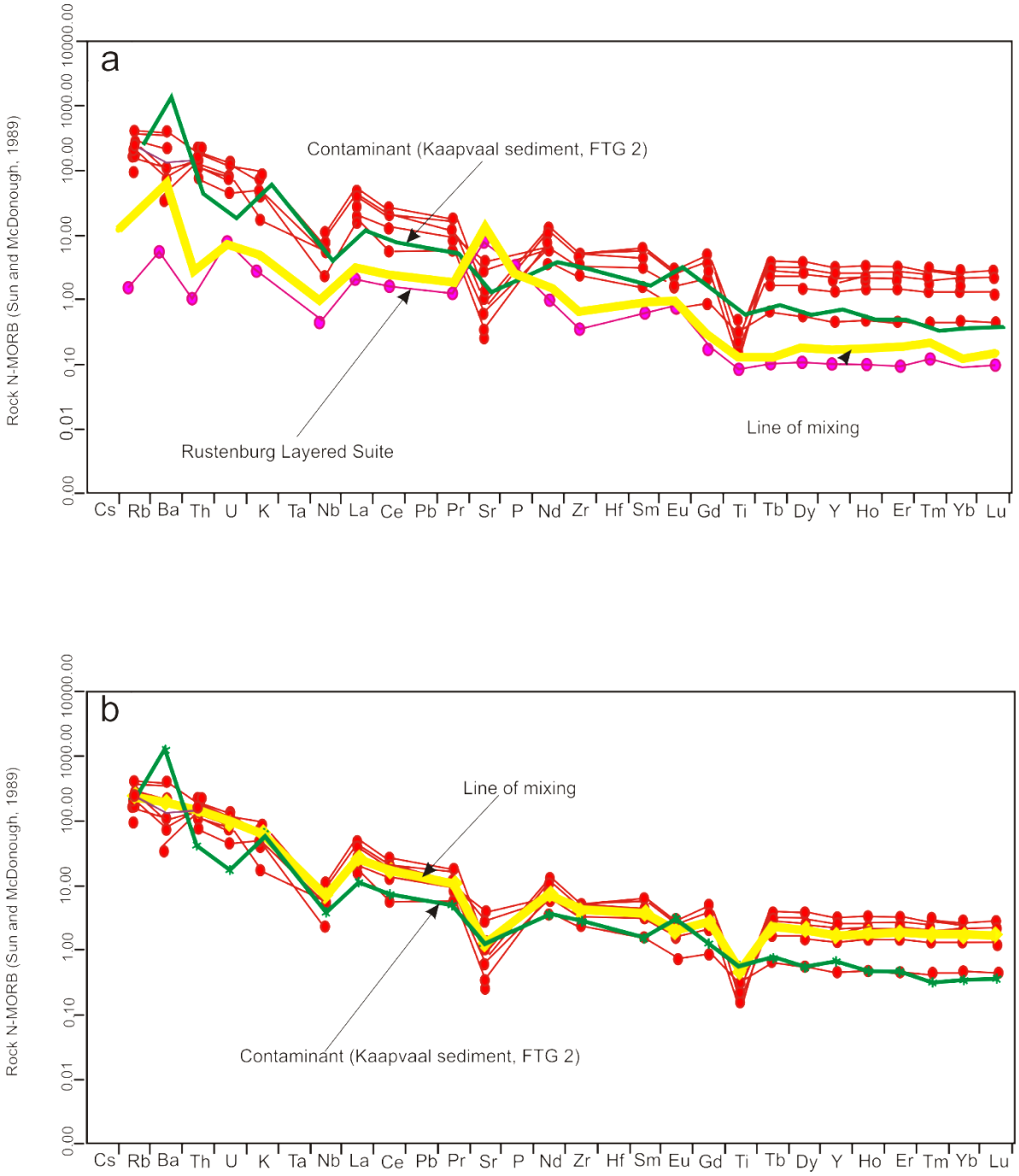

Figure 22: Plots showing the line of mixing between the Rustenburg Layered Suite (RLS), Rooiberg Group samples and Kaapvaal sediments (contaminant). (a) Mixing between RLS sample and FTG 2 (contaminant); (b) mixing between Rooiberg sample and FTG 2 (contaminant). Both samples, RLS and FTG 2 used in this model are obtained from Voordouw et al. (2009) and Toulkeridis et al. (1998) respectively.

CHAPTER 7

7.1 INTERNATIONAL SLIPS

Comparison between some geochemical signatures of the Rooiberg Group and other SLIPs from around the world is conducted to ascertain the evolution of SLIPs regardless of their location on earth. SLIPs used in comparison of geochemical characteristics to the Rooiberg Group include the Snake River Plain (USA) (McCurry et al., 2008), Keweenawan (Central Atlantic Magmatic Province) (Nicholson, 1992), Paraná-Etendeka (Brazil-Namibia) (Garland et al., 1995; Kirstein et al. 2000), Karoo-Ferrar (South Africa-Antarctica) (Peucat et al., 2002) and the Gawler Range Volcanics (Australia) (Kamenetsky et al., 2000) as shown in Fig. 2. Since trace and rare earth elements are used to decipher the source of the Rooiberg Group, these elements will also be used for the other SLIPs in comparison to the Rooiberg Group. Table 8 shows the different SLIPs used for comparison as well as the elements.

Table 7: Data of other SLIPs used in comparison with the Rooiberg Group.

Location	TiO_2	MgO	P_2O_5	Y	Zr	Nb	Ta	Nb	Yb
KAROO-FERRAR	0.31	0.40	0.05	44.0	225	16	1.40	16	4.50
KAROO-FERRAR	0.46	0.88	0.14	38.0	266	14	1.20	14	4.30
KAROO-FERRAR	0.47	0.96	0.12	34.0	270	13	1.10	13	3.70
KAROO-FERRAR	0.36	0.24	0.00	51.0	314	18	1.50	18	5.50
KAROO-FERRAR	0.47	0.84	0.14	34.0	286	12	1.00	12	3.60
KAROO-FERRAR	0.46	0.91	0.15	37.0	297	13	1.10	13	3.90
KAROO-FERRAR	0.47	0.90	0.13	34.0	277	12	1.00	12	3.70
KAROO-FERRAR	0.46	1.11	0.13	36.0	270	12	1.00	12	3.80
AUSTRALIA(GRV)	0.25	0.31	0.03	na	na	na	na	na	na
AUSTRALIA(GRV)	0.26	0.4	0.01	na	na	na	na	na	na
AUSTRALIA(GRV)	0.39	0.29	0.06	61.6	500	25	na	25	na
AUSTRALIA(GRV)	0.36	0.32	0.05	59.6	481	27	na	27	na
AUSTRALIA(GRV)	0.29	0.29	0.04	62.8	443	27	na	27	na
AUSTRALIA(GRV)	0.4	0.31	0.07	63.0	500	25	na	25	na
AUSTRALIA(GRV)	0.35	0.32	0.05	61.7	461	26	na	26	na
AUSTRALIA(GRV)	0.43	0.54	0.09	60.9	484	25	na	25	na
AUSTRALIA(GRV)	0.45	0.36	0.10	61.5	488	24	na	24	na
AUSTRALIA(GRV)	0.42	0.83	0.08	63.2	490	25	na	25	na
AUSTRALIA(GRV)	0.38	0.48	0.07	61.0	489	25	na	25	na
AUSTRALIA(GRV)	0.43	0.69	0.09	60.3	473	24	na	24	na
AUSTRALIA(GRV)	0.39	0.34	0.07	59.0	495	25	na	25	na
AUSTRALIA(GRV)	0.28	0.40	0.04	62.2	407	27	na	27	na

Location	TiO_2	MgO	P_2O_5	Y	Zr	Nb	Ta	Nb	Yb
AUSTRALIA(GRV)	na	0.21	0.06	35.2	321	18	1.62	18	3.29
AUSTRALIA(GRV)	na	0.36	0.02	17.5	95	17	1.75	17	1.77
AUSTRALIA(GRV)	na	0.44	0.02	60.4	231	22	2.50	22	5.97
AUSTRALIA(GRV)	na	0.34	0.05	44.1	233	20	2.35	20	5.05
AUSTRALIA(GRV)	na	0.16	0.03	101.9	147	43	7.93	43	14.09
AUSTRALIA(GRV)	0.35	0.75	0.03	48.0	413	22	na	22	na
AUSTRALIA(GRV)	0.32	0.36	0.06	53.0	312	24	na	24	na
AUSTRALIA(GRV)	0.31	0.32	0.04	60.0	298	23	na	23	na
CAMP	0.72	2.28	0.15	43.0	398	25	2.19	25	3.59
CAMP	0.64	1.69	0.13	48.0	431	26	2.14	26	4.69
CAMP	0.94	2.72	0.18	38.0	355	21	1.76	21	3.80
CAMP	0.04	0.07	0.01	na	na	na	na	na	na
PARANA-ETENDEKA	0.72	0.68	0.21	88.0	316	23	2.00	23	23.00
PARANA-ETENDEKA	0.66	0.62	0.2	55.0	317	25	na	25	25.00
PARANA-ETENDEKA	0.70	0.54	0.2	60.0	315	24	na	24	24.00
PARANA-ETENDEKA	0.73	0.59	0.21	47.0	309	23	na	23	23.00
PARANA-ETENDEKA	0.70	0.86	0.21	49.0	306	22	na	22	22.00
PARANA-ETENDEKA	0.72	1.32	0.21	55.0	304	22	na	22	22.00
PARANA-ETENDEKA	0.71	0.64	0.21	50.0	309	23	na	23	23.00
PARANA-ETENDEKA	0.73	0.90	0.2	53.0	309	24	2.07	24	24.00
PARANA-ETENDEKA	0.72	0.39	0.21	44.0	313	23	na	23	23.00
PARANA-ETENDEKA	0.68	0.47	0.2	67.0	317	23	na	23	23.00
PARANA-ETENDEKA	0.66	0.81	0.2	43.0	316	24	na	24	24.00
PARANA-ETENDEKA	0.70	0.74	0.19	43.0	315	24	na	24	24.00
PARANA-ETENDEKA	0.68	0.81	0.2	57.0	321	25	na	25	25.00
PARANA-ETENDEKA	0.67	0.65	0.19	51.0	321	25	na	25	25.00
PARANA-ETENDEKA	0.66	0.37	0.19	57.0	319	24	2.00	24	24.00
PARANA-ETENDEKA	0.64	0.56	0.19	53.0	321	25	na	25	25.00
PARANA-ETENDEKA	0.66	1.11	0.19	53.0	322	24	na	24	24.00
PARANA-ETENDEKA	0.70	0.56	0.2	54.0	319	25	na	25	25.00
PARANA-ETENDEKA	0.68	0.55	0.2	49.0	321	25	na	25	25.00
PARANA-ETENDEKA	0.95	1.48	0.25	42.0	254	21	1.74	21	21.00
PARANA-ETENDEKA	0.98	1.75	0.29	78.0	252	21	1.77	21	21.00
USA (Snake River Plain)	0.11	0.05	0.02	100.0	175	39	2.16	39	10.50
USA (Snake River Plain)	0.16	0.01	0.01	76.0	457	26	1.35	26	7.90
USA (Snake River Plain)	0.28	0.63	0.07	23.0	196	10	0.84	10	2.70
USA (Snake River Plain)	0.17	0.15	0.02	44.0	251	11	0.74	11	4.80
USA (Snake River Plain)	0.22	0.19	0.04	41.0	293	32	1.90	32	4.50

* CAMP-Central Atlantic Magmatic Province (Keweenawan); GRV-Gawler Range Volcanics.

Figure 23 shows the trace element and rare element plots of the different SLIPs and the Rooiberg Group (field data in black colour). The different SLIPs show identical negative spikes of elements such as Ba, Nb, Sr and Ti (Fig. 23a), although the Karoo-Ferrar province exhibit the greatest depleted concentrations of Ba and Sr while the Gawler Range Volcanics of Australia, though second in depleted Sr, display the highest depletion in Ti. The highest depletion of Ba and Sr in the Karoo-Ferrar province may be as a result of the high silicic composition of the province. In Fig. 23b all slips exhibit identical LREEs enrichment with minor depletion of the HREEs, with all exhibiting the negative Eu anomaly except for the Keweenawan of the Central Atlantic Magmatic Province (CAMP) which may be because the CAMP is a mafic-dominated province.

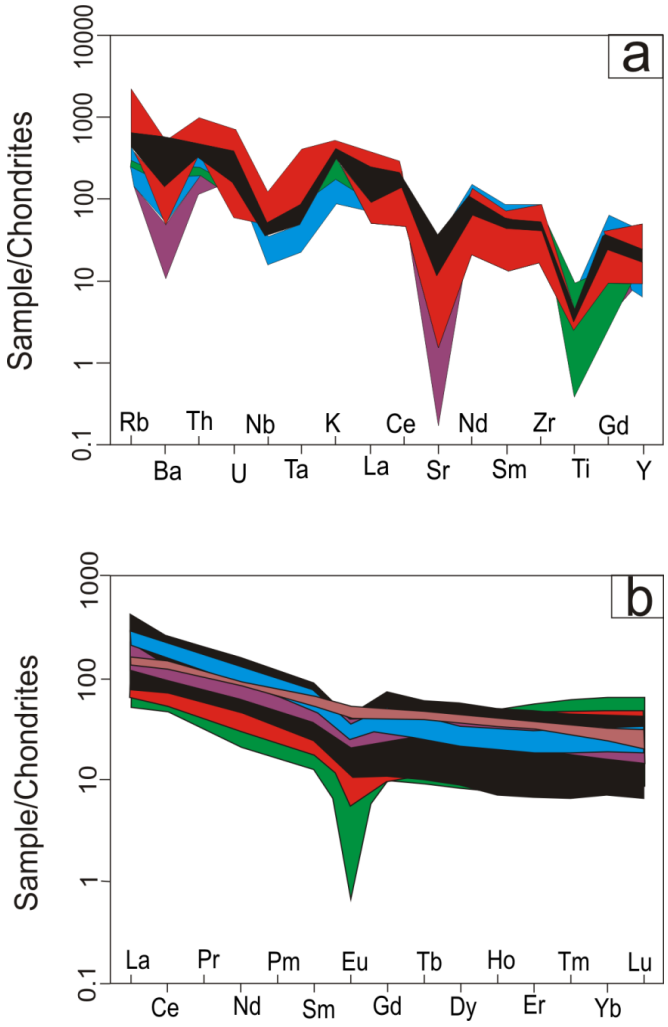

Figure 23: Trace element (a) and REE (b) plots of international SLIPS. Note- black colour represents the Rooiberg Group, red-Snake River Plain, brown-Central Atlantic Magmatic Province, Purple-Paraná-Etendeka, blue-Karoo-Ferrar and green-Gawler Range Volcanics.

Fig. 24 has been able to establish similar signatures of trace and rare earth elements between SLIPs around the world (including the Rooiberg Group), it is on this basis further comparisons between SLIPs is conducted using discrimination diagrams such as that used for the Rooiberg Group in Figs. 15 and 16 since these discrimination diagrams mainly use trace elements in their classification.

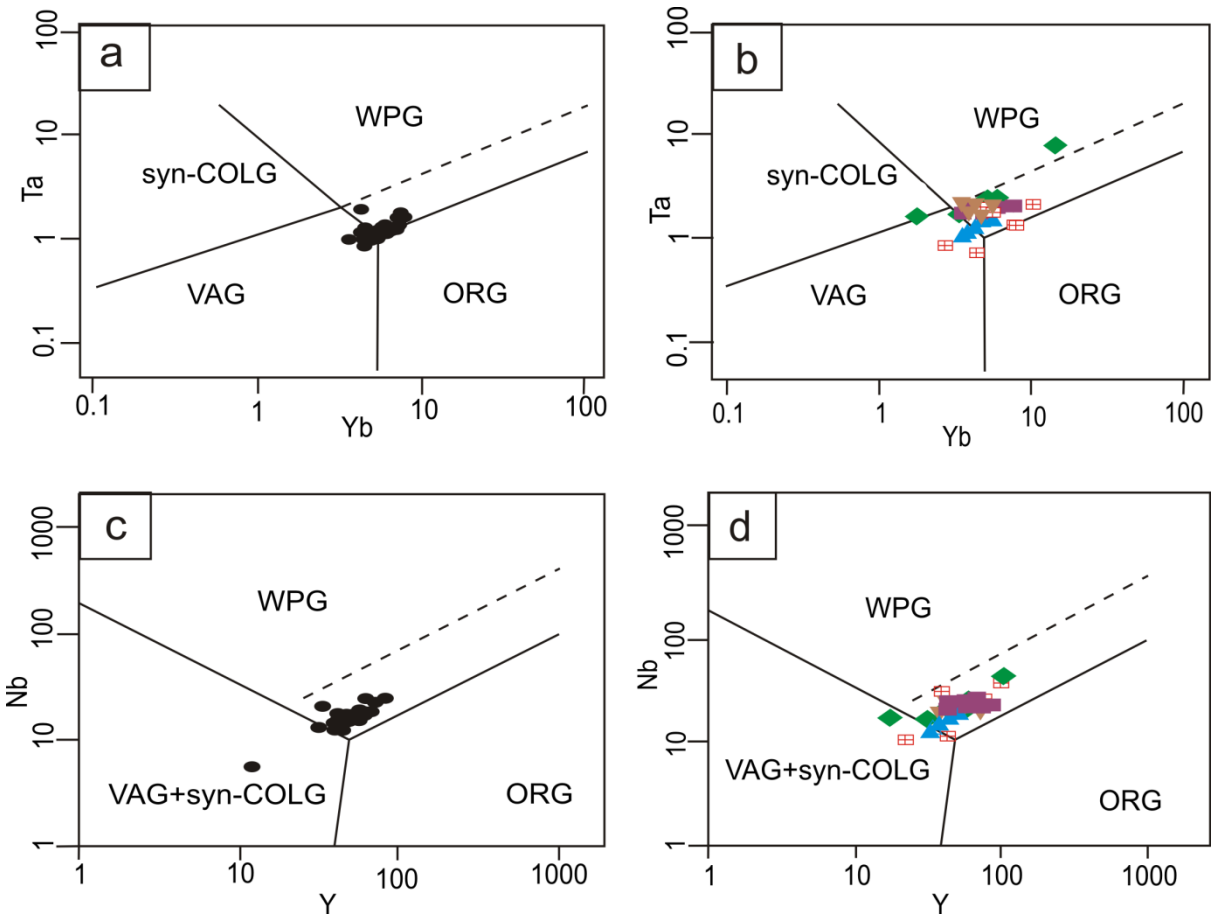

Figure 24: Comparison of the tectonic discrimination diagrams according to Pearce et al. (1984). (a) and (c) are Rooiberg plots while (b) and (d) are similar discriminant plots including data of other SLIPs.

Fig. 24b of the international SLIPs show that most of the samples plot in the WPG field with few samples plotting transitionally between the boundaries of the WPG and VAG and one

sample plot between the VAG and syn-COLG field. This plot is very similar to the Rooiberg Group plot in Fig. 24a, however, it important to note that the samples that plot across the boundaries in Fig. 24b are samples of the more silicic SLIPs such as samples from the Snake River Plain, the Karoo and Ferrar province and the Gawler Range Volcanics. Furthermore, samples of the Keweenawan Province of the Central Atlantic Magmatic Province plots only in the WPG field which is proposed to result from its mafic-dominated rocks. Also, similar to the plots of the Rooiberg Group in Fig. 24c the international SLIPs again plot mostly in the WPG field with few samples plotting transitionally across the WPG and VAG+syn-COLG fields (Fig. 24d). Of importance is the occurrence of fewer samples plotting across the WPG and VAG+syn-COLG fields in Fig. 24d (and Fig. 24c) when compared to Fig. 24b and d respectively. These plots can, therefore, be interpreted similar to Fig. 15 that the samples in the WPG field suggest a mantle-derived melt while those that plot along the boundaries of WPG and VAG+syn-COLG fields are evidence of contamination or assimilation.

Evidence supporting the evolution of SLIPs from a mantle-derived melt and contaminated by crustal material is shown in Fig. 25, utilizing the more accurate discriminant plots of Verma et al. (2013) for acidic rocks (as exhibited in Fig. 16 for the Rooiberg Group). International SLIPs in Fig. 25 mostly plot in the CR+OI field (representing the WPG field) with a few data points plotting across the CR+OI and CA and or Col fields. In all the plots (Figs 25a-e) the Karoo-Ferrar and Keweenawan provinces plot across the CR+OI and CA and or Col fields, this may indicate a high amount of contamination. The Snake River Plane samples do not plot in Fig. 25 and this is suggested to be due to the low TiO_2 content (< 0.3 wt.%) of the rocks as TiO_2 is one of the key parameters used in the classification scheme.

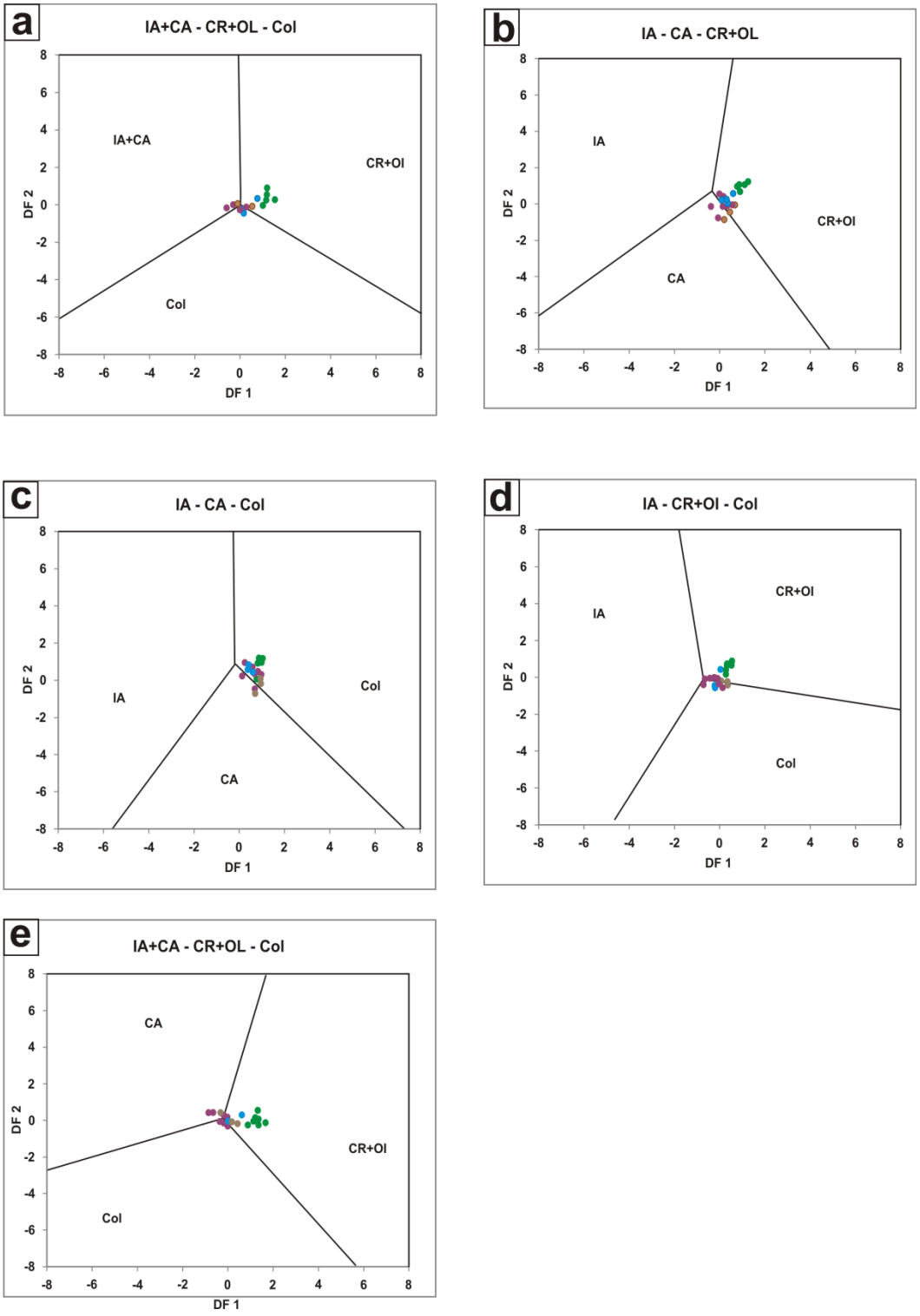

Figure 25: Acid rock discrimination plots (according to Verma et al., 2013) of other Slips around the world. Noteworthy is the absence of the Snake River Plain province, this might be due to the low TiO_2 content as shown in Table 8.

7.2 INTERPRETATION OF INTERNATIONAL SLIPs DATA

Different international SLIPs have exhibited similar trace and rare earth element geochemistry, regardless of their location on earth. Depleted amount of Ba and especially Sr indicates that these rocks evolve from a mantle-derived melt depleted in the fractionation of plagioclase. One significant characteristic exhibited by the SLIPs is depletion in Ti (as TiO_2) that decreases in concentration with increase in stratigraphic height in the different provinces. The depletion of TiO_2 with increase in stratigraphic height is thought as the compatibility of Ti with the crystallization of the mafic minerals that typically crystallize out early from the (usually more) mafic parental mantle-derived magma that evolve SLIPs. Evidence that support the decrease in TiO_2 is the presence of Fe-Ti bearing minerals such as ilmenite that crystallize during the early stages in SLIP evolution.

Despite the evidence of a mantle-derived melt for the formation of SLIPs, the markedly present negative Eu anomaly exhibited by SLIPs is interpreted as the involvement of crustal melting during the genesis of these rocks. All the SLIPs presented in this study as shown in Fig. 23b exhibit the Eu anomaly except for Keweenawan province. The lack of the Eu anomaly in the Keweenawan province is proposed to be due to the fact the province is mafic dominated (rhyolites are about 10-25% of the entire province, Vervoort et al., 2007) than the other SLIPs. Also supporting crustal involvement during the formation of the different SLIPs is the pattern of enriched LREEs and Slight depletion of HREEs exhibited in Fig. 23b. Figures 24 and 25 further show evidence of crustal melting or assimilation during the formational processes of SLIPs. In Fig. 24, data points that plot transitionally between the WPG and the VAG+syn-COLG fields are interpreted to indicate presence of crustal material during the formation of these SLIPs. Similar interpretation is executed in Fig. 25 where some SLIP samples plot transitionally between the CR+OI and CA and or Col fields and described as suggesting crustal involvement. However, it is important to note that the number of samples from the different SLIPs plotting transitionally between the WPG and the VAG+syn-COLG fields and the CR+OI and CA and or Col fields represented in Figs. 23 and 24 respectively are much fewer than those that plot in the WPG or CR+OI fields. The difference in samples plotting in the different fileds in Figs. 24 and 25 are an indication that the process of formation of the samples in the WPG or CR+OI fields (fractional crystallization) is more dominant than the process that form the samples plotting WPG and the VAG+syn-COLG fields and the CR+OI and CA and or Col fields (crustal contamination/assimilation).

CHAPTER 8

8.1 THERMOMETRY

In this chapter, estimates of the pressure (P), temperature (T) and water content present during the process of evolution of the Rooiberg Group is modelled. To model these three parameters, a modelling program according to Putirka (2008) is employed. Thermometers and barometers for volcanic systems (Putirka, 2008) are therefore used to execute modelling of P, T and water content of the Rooiberg Group. Putirka (2008) showed results of plagioclase- and alkali feldspar-liquid thermobarometers as well as orthopyroxene and orthopyroxene-liquid thermobarometers. This chapter however presents results of estimated P, T and water content of the Rooiberg Group using the plagioclase thermobarometer. The new thermobarometers (according to Putirka, 2008) are based on the earlier model of Putirka (2005b). Putirka (2005b) improves on the calibration of Sugawara (2001) and models of Ghiorso et al. (2002) of MELTS. Sugawara (2001) and Ghiorso et al. (2002) provided accurate estimates for T of existing models but failed for calculations of T <1100 °C and for hydrous systems.

The plagioclase thermobarometer of Putirka (2005b) yields high precision using data from Library of Experimental Phase Relation (LEPR) but a global regression of ~6 °C improvement in the standard error of estimate (SEE) (Putirka, 2008). However, the results of the thermobarometer of Putirka (2005b) are not reliable due to reasons such as potiential loss of Na when experiments were executed in an open furnace (Putirka, 2008). Putirka further highlighted that Na loss is not an issue as long as experiments to be modelled are conducted in sealed glass tubes, internally heated pressure vessels or in piston-cylinder apparatus. As a result, these thermobarometers perform well with some data sets and not for others. While the results of this plagioclase barometry may be unreliable, the plagioclase-liquid equilibrium might be used as a hygrometer, as long as T is well established (Putirka, 2008), although T does affect the estimates of water content obtained. For instance, a ± 38 °C error in T can produce a ±1.0 wt.% error in water content. However, Putirka (personal communication) stated that the pressure and water content estimates using this thermobarometer are not reliable because the program does not work with all compositions (does not work with all basaltic compositions) and water estimates are very sensitive to pressure. This barometer is more useful and reliable for the temperature estimates. Furthermore, the pressure and water estimates using the program according to Putirka (2008) yields high values (as shown in

Table 9), contrasting to other volcanic provinces such as the Snake River Plain that exhibit <5 Kbar pressure and described as water-undersaturated (Leeman et al., 2008).

Table 8: Results of microprobe analyses and thermobarometry using the spreadsheet of Putirka (2008)

Sample	Formation	SiO_2	TiO_2	Al_2O_3	Fe_2O_3	MnO	MgO	CaO	Na_2O	K_2O	BaO	Total	T(°C)	H_2O (wt. %)	P(kbar)
LD019 P2	Damwal	98.58	0.08	0.63	0.13	0	0	0.06	0.06	0.05	0	99.59	961.7264	6.969286	17.32746
LD019 P4	Damwal	69.28	0	21.06	0.05	0	0	0.78	8.56	0.3	0	100.03	1038.185	10.21858	38.8242
LD019 P5	Damwal	77.58	0.2	11.08	5.21	0.01	0.02	0.12	3.89	0.92	0.05	99.08	1012.127	11.30553	42.378
LD019 P6	Damwal	86.52	0.01	8.97	0.66	0	0	0.07	3.74	0.14	0.01	100.12	1002.073	10.49358	37.62332
LD019 P8	Damwal	70.36	0	20.66	0.33	0	0	0.14	7.98	0.25	0	99.73	1012.981	11.47916	43.30721
LD026 P6	Damwal	70.28	0	20.83	0.13	0	0	0.17	8.21	0.09	0.01	99.72	1042.785	10.70365	48.12119
LD026 P1	Damwal	67.62	0	19.8	0.15	0.06	0	0.64	11.62	0.09	0.01	99.99	1059.238	11.75181	55.08714
LD026 P2	Damwal	68.01	0.01	20.01	0.11	0.01	0.01	0.43	11.4	0.23	0.02	100.23	1080.058	13.4394	65.74201
LD007 P2	Kwaggasnek	70.98	0.03	20.88	0.1	0	0	0.03	7.38	0.08	0.01	99.49	1077.715	17.1197	75.40927
LD007 P3	Kwaggasnek	70.17	0.01	20.58	0.07	0	0	0	8.96	0.05	0	99.85	1090.413	18.00854	80.75835

Note: The different values of temperature, Pressure and water content are obtained from results of microprobe analysis on plagioclase grains occurring within the Damwal and Kwaggasnek formations. Different “P” numbers on the samples indicate a different microprobe analysis.

Estimates of T, P and water content using Putirka (2008) was successful using both major element and electron microprobe data of feldspar (plagioclase) of some samples that represent the Rooiberg Group. Table 9 shows the results obtained for T, P and water content using the thermobarometer. Plagiclase data of four samples representing the Rooiberg Group were used in this chapter. At first, samples were selected to represent the four formations within the Rooiberg Group, however, samples representing Schrikkloof (and many of the Kwaggasnek) Formation did not yield any result. Investigation into the inability of the Schrikkloof Formation to yield any result is in progress and subsequent studies will give details on this issue, however, the idea that the Schrikkloof samples are too altered to yield any result may be responsible for the failure of the Schrikkloof samples to yield any results. At the moment, three samples representing the Damwal Formation and one sample representing the Kwaggasnek Formation were successfully accounted for using the program according to Putirka (2008). These samples are exhibited in Table 9. Temprature (T) increases from ~961.7 °C in the Damwal Formation to ~1090.4 °C in the Kwaggasnek Formation. This range of temperature occurs within the estimated range of temperatures for the Rooiberg Group according to Lenhardt and Eriksson (2012). Pressure (P) increases from ~17.3 kbar in the Damwal Formation to ~80.8 kbar in the Kwaggasnek Formation. Also increasing with increase in stratigraphic height from the Damwal Formation to the Kwaggasnek Formation is the water content. The water content increases from ~6.5 wt.% in the Damwal Formation to ~18.0 wt.% in the Kwaggasnek Formation.

8.2 DISCUSSION OF THERMOMETRY

A change in composition from dacitic to rhyolitic flow is usually accompanied by a temperature drop. However, the results of modelling (using Putirka, 2008) for the Rooiberg Group indicate an increase in the temperature from the Damwal Fromation to the Kwaggasnek Formation. The best possible explanation for this increase is proposed to be the subsequent rise in the the heat source that induce melting of the crust. It is proposed that the possible source of heat, Bushveld (Rustenburg Layered Suite) magma, rises from depth as it melts the overlying (upper) continental crust. Melting of the crust with simultaneous fractional crystallization and eruption can therefore lead to the creation of space for the ponding magma. The space formed will also result in a higher density of the underlying and ponding magma, thus, resulting in an upward movement due to density difference between the underlying ponding magma and the overlying melting crust. This idea further supports partial melting of the crust for the formation of the Rooiberg Group.

Mangan et al. (2004) described the effect of water content (and CO_2) in the nucleation and exsolution of gass bubbles (vesicles). These authors performed experiments of both homogenous and heterogenous nucleation. Mangan et al. (2004) and Mangan and Sisson (2000) both agreed that heterogenous nucleation containing crystals occur more in nature. Mangan et al. (2004) further stated that in heterogenous systems a minor change in the pressure triggers bubble nucleation in water saturated rhyolites, opposing the substantial pressure change required in homogenous nucleation (Mangan and Sisson, 2000). Mangan et al. (2004) used a 5.5 wt.% water saturated rhyolite. From the Rooiberg samples, water content is observed to increase from ~6.5 wt.% in the Damwal Formation to ~18.00 wt.% in the Kwaggasnek Formation. The wide range in water content exhibited by the Rooiberg Group contradicts the subtle pressure change suggestion of natural, heterogenous (crystal-bearing) nucleation of Mangan et al. (2004). This wide range in water content is again proposed to result from the close proximity of the source of melting to the melted crust. It is therefore interpreted that the Fe-Ti oxide surface described as commencing heterogenous nucleation (Mangan et al., 2004) located in the lower part of the Rooiberg Group would have formed first, and if we consider the suggestion of the upward movement of the source of heat closer to the melted liquid from the crust, bubbles/volatiles will exhibit increase kinetic energy leading to increase volatile exsolution. Hort (1998) interpreted that the exsolution of volatiles from a crystallizing system does not necessarily decrease the temperature but may keep the temperature constant or even increase it. The presence of vesciles in the Rooiberg Group especially in the Damwal, Kwaggasnek and Schrikkloof formations support the presence of gass bubbles in these rocks prior eruption and that exsolution of gas bubbles in the rocks may have increased the temperature.

CHAPTER 9

DISCUSSION

Detailed petrography shows some distinction between the more mafic, lower part of the Rooiberg SLIP stratigraphy and the upper silicic unit. The lower part (the Dullstroom, and to a certain degree the lower part of the Damwal Formation) of the Rooiberg Stratigraphy exhibit fewer phenocrysts, making it less porphyritic than the upper parts of the stratigraphy. The Dullstroom Formation exhibit fewer pyroclastic units (ignimbrites) when compared with the upper formations. Phenocrysts are mostly plagioclase with some K-feldspar and minor pyroxene, similar to the observation of Twist (1985). It should be noted that the Na-rich plagioclase dominates throughout the Rooiberg stratigraphy while the Ca-richer feldspar such as anorthite occurs mainly in the Dullstroom (more mafic) area. The dominant presence of plagioclase is similar to the observation of Janasi et al. (2007) where trachydacites (less silicic) of the Paranà are described to mainly contain phenocrysts of plagioclase and clinopyroxene. However, the Damwal, Kwaggasnek and Schrikkloof formations, composed of a microcrystalline groundmass similar to the lower part, lacks the presence of mafic minerals such as clinopyroxene and the Fe-Ti bearing minerals but exhibit distinct layers of pyroclastic units in the Damwal, Kwaggasnek and Schrikkloof formations. Occurrence of pyroclastics is in accordance with the description of the upper units in the Gawler Range Volcanics, where the rocks are described to be dominated by ignimbrites (Agangi et al., 2012). Similarly, pyroclastic rocks occur in the rhyolitic ignimbrites of the Rogerson Graben (Snake River Plain) (Andrews et al., 2008) but are absent in the McKinney Basalt of the same province (Snake River Plain) (Leeman and Vitaliano, 1976). With “caution thrown to the wind” due to absence of any geochemical data, it can be interpreted that pyroclastic material, breccias and ignimbrite are more commonly found in the silicic part of SLIPs than the lower mafic portion.

Flow banding is much more commonly exhibited in the upper part of the Rooiberg Group stratigraphy, the Damwal, Kwaggasnek and Schrikkloof formations, than in the Dullstroom Formation. The occurrence of flow banding in the upper parts of the Rooiberg is similar to the reports of Agangi et al. (2012) and Blissett (1985) for the upper parts of the Gawler Range Volcanics (GRV). Agangi et al. (2012) also reported the occurrence of flow folds (similar to flow-bands) in the upper parts of the GRV. Flow-banding is, therefore, proposed as more synonymous with the silicic part of volcanic rocks than the mafic part; after all flow-bands are structures that represent evidence of viscosity which is greater in the silicic units

than the mafic units within a succession of volcanic rocks. Subsequently, it is proposed in this study that the occurrence of mafic minerals such as pyroxene in the lower parts of SLIP stratigraphy along with other crystallizing minerals such as apatite and Fe-Ti rich minerals indicate that the crystallizing liquid that commence the formation of SLIPs is mafic in composition. This further implies that the melt which evolved the Rooiberg Group, especially the Dullstroom Formation, is mantle-derived in accordance with the suggestions of Schweitzer and Hatton (1995), Schweitzer et al. (1995) and Buchanan et al. (2002; 2004). The distinction between the mineral compositions of the Damwal, Kwaggasnek and Schrikkloof formations and the Dullstroom Formation could imply difference in the processes of evolution between the upper and lower parts of the Rooiberg Group.

As results have shown in this study, a chemostratigraphy is possible within the area north of Loskop Dam area. The concentrations of the elements used could therefore be useful for regional comparison as already proposed by Schweitzer et al. (1995) and Schweitzer and Hatton (1995). Nevertheless, as no detailed geochronological framework for the Rooiberg Group formations exists regional correlations are executed with utmost caution.

Despite some work in recent history (Schweitzer et al., 1995; Hatton and Schweitzer, 1995; Buchanan et al., 2002; 2004), the petrogenesis and crystallization history of the Rooiberg Group rocks is still not completely solved. Geochemical evidence of this study support the hypothesis that fractional crystallization was one of the dominant processes during the formational history of the Rooiberg Group, i.e. from relatively Mg-rich rocks in the Dullstroom Formation to Si-rich rocks in the Schrikkloof Formation (Figs. 12 and 13). However, some samples show high SiO_2 (Fig. 13) in the Dullstroom area and are described as samples representing the low-Mg felsites magma type that occur in this region (described as Basal rhyolite by Schweitzer et al., 1994; Hatton and Schweitzer, 1995). The decrease in Ti (TiO_2) concentration up-section as shown in Figs. 12 and 13 suggests that the magma that formed the lower part of the Rooiberg Group, the Dullstroom, was enriched in TiO_2. This is supported by the occurrence of Fe- and Ti-rich mineral phases (such as magnetite and ilmenite) in the Dullstroom (c.f. Buchanan et al., 1999) and Damwal formations. Furthermore, the crystallization of these Fe-Ti rich mineral phases led to the partitioning of compatible elements such as P (P_2O_5), Mg (MgO), Fe (Fe_2O_3) and Lu into the suite of crystallizing minerals. P (P_2O_5), forming apatite, was observed to be more prominent in the Damwal Formation than in the overlying Kwaggasnek Formation in the area north of Loskop Dam. The reduced concentration of P, Mg and Fe along with the subsequent enrichment of Si

in the residual melt, at a later stage, formed the less mafic and more silica-rich rocks of the upper parts of the Rooiberg Group, the Kwaggasnek and Schrikkloof formations. Mathez et al. (2013) stated that during the middle stages of fractionation, where SiO_2 is about 60 to 66 wt.%, Fe-enrichment of residual liquids is almost always accompanied by SiO_2 enrichment. This middle stage of fractionation is likened to the Damwal Formation (where SiO_2 composition is mainly between 60 and 73 wt.%) after which there is an observed increase in the SiO_2 in the Kwaggasnek and Schrikloof formations. The described trend of fractionation strongly supports the evidence of fractional crystallization in the evolution of these rocks, especially in the Damwal Formation within the area north of Loskop Dam. Further evidence strongly supporting fractional crystallization of a mantle-derived source for the evolution of the Rooiberg Group are the $^{87}Sr/^{86}Sr$ and ε_{Nd} isotope plot in Fig. 20. The Rooiberg Group show isotopic signatures similar to the mafic cumulate of the RLS of the Bushveld Complex and not the rocks of the Kaapvaal Craton, despite its acidic composition. Both the RLS and Rooiberg Group (Fig. 20) plot close to the bulk-silicate-earth (BSE) compositions and within the mantle array. Thus, the remarkable identical isotopic signatures of both acidic (Rooiberg Group) and mafic (RLS) rocks of the Bushveld Complex reflect a mantle origin with no crustal contamination, posing a "mystery" about these rocks that continues to elude scientists studying the Bushveld province. According to plots using discrimination diagrams modified after Pearce et al. (1984) and Verma et al. (2013) in Figs. 15 and 16 respectively, results also suggest a mantle-derived melt for the origin for the Rooiberg Group with no evidence for substantial and observable amount of crustal contamination. Isotope plots in Figs. 17, 18 and 19 also show a general trend of fractional crystallization especially in the Dullstroom Formation, which forms a scatter od data points with decrease in stratigraphic height in the Damwal and Kwaggasnek formations due to crustal assimilation.

Despite evidence of fractional crystallization of a mantle-sourced liquid for the evolution of the Rooiberg Group, evidence of crustal origin cannot be ignored. The negative spike in Eu exhibited by the Rooiberg Group is typical of crustal rocks. The Rooiberg Group rocks used in this study are metaluminous to peraluminous, similar to the findings of Mathez et al. (2013). Metaluminous rhyolites are usually anorogenic (Whalen et al., 1987; Andrews et al., 2008), similar to Eby's (1992) A_2 granitoids, representing a crustal origin, hence crustal source is again merited as the origin of these rocks. Further evidence that strongly supports crustal involvement (melting/assimilation) for the evolution of the Rooiberg Group is observed in the Nb/Ta values. Pfander et al. (2007) described the Nb/Ta of the continental

crust to range between ~12-13 while mantle derived compositions such as OIBs and MORBs have higher values that are usually greater than 14 (~15-16). Nb/Ta values as observed in the upper part of the Rooiberg Group range mainly between 10.91 and 14.83, with only four samples exhibiting values between 15.13 and 16.02 in the Damwal Formation. These values exhibited by the upper part of the Rooiberg Group are identical to crustal values although the high Nb/Ta values displayed by some of the Damwal samples suggest otherwise. At this point it is important to consider that the similarities between some geochemical signatures between the Rooiberg Group and deeper sourced liquid (possibly from the mantle) suggest possible magma mixing. Barth et al. (2000) also showed that the Nb/Ta values of the crust is ~11-12 which is usually lower than the primitive and depleted mantle having values of 17.4±5 and 15.5±1 respectively. Again the crustal values of Nb/Ta which are lower than the values of mantle-derived compositions are likened to the upper part of the Rooiberg Group in this study. However, those samples that show high Nb/Ta values are interpreted to represent magma mixing between the source of melting (mafic magma) and melt generated from the crust. Barth et al. (2000) also stated that Nb and Ta are concentrated in the upper continental crust, as such, comparison of the Nb and Ta values between the upper part of the Rooiberg Group used in this study, the continental and mantle compositions are conducted. The upper part of the Rooiberg Group exhibit Nb and Ta compositions of 5.38-24.2 and 0.45-1.86 ppm respectively (Table 6). White (2013) showed that mantle concentrations of Nb and Ta are 0.0651 and 0.037 ppm respectively, this low concentrations also support that mantle derived compositions are Nb and Ta poor. However, Taylor and McLennan (1985; 1995) and Wedepohl (1995) showed that Nb and Ta values in the crust are much higher. Taylor and McLennan (1985; 1995) assumed that Nb and Ta are 25 and 2.2 ppm respectively while Wedepohl (1995) showed 26 and ~1.5 ppm for Nb and Ta respectively. Plank and Langmuir (1998) also showed the Nb and Ta concentrations of the upper crust as 13.7 and 0.96 ppm respectively. It can be seen that the upper part of the Rooiberg Group shows Nb and Ta values that are similar to crustal compositions than mantle-derived sources. This evidence also support that crust is a major source in the origin of the upper part of the Rooiberg Group. It is therefore suggested that the lava types described by Schweitzer et al. (1995) and Schweitzer and Hatton (1995) for the Dullstroom Formation could be the products of partial melting of a lower part of the crust (lower part of the upper crust or the boundary between the upper and lower crust) and possible mixing with the source of melting as suggested by the ε_{Nd} and Nb/Ta values, while the Damwal, Kwaggasnek and Schrikkloof formations are

interpreted as sole products of partial melting of the upper part of the continental crustal material. However, some evidence such as the higher Nb/Ta value exhibited by some samples of the Damwal Formation also show mixing between magmas or mixing between magma and partially melted crust. The mixture is therefore suggested to result in the two groups described in Fig. 16 which shows the distinction between the Damwal Formation from the Kwaggasnek and Schrikkloof formations.

Strong isotopic evidence for mantle origin for the Rooiberg Group is shown in Fig. 20. There is great similarity between the ε_{Nd} values exhibited by the Rooiberg Group and the values exhibited by the continental crust. The Rooiberg Group ε_{Nd} values range between ~-10 to ~-6, similar to the continental crust compositions (~-20 to -5, Dickin, 2002) as well as the continental basalts formed in the crust. The ε_{Nd} value of the Rooiberg Group again suggests possible crustal involvement in the evolution of these volcanics. Similarities in the ε_{Nd} and Rb/Sr values (isotope compositions as shown in Figs. 17 and 19) exhibited by the different lava types in the Dullstroom Formation suggests that this formation evolved from fractional crystallization of a mafic liquid whereas the Damwal and Kwaggasnek formations, which show variations in isotopic values with decrease in the stratigraphic height, suggest a more crustal involvement. The variation in ε_{Nd} and Rb/Sr signatures between in the Dullstroom Formation and the Damwal and Kwaggasnek formations as observed in Fig. 17 and 19 again suggests that the process of evolution of the lower part of the Rooiberg Group may not be identical to the process that led to the formation of the upper part.

In general, it is observed that major, trace, as well as isotope signatures of the Rooiberg Group exhibit both fractional crystallization (mantle source) and characteristics of partial melting of the crust. This observation led to modelling the assimilation and fractional crystallization as the mechanism that evolved the Rooiberg Group. Results of the model (Fig. 22) show that a mafic liquid contaminated by crustal material do not evolve compositions exhibited by the Rooiberg group. Furthermore, the mixture of the Rooiberg Group and crustal material show that the two rocks could have evolved from identical sources as the line of mixing shown in Fig. 22b is the same as the Rooiberg sample after contamination. The observed change of Ba composition between the Rooiberg Group and Kaapvaal rock samples could imply that though the Rooiberg Group, similar to crustal composition, does exhibit

some mantle-derived signatures as well. Again, Rooiberg Group exhibits both crustal and mantle properties.

The Rooiberg Group exhibiting both mantle and crustal signatures is, therefore, proposed in this study to result from the occurrence of a thick crust and a possible shallow, lower upper mantle within the Bushveld Province similar to the suggestion of Nguuri et al. (2001). The suggestion of Nguuri et al. (2001) is also consistent with the interpretation of James et al. (2001), where cratonic roots are described as extending into 250 to 300 km depth and into the mantle. Therefore, liquid from the lower upper mantle could have also mixed with crustal material to result in the magnesian lava type of the lower part of the Rooiberg Group. James et al. (2001) also stated that there was chemical modification of the mantle during magma emplacement in the Proterozoic (Bushveld region) where cratonic (crustal) material was added to the mantle. This could also explain why the lower part of the Rooiberg Group exhibiting mantle-derived properties. The suggestion by James et al (2001) is consistent with Carlson et al. (2000) where Proterozoic peridotites from the mantle were described as showing evidence of crust-mantle coupling. This unique mantle could have been the source of the mafic liquid that evolved the Dullstroom Formation. Furthermore, Nguuri et al. (2001) and Webb et al. (2000) stated that the Bushveld event resulted in a downward flexure of the crust within the Bushveld Magmatic Province. This downward flexure is interpreted in this study to reduce the distance between the crust and the heat source that is inducing the melting. The reduction of this distance is suggested to generate the “unusual” high temperatures exhibited by the Rooiberg Group as reported by Lenhardt and Eriksson (2012). As a result, temperature estimates were modelled using the modelling spreadsheet of Ersoy (2013). Temperatures modelled show high temperatures for the Rooiberg Group which range between ~961.7 °C in the Damwal Formation to ~1090.4 °C in the Kwaggasnek Formation (Table 9). These temperature estimates are similar to the 880-1120 °C proposed by Lenhardt and Eriksson (2012) and much greater than the estimated and modelled range of temperatures (~800 °C) that can partially melt the crust as a result of basalt injection (Annen and Sparks, 2002; Shellnutt et al., 2012).

This mode of formation described for the Rooiberg Group is similar to the process described for the evolution of rhyolites of the Yellowstone volcanism (Pierce and Morgan, 2009) in which basalts from a plume are interpreted to melt the Paleozoic crust. The high temperature exhibited by the Rooiberg Group is typical of a mantle-derived liquid; however, it is observed that temperature increases with decrease in stratigraphic height from the Damwal

Formation to the Kwaggasnek Formation (Table 9). Increase in temperature with reduction in stratigraphic height is therefore suggested to result from the reduction in distance between the heat source and the crustal material melted. The distance reduction is suggested to possibly commence crustal melting.

However, it is not certain how much heat as well as volume of mafic liquid will be required to melt the crust to generate such volume as exhibited by the Rooiberg Group. Furthermore, Frost and Frost (2011) described from experiments that ferroan granitoids produced by partial melting of tonalitic to granodioritic crust exhibit calc-alkalic characteristics while high degrees of partial melting would be required for any composition to reach the alkali-calcic boundary. All formations within the Rooiberg Group have a composition ranging from calcic through calc-alkalic to alkali-calcic, with the low-magnesian felsites all occurring in the alkali-calcic compositions (Mathez et al., 2013). This composition supports the occurrence of high degree of melting that might have resulted due to the increase in temperature with decrease in stratigraphic height from the Dullstroom Formation to the Schrikkloof Formation.

It is, therefore, proposed that the Rooiberg Group fractionally crystallized from partial melting of the crust by a mantle plume, basaltic magma beneath or within the crust or mantle-melt with addition of crustal material during crustal melting. In the Bushveld Magmatic Province, the possible source of heat that can induce crustal melting is suggested as the ponding of the mafic magma of the Rustenburg Layered Suite (RLS) from a main magma chamber in a shallow and within crustal depth (the reason why the RLS was used in the assimilation and fractional crystallization model as the mantle source). Mixing between the mafic magma and melted crust is proposed to result in the initial liquid composition being Ti-, Mg- and Fe-rich in the Dullstroom Formation (and in Damwal Formation), followed by more melting of the crust which increased the silica content. However, since the result of mixing between the RLS and the crustal material (Fig. 22a) does not produce any Rooiberg composition, there is a possibility that the shallow mantle composition was altered during magmatism (James et al., 2001; Nguuri et al., 2001).

Silicic volcanic rocks formed by partial melting of the crust induced by a mantle plume are subdivided into two types of melting processes: first type is the conductive heating from an underlying mantle and the second involves the advective heating of the crust by a basaltic magma ponding below the crust-mantle boundary (Xu et al., 2008). Frost et al. (2001) interpreted that crustal melting resulting from flood basalt volcanism can only be caused by advective heating transferred by underplated basaltic magma. When such magmas are

emplaced in crustal levels, melting of the crust is imminent and generation of silicic magma can therefore be expected (Annen and Sparks, 2002; Annen et al., 2006). Contrary to the two processes described for the formation of the silicic volcanics of the Rooiberg Group, Buchanan et al. (2002) and Mathez et al. (2013) interpreted that the Rooiberg Group evolved from fractional crystallization of mantle-derived magma that was contaminated by crustal material. However, on the basis of the signatures presented in this study between the Rooiberg Group and crustal composition, partial melting of the crust is suggested as a major process that evolved (at least) the upper part Rooiberg Group by ponding of mafic magma at crustal levels. One major source of heat that could induce partial melting of the crust to form the Rooiberg Group is the mafic magmas of the Rustenburg Layered Suite. It is suggested that the c. 1200°C mafic magmas that also led to the Rustenburg Layered Suite (Buick et al., 2001), much hotter than the ~800 °C required to melt the continental crust (Annen and Sparks, 2002; Shellnutt et al., 2012), is the source of heat that melted the crust to generate silicic compositions. Also, Frost and Frost (2011) interpreted that the high, >900 °C temperature of ferroan granitoids suggest the involvement of hot mafic magmas, which provides sufficient heat for melting or may contribute mass via differentiation and assimilation of crustal melts. Temperature estimates of the Rooiberg Group are within the estimated modelled range of temperatures that can result from partial melting of the crust as a result of basalt injection.

Finally, comparison between the Rooiberg Group samples used in this study (upper part of the Rooiberg) and other silicic large igneous provinces around the world such as the Snake River Plain, Central Atlantic Magmatic Province, Paraná-Etendeka, Karoo-Ferrar and Gawler Range Volcanics, all exhibit similarities. Notable depletion of Ba, Nb, and Sr (Fig. 23) in the upper Rooiberg Group and other SLIPs are described as representing mantle melts in which fractional crystallization was a dominant process. However, depleted amount of Eu, though representing fractional crystallization of plagioclase, is typical of the crust. The similarity between the Rooiberg Group, the Snake River Plain, Central Atlantic Magmatic Province, Paraná-Etendeka, Karoo-Ferrar and Gawler Range Volcanics suggest that though fractional crystallization played an important part in the evolution of SLIPs, however, partial melting and or assimilation of the crust during this process cannot be ignored. Further investigation on the type of process incorporating the crustal material into the mafic melt and detailed comparison between the entire Rooiberg Group and the other SLIPs will be undertaken in future studies.

CHAPTER 10

CONCLUSIONs

In summary, the Rooiberg Group as a whole exhibits both mantle and crustal signatures. A mantle signature is most evident in the Dullstroom Formation (and to a certain degree the lower parts of the Damwal Formation) whereas a crustal signature becomes more prominent throughout the Kwaggasnek and Schrikkloof formations. This change can be explained by the existence of the thick crust of the Kaapvaal Craton and a shallow mantle source within the Bushveld province, and the interaction of these two sources during magmatism. During the evolution of the Rooiberg Group, melting of the crust occurred with a simultaneous decrease in distance between the melted crust and the source of heat that generated high temperatures for the Rooiberg Group.

Similarities in geochemical signatures between the Rooiberg Group and selected SLIPs around the world suggest a similar origin for SLIPs by fractional crystallization of a mafic melt and melted (or assimilated) crustal material. However, the level at which different SLIPs will start crustal assimilation is not known as the thickness of the crust varies between location. For mantle-related melts, only relatively small amounts of assimilation of crustal material is necessary in order to produce the large amounts of rhyolitic magma of silicic large igneous provinces. Therefore, the majority of the material can be produced by rather simple fractional crystallization from a mantle-derived melt. For crustal melting, a large amount of heat is required to melt high amounts of the crusts in order to produce an enormous accumulation of silicic rocks such as the upper parts of the Rooiberg Group.

REFERENCE

Agangi, A., Kamentesky, V.S., McPhie, J., 2012. Evolution and emplacement of high fluorine rhyolites in the Mesoproterozoic Gawler silicic large igneous province, South Australia. Precambrian Research, volume 208, p. 124-144.

Allen, S.R., McPhie, J., 2002. The Eucarro Rhyolite, Gawler Range Volcanics, South Australia: a >675 km^3, compositionally zoned lava of Mesoproterozoic age. Geological Society of America Bulletine, volume 114, p.1592-1609.

Allen, S.R., Simpson, C.J., McPhie, J., Daly, S.J., 2003. Stratigraphy, distribution and geochemistry of widespread felsic volcanic units in the Mesoproterozoic Gawler Range Volcanics, South Australia. Australian Journal of Earth Sciences, volume 50, p. 97-112.

Allen, S.R., McPhie, J., Ferris, G., Simpson, C., 2008. Evolution and architecture of a large felsic igneous province in western Laurentia: the 1.6 Ga Gawler Range Volcanics, South Australia. Journal of Volcanology and Geothermal Research, volume 172, p., 132-147.

Altermann, W., Lenhardt, N., 2012. The volcano-sedimentary succession of theArchean Sodium Group, VentersdorpSupergroup. South Africa: Volcanology, sedimentology and geochemistry. Precambrian Research 214–215, p. 60–81.

Andrews, G.D.M., Branney, M.J., Bonnichsen, B., McCurry, M., 2008. Rhyolitic ignimbrite in the Rogerson Graben, Southern Snake River Plain volcanic province: Volcanic stratigraphy, eruption history and basin evolution. Bulletin of Volcanology, volume 70, p. 269-291.

Annen, C., Sparks, R.S.J., 2002. Effects of repetitive emplacement of basaltic intrusions on thermal evolution and melt generation in the crust. Earth and Planetary Science Letters volume 203, p. 937-955.

Annen, C., Blundy, J.D., Sparks, R.S.J., 2006. The genesis of intermediate and silicic magmas in deep crustalhot zones. Journal of Petrology volume 46, p. 605-626.

Barth, M.G., McDonough, W.F., Rudnick, R.L., 2000. Tracking the budget of Nb and Ta in the continental crust. Chemical Geology 165, 197-213.

Belleini, G., Comin-Chiaramonti, P., Marques, L.S., Melfi, A.J., Nardy, J.R., Papatrechas, C., Piccirillo, E.M., Roisenberg, A., Stolfa, D., 1986. Petrogenic aspects of acid and basaltic lavas from the Paraná Plateau (Brazil): geological, mineralogical and petrochemical relationships. Journal of Petrology, volume 27, p. 915-944.

Betts, P.G., Giles, D., Foden, J., Schaefer, B.F., Mark, G., Pankhurst, M.J., Forbes, C.J.,Williams, H.A., Chalmers, N.C., Hills, Q, 2009. Mesoproterozoic plume-modified orogenesis in eastern Precambrian Australia. Tectonics, volume 28, TC3006.

Blissett, A.H., 1985. Gairdner, South Australia. Explanatory notes, 1:250 000 geological series. Geological Survey of South Australia, Adelaide.

Blissett, A.H., Creaser, R.A., Daly, S.J., Flint, R.B., Parker, A.J., 1993. Gawler Range Volcanics. In: Drexel, J.F., Preiss, W.V., Parker, A.J. (Eds.), The Geology of South Australia. Geological Survey of South Australia, Adelaide.

Bonnichsen, B., Citron, G.P., 1982. The Cougar Point Tuff, southwestern Idaho. In: Bonnichsen, B, Breckinridge, R.M., (eds) Cenozoic Geology of Idaho. Idaho Buruea of Mines and Geological Bulletin, volume 26, p. 255-281.

Bottinga, Y, Richet, P., Sipp, A, 1995. Viscosity regimes of homogenous silicate melts. American Mineralogist, volume 80, p. 305-318.

Boudreau, A.E., 1999. PELE—a version of the MELTS software program for the PC platform. Computers and Geosciences, volume 25, p. 201–203.

Boynton, W. V., 1984. Cosmochemistry of the rare earth elements: meteorite studies. In: Henderson P (eds) Rare Earth Element Geochemistry. Elsevier, Amsterdam, p. 63-114.

Branney, M. J., Kokelaar, B. P., 1992. A reappraisal of ignimbrite emplacement: progressive aggradation and changes from particulate to non-particulate flow during emplacement of high-grade ignimbrite. Bulletin of Volcanology, volume 54, p. 504-520.

Bryan, S.E., 2007. Silicic large igneous provinces. Episodes 30, p. 20-31.

Bryan, S.E., Riley, T.R., Jerram, D.A., Leat, P.T., Stephens, C.J., 2002. Silicic volcanism: an under-valued component of Large Igneous Provinces and Volcanic Rifted Margins. In: Menzies, M.A., Klemperer, S.L., Ebinger, C.J., Baker, J. (Eds.), Magmatic Rifted Margins: Geological Society of America Special Paper, volume 362, p. 99-118,

Breitsprecher, K., Thorkelson, D.J., Shwab, D.L., Thompson, R.I., 2000. Volcanic stratigraphy and petrology of the eastern margin of the Kamloops Group near Enderby, British Columbia. Geological Survey of Canada, p. 1-7.

Buchanan, P.C., 2006. The Rooiberg group. In: Johnson, M.R., Anhaeusser, C.R., Thomas, R.J. (Eds.), The Geology of South Africa. Geological Society of South Africa/Council for Geoscience, Johannesburg/Pretoria, p. 283–289.

Buchanan, P.C., Reimold, W.U., 1998. Studies of the Rooiberg Group, Bushveld Complex, South Africa: No evidence for an impact origin. Earth and Planetary Science Letters, volume 155(1998), p.149-165.

Buchanan, P.C., Koeberl, C., Reimold,W.U., 1999. Petrogenesis of the Dullstroom Formation, Bushveld Magmatic Province, South Africa. Contributions to Mineralogy and Petrology, volume 137, p.133-146.

Buchanan, P.C., Reimold, W.U., Koeberl, C., Kruger, F.J., 2002. Geochemistry of intermediate to siliceous volcanic rocks of the Rooiberg Group, Bushveld Magmatic

Province, South Africa. Contributions to Mineralogy and Petrology, volume 144, p.131-143.

Buchanan, P.C., Reimold, W.U., Koeberl, C., Kruger, F.J., 2004. Rb–Sr and Sm–Nd isotopic compositions of the Rooiberg Group, South Africa: early Bushveld-related volcanism. Lithos volume 29, p. 373–388.

Buick, I.S., Maas, R., Gibson, R., 2001. Precise U-Pb titanite age constraints on the emplacement of the Bushveld Complex, South Africa. Journal of the Geological Society of London, volume 158, p. 3-6.

Cannon, W.F., 1992. The North American Midcontinental Rift beneath the Lake Superior regionwith emphasis on its geodynamic evolution. Tectonophysics, volume 213, p. 41-48.

Carlson, R.W., Boyd, F.R., Shirey, S.B., Janney, P.E., Grove, T.L., Bowring, S.A., Schmitz, M.D., Dann, J.C., Bell, D.R., Gurney, J.J., Richardson, S.H., Tredoux, M., Menzies, A.H., Pearson, D.G., Hart, R.J., Wilson, A.H. Moser, D., 2000. Continental growth, preservation and modification in southern Africa, GSA Today, 10, 1-7.

Cathey, H.E., Nash, B.P., 2004. The Cougar Point Tuff; implications for thermochemical zonation and longevity of high-temperature, high-volume silicic magmas of the Miocene Yellowstone hotspot. Journal of Petrology volume 45, p. 27-58.

Catuneanu, O., Wopfner, H., Eriksson, P.G., Cairncross, B., Rubidge, B.S., Smith, R.M.H., Hancox, P.J., 2005. The Karoo basins of south-central Africa. Journal of African Earth Sciences, volume 43, p. 211-253.

Cawthorn, R.G., 2013. The residual or roof zone of the Bushveld Complex, South Africa. Journal of Petrology volume 54, p. 1875-1900.

Cawthorn, R.G., Webb, S.J., 2001. Connectivity between the western and eastern limbs of the Bushveld Complex. Tectonophysics volume 330, p. 195-209.

Cawthorn, R.G., Walraven, F., 1998. Emplacement and Crystallization time for the Bushveld Complex. Journal of Petrology, volume 39, p. 1669-1687.

Cawthorn, R.G., Spies, L., 2003. Plagioclase content of cyclic units the Bushveld Complex, South Afrcia. Contributions to Mineralogy and Petrology, volume 145, p. 47-60.

Chen, B., Jahn, B.-m., Wilde, S. & Xu, B., 2000. Two contrasting Paleozoic magmatic belts in northern Inner Mongolia, China: petrogenesis and tectonic implications. Tectonophysics, volume 328, p. 157-182.

Cheney, E.S., Twist, D., 1991. The comformable emplacement of the Bushveld mafic rocks along a regional uncomformity in the Transvaal succession of South Africa. Precambrian Research, volume 52, p. 115-132.

Christiansen, R.L., 2001. The Quartenary and Pliocene Yellowstone Plateau volcanic field of Wyoming, Idaho and Montana. Geology of Yellowstone National Park, US Geological Survey National Paper, p. 729.

Christiansen, E.H., McCurry, M., 2008. Contrasting origins of Cenozoic silicic volcanic rocks from the western Cordillera of the United States. Bulletin of Volcanology, volume 70, p. 251-267.

Clubley-Armstrong, A.R., 1977. The geology of the Selonsrivier area, north of Middelburg, Transvaal, with special reference to the structure of the regions southeast of the Dennilton Dome. MSc thesis, University of Pretoria.

Coertze, F.J., Jansen, H., Walraven, F., 1977. The transition from the Transvaal sequence to the Waterberg Group. Geological Society of South Africa Transactions, volume 80, p. 145-156.

Creaser, R.A., 1995. Neodymium isotopic constraints for the origin of Mesopro-terozoic felsic magmatism, Gawler-Craton, South Australia. Canadian Journal of Earth Sciences volume 32, p. 460–471.

Davies, D.W., Paces, J.B., 1990. Time resolution of geologic events on the Keweenaw Peninsula and implications for development of the Midcontinent Rift system. Earth and Planetry Science Letters, volume 97, p. 54-64.

DePaolo, D.J., 1981. A neodymium and strontium isotopic study of the of the Mesozoic calc-alkaline granitic batholiths of the Seirra Nevada and Peninsula Ranges, California. Journal of Geophysical Research volume 86, p. 10470-10488.

Dickin, A.P., 2002. Radiogenic Isotope Geology, Cambridge Univ Press, New York, p. 490.

Dingwell, D.B., 1996. Volcanic dilemma- flow or blow? Science, volume 273, p. 1054-1055.

Du Plessis, M.D., 1976. The Bushveld Granites and associated rocks in the area northwest of Warmbaths, Transvaal. MSc. Thesis, University of Pretoria.

Duncan, A.R., Armstrong, R.A., Erlank, A.J., Marsh, J.S., Watkins, R.T., 1990. MORB-related dolerites associated with the final phases of Karoo flood basalt volcanism in southern Africa. In: Parker, A., Rickwood, B., (eds) Mafic Dykes and Emplacement Mechanism. Balkelma, Rotterdam, p. 119-129.

Duncan, R.A., Hooper, P.R., Rehacek, J., Marsh, J.S., Duncan, A.R., 1997. The timing and duration of the Karoo igneous event, southern Gondwana. Journal of Geophysical Research volume 102, p. 18127–18138.

Eby, G.N., 1992. Chemical Subdivision of the A-type granitoids: petrogenetic and tectonic implications. Geology, volume 20, p. 641-644.

Ehrenborg, J., 1996. A new stratigraphy for the Tertiary volcanic rocks of the Nicaraguan Highland. Bulletin of the Geological Society of America, volume 108, p. 830-842.

Ekren, E.B., McIntyre, D.H., Bennett, E.H., 1984. High-temperature, largevolume, lava-like ash-flow tuffs without calderas in southwestern Idaho. US Geological Survey Proffessional Papper 1272:76.

Elston, W.E., Twist, D., 1989. Vredefort- Bushveld enigma of South Africa and the recognition of large terrestrial impact structures: mental leaps and mental obstacles. Abstract of International Geology Congress, volume 28, p. 449.

Elston, W.E., 1992. Does the Bushveld –Vredefort system (South Africa) record the largest known terrestrial catastrophe? In: Submitted to the International Conference on Large Meteorite Impacts and Planetary Evolution. Lunar Planets Institute of Contribution, volume 799, p. 24-25.

Eriksson, P.G., Schweitzer, J.K., Bosch, P.J.A, Schereiber, U.M., Van Deventer, J.L., Hatton, C.J., 1993. The Transvaal sequence: an overview. Journal of African Earth Sciences volume 16, p. 25-51.

Erlank, A.J., Marsh, J.S., Dancan, A.R., Miller, R.M., Hawkesworth, C.J., Betton, P.J., Rex, D.C., 1984. Geochemistry and petrogennesis of Etendeka volcanic rocks from SW A/Namibia. In Erlank, A.J. (ed) Petrogenesis of the volcanic rocks of the Karoo Province. Geology Society of South Africa Special Publication volume 13, p.195-247.

Ersoy, E.Y., 2013. PETROMODELER (Petrological modeler): a Microsoft® Excel© spreadsheet program for modelling melting, mixing, crystallization and assimilation processes in magmatic systems. Turkish Journal of Earth Sciences, volume 22, p. 115-125.

Ferris, G., 2003. Volcanic textures within the Glyde Hill Volcanic Complex. Quarterly Earth Resources Journal of Primary Industries and Resources, South Australia, volume 29, p. 36-41.

French, B.M., Twist, D., 1983. Status of the Rooiberg Felsite in the Bushveld Complex: A review. Institute of geological research on the Bushveld Complexresearch report, volume 39.

Frost, B.R., Barnes, C.G., Collins, W.J., Arculus, R.J., Ellis, D.J., Frost, C.D., 2001. A geochemical classification for granitic rocks.Journal of Petrology, volume 42, p. 2033–2048.

Frost, C.D., Bell, J.M., Frost, B.R., Chamberlain, K.R., 2001. Crustal growth by magmatic underplating: isotopic evidence from the northern Sherman batholith. Geology, volume 29, p. 515–518.

Frost C.D., Frost B.R., 2011. On ferroan (A-type) granitoids: their compositional variability and modes of origin. J Petrol 52, 39–53.

Ganju, P.N., 1944. The Panjal Traps: acid and basic volcanic rocks. Proceedings of the Indian Academy of Science, volume 18, p.125-131.

Garland, F., Hawkesworth, C.J., Mantovani, M.S.M., 1995. Description and Petrogenesis of the Paraná rhyolites, Southern Brazil. Journal of Petrology, volume 36, p. 1193-1227.

Ghiorso, M.S., Hirschmann, M.M., Reiners, P.W., Kress, V.C. III, 2002. The pMELTS: a revision of MELTS for improved calculation of phase relations and major element partitioning related to partial melting of the mantle to 3 GPa. Geochemistry Geophysics Geosystems 3:1-36, 10.1029/2001GC000217.

Glen, J.M.G., Renne, P.R., Milner, S.C., Coe, R.S., 1997. Magma flow inferred from anisotropy of magnetic susceptibility in the coastal Paraná-Etendeka Igneous Province: Evidence for rifting before flood volcanism. Geology volume 25, p. 1131-1134.

Green, J.C., Fitz III, T.J., 1993. Extensive felsic lavas and rheoignimbrites in the Keweenawan Midcontinental Rift plateau volcanics, Minnesota: petrographic and field recognition. Journal of volcanology and geothermal research, volume 54, p. 177-196.

Greenough, J.D., Dostal, J., 1992. Cooling history and differentiation of a thick north mountain basalt flow (Nova Scotia, Canada). Bulletine of Volcanology volume 55, p. 63-73.

Gresens, R.L., 1967. Composition-volume relationships of metasomatism: Chemical Geology, volume 2, p. 47–65.

Harris, C., Marsh, J.S., Duncan, A.R., Erlank, A.J., 1990. The petrogenesis of the Kirwan Basalts of Dronning Maud Land, Antarctica. Journal of Petrology, volume 31, p. 341-369.

Harmer, R. E. and Farrow, D. 1995. An isotopic study on the volcanics of the Rooiberg Group: age implications and a potential exploration tool. Mineralium Deposita volume 30, p. 188-195.

Harris, C., Pronost, J.J.M., Ashwal, L.D., Cawthorn, R.G., 2005. Oxygen and hydrogen isotope stratigraphy of the Rustenburg Layered Suite, Busheld Complex: Constraints on crustal compositions. Journal of Petrology volume 46, p. 579-601.

Hatton, C.J., 1988. Formation of the Busxhveld Complex at a plate margin. Abstract Congress Geology Society of South Africa, volume 22, p. 251-254.

Hatton, C.J., 1995. Mantle plume origin for the Bushveld and Ventersdorp magmatic provinces. Journal of Africa Earth Science, volume 21, p. 571-577.

Hatton, C.J, Schweitzer, J.K., 1995. Evidence for synchronous extrusive and intrusive Bushveld magmatism. Journal of Africa Earth Science, volume 21, p. 579-594.

Hubbard, H.A., 1975b. Lower Keweenawan volcanic rocks of Michigan and Wisconson. Journal of research of the United States Geological Survey, volume 3, p. 529-541.

Hort, M., 1998. Abrupt change in magma liquidus temperature because of volatile loss or magma mixing: effects of nucleation, crystal growth and thermal history of the magma. Journal of Petrology, volume 39, p. 1063–1076.

Huppert, H.E., Stephen, R., Sparks, J., 1985. Cooling and contamination of mafic and ultramafic magmas during ascent through continental crust. Earth and Planetry Science Letters volume 74, p. 371-386.

Hurwitz, S., Navon, O., 1994. Bubble nucleation in rhyolitic melts: Experiments at high pressure, temperature, and water content. Earth and Planetry Science Letters, volume 122, p. 267-280.

James, D.E., M.J. Fouch, J.C. VanDecar, S. van der Lee, Kaapvaal Seismic Group, 2001. Tectospheric structure beneath southern Africa. Geophys. Res. Lett. 28, p. 2485-2488.

Janasi, V.D.A., de Freitas, V.A., Heaman, L.H., 2011. The onset of flood basalt volcanism, North Paraná Basin, Brazil: A precise U-Pb baddeleyite/zircon age for a Chapecó-type dacite. Earth and planetry science letters 302(1-2), p. 147-153.

Janasi, V.D.A., Montanheiro, T.J., de Freitas, V.A., Reis, P.M., Negri, F.D.A., Dantas, F.A., 2007. Geology, petrography and geochemistry of the acid volcanism of the Paranà Magmatic Province in the Piraju-Ourinhos region, SEBrazil. Revista Brasileira de Geociências volume 37 (4), p. 745-759.

Jourdan, F., Bertrand, H., Scharer, U., Blichert-Toft, J., Feraud, G., Kampunzu, A.B., 2007b. Major and trace element and Sr, Nd, Hf and Pb isotope compositions of the Karoo Large Igneous Province, Botswana-Zimbabwe: lithosphere vs mantle plume contribution. Journal of Petrology, volume 48, 1043-1077.

Kamenetsky, V.S., Morrow, N., McPhie, J., 2000. Origin of high-Si dacite from rhyolitic melt: evidence from melt inclusions in mingled lavas of the 1.6GA Gawler Range Volcanics, South Australia. Mineralogy and Petrology, volume 69, p. 183-195.

Karsli, O., Dokuz, A., Kaliwoda, M., Uysal, I., Aydin, F., Kandemir, R., Fehr, K.-T., 2014. Geochemical fingerprints of Late Triassic calc-alkaline lamprophyres from the Eastern

Pontides, NE Turkey: A key to understanding lamprophyre formation in a subduction-related environment. Lithos 196-197, p. 181-197.

Kirtsein, L.A., Peate, D.W., Hawkesworth, C.J., Turner, C.P., Harris, C., Mantovani, M.S.M., 2000. Early Cretaceous basaltic and rhyolitic magmatism in southern Uruguay associated with the opening of the south Atlantic. Journal of Pterology, volume 41, p. 1413-1438.

Leeman, W. P., Annen, C., Dufek, J., 2008. Snake River Plain-Yellowstone silicic volcanism: Implications for magma genesis and magma fluxes, in Dynamics of Crustal Magma Transfer, Storage, and Differentiation—Integrating Geochemical and Geophysical Constraints, Geological Society of London special publications, volume 304, p. 235-259.

Leeman, W.P., Vitaliano, C.J., 1976. Petrology of McKinney basalt, Snake River Plain, Idaho. Geological Society of America Bullettin volume 87, p. 1777-1792.

Lenhardt, N., Eriksson, P.G., 2012. Volcanism of the Paleoproterozioc Bushveld Large Igneous Province: The Rooiberg Group, Kaapvaal Craton, South Africa. Precambrian Research volume 214-215, p. 82-94.

Li, X.H., 2000. Cretaceous magmatism and lithospheric extension in southeast China, Journal of Asian Earth Sciences, volume 18, p. 293– 305.

Liu, H.-Q., Xu, Y.-G., Tian, W., Zhong, Y.,-T., Mundil, R., Li, X.,-H., Yang, Y.-H., Luo, Z.-Y.,Shang-Gaun, S.-M., 2014. Origin of two types of rhyolites in the Tarim Large Igneous Province: consequences of incubation and melting of a mantle plume. Lithos, volume 204, p. 59-72.

Loubser, M., Verryn, S., 2008. Combining XRF and XRD analyses and sample preparation to solve mineralogical problems. South African Journal of Geology, volume 111, p. 229-238.

Mangan, M., Mastin, L., Sisson, T., 2004. Gas evolution in eruptive conduits: combining insights from high temperature and pressure decompression experiments with steady-state flow modeling. Journal of Volcanology and Geothermal Research volume 129, p. 23–36.

Mangan, M., Sisson, T., 2000. Delayed, disequilibrium degassing in rhyolite magma: decompression experiments and implications for explosive volcanism. Earth and Planetry Science Letters, volume 183, p. 441-455.

Marsh, J.S., Ewart, A., Milner, S.C., Duncan, A.R., Miller, R.McG., 2001. The Etendeka Igneous Province, Magma types and their stratigraphic distribution with implications for the evolution of the Paranà-Etendaka flood basalt province. Bulletin of Volcanology volume 62 (6-7), p. 464-486.

Mathez, E.A., VanTongeren, J.A., Schweitzer, J., 2013. On the relationships between the Bushveld Complex and its felsic roof rocks, part 1: petrogenesis of Rooiberg and related fesites. Contributions to Mineralogy and Petrology, volume 166, p. 435-449.

McCurry, M., Hayden, K.P., Morse, L.H., Mertzman, S.A. Jr., 2008. Genesis of post-hotspot, A-type rhyolite of the eastern Snake River Plain volcanic field by extreme fractional crystallization of olivine tholeiite. Bullettin of Volcanology, volume 70, p. 361-383.

McPhie, J., DellaPasqua, F., Allen, S.R., Lackie, M.A., 2008. Extreme effusive eruptions: paleoflow data on an extensive felsic lava in the Mesoproterozoic Gawler Range Volcanics. Journal of Volcanology and Geothermal Research, volume 172, p. 148-161.

Melluso, L., Cucciniello, C., Petrone, C.M., Lustrino, M., Morra, V.,Tiepolo, M., Vasconcelos, L., 2008. Petrology of Karoo volcanic rocks in the southern Lebombo monocline, Mozambique. Journal of African Earth Sciences, volume 52, p. 139-151.

Milner, S. C., Duncan, A. R., Ewart A., 1992. Quartz latite rheoignimbrite flows of the Etendeka Formation, northwestern Namibia. Bulletin of Volcanology, volume 54, p. 200-219.

Milner, S. C., Duncan, A. R., Whittingham, A. M., and Ewart, A., 1995. Trans-Atlantic correlation of eruptive sequences and individual silicic volcanic units within the Paraná-Etendeka igneous province: Journal of Volcanology and Geothermal Research, volume 69, p. 137–157.

Mingram, B., Trumbull, R.B., Littman, S., Gerstenberger, H., 2000. A petrogenetic study of anorogenic felsic magmatism in the Cretaceous Paresis ring complex, Namibia: evidence for mixing of crust and mantle-derived components. Lithos, volume 54, p. 1-22.

Moghadam, H.S., Li, X-H., Ling, X-X., Santos, J.F., Stern, R.J., Li, Q-L., Ghorbani, G., 2015. Eocene Kashmar granitoids (NE Iran): Petrogenetic constraints from U–Pb zircon geochronology and isotope geochemistry. Lithos 216-217, p. 118-135.

Morris, C. G., 1992. Academic Press Dictionary of Science and Technology, Gulf Professional Publishing, p. 852, ISBN 0122004000.

Nakazawa, K., Kapoor, H.M., Ishii, K-I., Bando, O.Y., Tokuoka, T.,Murata, M., Nakamura, K., Nogami, S.S., Shimizu, D., 1975. The upper Permian and lower Triassic in Kashmir, India. Memoirs of the Faculty of Science, Kyoto University, Series of Geology and Minerlogy, volume 39, p. 83-98.

Nesbitt, H.W., Young, G.M., 1982. Early Proterozoic climates and plate motions inferred from major element chemistry of lutites. Nature, volume299, p. 715-717.

Nguuri, T.K., Gore, J., James, D.E., Webb, S.J., Wright, C., Zengeni, T.G., Gwavava, O., Snoke, J.A., Kaapvaal Seismic Group, 2001. Crustal structure beneath southern Africa and its implications for the formation and evolution of the Kaapvaal and Zimbabwe cratons. Geophysical Research Letters 28, 2501-2504.

Nicholson, S.W., 1992. Geochemistry, petrography and volcanology of rhyolites of the Portage Lake Volcanics, Kweenaw Peninsula. United States Geologigical Surbey and Bullettine 1970- A, B; B1-B57.

Pankhurst, R.J., Leat, P.T., Srouga, P., Rapela, C.W., Marquez, M., Storey, B.C., Riley, T.R., 1998. The Chon-Aike silicious province of Patagonia and related rocks in Artactica: a silicic large igneous province. Journal of Volcanology and Geothermal Research, volume 81, p. 113-136.

Pankhurst, M.J., Schaefer, B.F., Betts, P.G., 2011. Geodynamics of rapid voluminous felsic magmatism through time. Lithos 123, p. 92-101.

Parker, D.F., Ghosh, A., Price, C.W., Rinard, B.D., Cullers, R.L., Ren, M., 2005. Origin of rhyolite by crustal melting aand the nature of parental magmas in the Oligocene Conejos Formation, San Juan Mountains, Colorado, USA. Journal of Volcanology and Geothermal Research, volume 139, p. 185-210.

Peate, D.W., 1997. The Paraná-Etendeka Province. In Mahoney, J.J., Coffin, M.F. (eds), Large Igneous Provinces: Continental, Oceanic, and Planetry flood volcanism, volume 100. American Geophysical Union, p. 217-245.

Peate, D.W., Hawkesworth, C.J., Mantovani, M.S.M, 1992. Chemical stratigraphy of the Paraná lavas (South America): classification of magma types and their spatial distribution. Bulletin of Volcanology, volume 55, p. 119-139.

Pearce, J.A., Harris, N.B.W., Tindle, A.G., 1984. Trace element discrimination diagrams for the tectonic interpretation of granitic rocks. Journal of Petrology, volume 25, p. 956–983.

Peucat, J. J., Capdevila, R., Fanning, C. M., Menot, R. P., Pecora, L., Testut, L., 2002. 1.60 GA Felsic volcanic blocks in the moraines of the Terre Adélie Craton, Antartica: comparisons with the Gawler Range Volcanics, South Australia. Australian Journal of Earth Sciences, volume 49, p. 831-845.

Pfander, J.A., Münker, C., Stracke, A., Mezger, K., 2007. Nb/Ta and Zr/Hf in ocean island basalts- Implications for crust-mantle differentiation and the fate of Niobium. Earth and Planetry Science Letters 254, 158-172.

Pierce, K.L., Morgan, L.A., 1992. The track of the Yellowstone hotspot: volcanism, faulting, and uplift. In: Limk, P.K., Kuntz, M.A., Platt, L.P. (eds) Regional Geology of eastern Idaho and western Wyoming. Geological Society of America Memoir, volume 179, p. 1-53.

Pierce, K.L., Morgan, L.A., 2009. Is the track of the Yellowstone hotspot driven by a mantle plume? –A review of volcanism, faulting, and uplift in the light of new data.Journal of Volcanology and Geothermal Research, volume 188, p. 1-25.

Plank, T. and C. H. Langmuir. 1998. The chemical composition of subducting sediment and its consequences for the crust and mantle. Chemical Geology 145, 325-394.

Pronost, J., Harris, C., Pin, C., 2008. Relationship between footwall composition, crustal contamination, and fluid-rcok interaction in the Platreef, Bushveld Complex, South Africa. Mineralium Deposita, volume 43, p. 825-848.

Putirka, K., 2005b. Igneous thermometers and barometers based on plagioclase + liquid equilibria: tests of some existing models and new calibrations. American Mineralogist volume 90, p. 336-346

Putirka, K.D., 2008. Thermometers and barometers for volcanic systems. Reviews in Mineralogy and Geochemistry volume 69, p. 61–120.

Renne, P.R., Deckart, K., Ernesto, M., Féraud, G., Piccirillo, E.M., 1996a. Age of the Ponta Grossa dyke swarm (Brazil), and implications to Parana flood volcanism. Earth and Planetary Science Letter volume 144, p. 199–211.

Renne, P.R., Glen, J.M., Milner, S.C., Duncan, A.R., 1996b. Age of the Etendeka volcanism and associated intrusions in southwestern Africa. Geology volume 24, p. 659-662.

Rhodes, R.C., 1975. New evidence for impact origin of the Bushveld complex, South Africa. Geology volume 3, p. 549-554.

Rhodes, R.C., Du Plessis, M.D., 1976. Notes on some stratigraphic relations in the Rooiberg felsites. Transactions of the geological society of South Africa, volume 79, p. 183-185.

Riley, T.R., Knight, K.B., 2001. Age of pre-break-up Gondwana magmatism. Antarctic Science, volume 13(2), p. 99-110.

Riley, T.R. and Leat, P.T., 1999. Large volume silicic volcanism along the proto-Pacific margin of Gondwana: lithological and stratigraphical investigation from the Antarctic Peninsula. Geological magazine, volume 136, p. 1-16.

Schweitzer, J.K., 1987. The transition from the Dullstroom Basalt formation to the Rooiberg Felsite Group, Transvaal Supergroup: a volcanological, geochemical and petrological investigation. Ph.D. thesis, University of Pretoria.

Schweitzer, J.K., Hatton, C.J., de Waal, S.A., 1995. Regional lithochemical stratigraphy of the Rooiberg Group, upper Transvaal Supergroup: A proposed new subdivision. South African Journal of Geology, volume 98, p. 245-255.

Schweitzer, J.K., Hatton C.J., 1995. Chemical alteration within the volcanic roof rocks of the Bushveld Complex. Economic Geology and the Bulletin of the Society of Economic Geologists, volume 90, p. 2218-2231.

Schneiderhan, E.A., 2007. Neoarchean clastic rocks on the Kaapvaal Craton: provenance analysis and geotectonic implications. PhD Thesis, University of Johannesburg, South Africa.

Shellnut, J.G., Bhat, G.M., Wang, K-L., Brookfield, M.E., Dostal, J., Jahn, B-M., 2012. Origin of the silicic volcanic rocks of the Early Permian Panjal Traps, Kashmir, India Chemical Geology, volume 334, p.154-170.

Shellnutt, J.G., Jahn, B.,-M., 2010. Formation of the late Permian Panzhihua plutonic-hypabyssal-volcanic igneous complex: implications for the genesis of Fe-Ti oxide deposits and A-type granites of SW China. Earth and Planetry Science Letters volume 289, p. 509-519.

South African Commission on Stratigraphy, 1980. Stratigraphy of South Africa. Geological Survey of South Africa, Handbook 8. Pretoria: Geological Survey of South Africa, p. 690.

Stewart, K.P., 1994. High temperature silicic volcanism and the role of mantle magmasin Proterozoic crustal growth: The Gawler Range Volcanic Province. University of Adelaide, Adelaide.

Sugawara, T., 2001. Ferric iron partitioning between plagioclase and silicate liquid: thermodynamics and petrological applications. Contributions Mineralogy and Petrology volume 141, p.659-686.

Sun S. S., Bailey, D. K., Tarney, J., Dunham, K., 1980. Lead isotopic study of young volcanic rocks from mid-ocean ridges, ocean islands and island arcs. Philos. Trans. R. Soc. London A297, 409-445.

Sun, S.S., McDonough, W.F., 1989. Chemical and isotopic systematics of oceanic basalts: implications for mantle composition and processes. In: Sanders, A.D., Norry, M.J. (Eds.), Magmatism in the Ocean Basins. Geological Society of London Special Publication, volume 42, p. 313-345.

Sweeney, R.J., Duncan, A.R., Erlank, A.J., 1994. Geochemistry and petrogenesis of Central Lebombo basalt s of the Karoo Igneous Province. Journal of Petrology, volume 35, p. 95-125.

Tankard, A.J., Jackson, M.P.A., Eriksson, K.A., Hobday, D.K., Hunter, D.R., Minter, W.E.L., 1982. Crustal evolution of southern Africa. Springer, Berlin, 523 pp.

Taylor, S. R., McLennan, S. M., 1985. The Continental Crust: its composition and evolution. Oxford: Blackwell Scientific Publishers.

Taylor, S. R., McLennan, S. M., 1995. The geochemical evolution of the continental crust. Reviews of Geophysics 33, 241-265.

Tegner, C., Robins, B., Reginiussen, H., Grundvig, S., 1998. Assimilation of crustal xenoliths in a basaltic magma chamber: Sr and Nd Isotopic constraints from the Hasvik Layered Intrusion, Norway. J. Petrol. 40, 363-380.

Thiede, D.S., Vasconcelos, P.M., 2010. Parana flood basalts: rapid extrusion hypothesis confirmed by new $^{40}Ar/^{39}Ar$ results. Geology volume 38, p. 747–750.

Thompson, R.N., Morrison, M.A., Dickin, A.P., Hendry, G.L., 1983. Continental food basalts. arachnids rule OK? In: Hawkesworth CJ, Norry MJ (eds.) Continental basalts and mantle xenoliths. Shiva Publishing, Nantwich, p. 158-185.

Thompson, R.N., Morrison, M.A., Hendry, G.L., Parry, S.J., Simpson, P.R., Hutchison, R., O'Hara, M. J., 1984. An assessment of the relative roles of crust and mantle in magma genesis: an elemental approach. Philosophycal Transaction Royal Society of London A310: p. 549-590.

Toulkeridis, T., Goldstein, S.L., Clauer, N., Kröner, A., Todt, W., Schildowski, M., 1998. Sm-Nd, Rb-Sr and Pb-Pb dating of silicic carbonates from the early Archean Barberton Greenstone Belt, South Africa: Evidence for post-depositional isotopic resetting at low temperature. Precambrian Research, volume 92, p. 129-144.

Twist, D., Bristow, J.W., 1990. Extensive lava-like siliceous flows in southern Africa: a review of occurrences. Institute for geological research of the Bushveld Complex research report, volume 82.

Twist, D., 1985. Geochemical evolution of the Rooiberg Silicc Lavas in the Loskop Dam Area, Southeastern Bushveld. Economic Geology, volume 80, p. 1153-1165.

Twist, D., French, B.M., 1983. Voluminous acid volcanism in the Bushveld Complex: a review of the Rooiberg Felsite. Bulletine volcanologique, volume 46(3), p. 225-242.

VanTongeren, J.A., Mathez, E.A., 2012. Large scale liquid immiscibility at the top of the Bushveld Complex, South Africa. Geology 40, p. 491–494.

VanTongeren, J.A., Mathez, E.A., Kelemen, P.B., 2010. A felsic end to Bushveld differenciation. Journal of Petrology, volume 51, p. 1891-1912.

Verma, S.P., Pandarinath, K., Verma, S.K., Agrawal, S., 2013. Fifteen new discriminant-function-based multi-dimensional robust diagrams for acid rocks and their application to Precambrian rocks. Lithos 168-169, 110-118.

Vervoort, J.D., Green, J.C., 1997. Origin of evolved magmas in the Midcontinental Rift System, northeast Minnesota: Nd-isotope evidence for melting of Archean crust. Canadian Journal of Earth Sciences, volume 34, p. 521-535.

Vervoort, J.D., Wirth, K., Kennedy, B., Sandland, T., Harpp, K.S., 2007. The magmatic evolution of the Midcontinental Rift: new geochronological and geochemical evidence from felsic magmatism. Precambrian Research, volume 157, p. 235-268.

Voordouw, R., Gutzmer, J, Beukes, N.J., 2009. Intrusive origin for upper group (UG1, UG2) stratiform chromitite seams in the Dwars River area, Bushveld Complex, South Africa. Miner Petrol 97, 75-94.

Wade, C.E., Reid, A.J., Wingate, M.T.D., Jagodzinski, E.A., Barovich, K., 2012. Geochemistry and geochronology of the c. 1585 Ma Benagerie Volcanic Suite, southern Australia: Relationship to the Gawler Range Volcanics and implications for the petrogenesis of a Mesoproterozoic silicic large igneous province. Precambrian Research 206-207, p. 17-35.

Walraven, F., 1995. Genetic aspects of the granophyric rocks of the Bushveld Complex. Economic Geology, volume 80, p. 1166-1180.

Walraven, F., 1997. Geochronology of the Rooiberg Group, Transvaal Supergroup, South Africa. Information circular, Economic Research Unit, University of Witwatersrand, Johannesburg, South Africa, volume 97, p. 316.

Warren, I., Simmons, S.F., Mauk, J.L., 2007. Whole-Rock Geochemical Techniques for Evaluating Hydrothermal Alteration, Mass Changes, and Compositional Gradients Associated with Epithermal Au-Ag Mineralization. Economic Geology, volume 102, p. 923-948.

Watts, K.E., Bindeman, I.N., Schmitt, A.K., 2011. Large volume rhyolite gneiss in cladera complexes of the Snake River Plain: insights from the Kilgore Tuff of the Heise Volcanic Field, Idaho, with comparison to the Yellowstone and Bruneau-Jarbidge rhyolites. Journal of Petrology volume 52, p. 857-890.

Webb, S.J., T. Nguuri, D.E. James, and T.H. Jordan, 2000. Crustal thickness supports Bushveld continuity, Eos Trans. AGU, Supplement, 81 (19), S175.

Wedepohl, K. H. 1995. The composition of the continental crust. Geochimica et Cosmochimica Acta, 59: 1217-1232.

Whalen, J.B., Currie, K.L., Chappell, B.W., 1987. A-type granite: geochemical characteristics, discrimination and petrogenesis. Contributions to Mineralogy and Petrology, volume 95, p. 407–419.

White, W.M., 2013. Geochemistry. John Wiley and Sons Ltd, USA.

White, J.C., Holt, G.S., Parker, D.F., Ren, M.H., 2003. Trace-element partitioning between alkali feldspar and peralkalic quartz trachyte to rhyolite magma. Part I: systematics of trace-element partitioning. American Mineralogist volume 88, p. 316–329.

Winchester, J.A., Floyd, P.A., 1977. Geochemical discrimination of different magma series and their differentiation products using immobile elements. Chemical Geology, volume 20, p. 325-343.

Workman, R.K., Hart, S.R., 2005. Major and trace element composition of the depleted MORB mantle (DMM). Earth and Planetry Science Letters 581.

Wright, K.E., McCurry, M., Hughes, S.S., 2002. Petrology and geochemistry of the Miocene Tuff of McMullen Creek, central Snake River Plain, Idaho. In: Bonnichsen, B., White, C.M., McCurry, M. (eds) Tectonic and magmatic evolution of the Snake River Plain volcanic province. Idaho Geological Survey and Bulletin, volume 30, p. 177-194.

Xu, Y-G., Chung, S-L., Shao, H., He, B., 2010. Silicic magmas from the Emeishan large igneous province, southwest China: petrogenesis and their link with the end-Guadalupian biological crisis. Lithos, volume 119, p.47-60.

Xu, Y.G., Luo, Z.Y., Huang, X.L., He, B., Xiao, L., Xie, L.W., Shi, Y.R., 2008. Zircon U–Pb and Hf isotope constraints on crustal melting associated with the Emeishan mantle plume. Geochimica et Cosmochimica Acta 72, p. 3084–3104.

Zartman, R.E., Nicholson, S.W., Cannon, W.F., Morey, G.B., 1996. U-Th-Pb zircon ages of some Keweenawan Supergroup rocks from the south shore of Lake Superior. Canadian Journal of Earth Sciences, volume 34(4), p. 549-561.

Zhou, M.F., Yan, D.P., Kennedy, A.K., Li, Y.Q., Ding, J., 2002. SHRIMP U–Pb zircon geochronological and geochemical evidence for Neoproterozoic arc-magmatism along the western margin of the Yangtze Block South China. Earth Planetry Science Letters, volume 196, p. 51–67.

Index

Abbreviations

CAMP -	Central Atlantic Magmatic Province
CIA-	Chemical Index of Alteration
GRV-	Gawler Range Volcanics
HTI-	High-Ti basalt
LIP-	Large Igneous Province
LMF-	Low-Mg felsite
LTI-	Low-Ti basalt
LOI-	Loss on Ignition
SLIP-	Silicic Large Igneous Province
XRF-	X-ray Flourescence